Smoke Spreading

in Vertical Shafts in Buildings

with Scale Modelling Technique

TANG POK MAN

BEng (Hons), The Hong Kong Polytechnic University

Department of Building Services Engineering

A thesis submitted in partial fulfilment of

the requirements for the

Degree of Master of Philosophy

(February 2004)

CERTIFICATE OF ORIGINALITY

I hereby declare that this thesis is my own work and that, to the best of my knowledge and belief, it reproduces no material previously published or written nor material which has been accepted for the award of any other degree or diploma, except where due acknowledgement has been made in the test.

TANG POK MAN

Department of Building Services Engineering

The Hong Kong Polytechnic University

Hong Kong

February 2004

Abstract

Abstract of a thesis entitled 'Smoke spreading in vertical shafts in buildings with scale modelling technique' submitted by TANG POK MAN for the degree of Master of Philosophy at The Hong Kong Polytechnic University in August 2003.

A vertical shaft is a building enclosure with large height-to-span ratio passing through floors vertically with openings to different levels. Smoke spreading through a vertical shaft is identified as an important key issue and of the primary concern of fire safety for old highrise buildings in Hong Kong. This study investigates the smoke movement in vertical shafts due to a fire at various locations in a building. A scale-down model was constructed and the scaling laws were applied to study the smoke travelling time from the fire location to other building locations through the shaft. Scaling parameters considering the conservation of enthalpy were selected for the experimental study. It found that the location of fire would be important in determining the smoke travelling time in vertical shafts. Scenarios of a fire in a compartment at different levels adjacent to the shaft were considered. Five different locations were studied with different fire sizes. Smoke spreading patterns were observed and empirical correlations were derived to predict the smoke travelling time of the plume front in the shaft. These empirical correlations would be very useful for professionals such as building design engineer, law draftsmen and property owners in predicting the smoke travelling time in full scale buildings. Finally, the experimental results were used to describe the smoke spreading through a lift shaft in a reported fire case, the Garley building fire. The times required for smoke to travel inside the lift shaft were obtained from the correlation derived. This information would be helpful for fire investigation.

Acknowledgements

I wish to thank my chief supervisor, Assistant Professor L. T. Wong, for his guidance, encouragement and support over the past years.

Contents

Chapter 1 Introduction

'Concrete jungles' in Hong Kong, include modern buildings with new design features and old highrise buildings constructed years ago. A building in Hong Kong of which the floor of the uppermost storey exceeds 30 m above the point of staircase discharge at ground floor level is defined as highrise building (Hong Kong Fire Services Department 1998). Vertical shaft is an essential architectural element in buildings for service installation and transportation. A vertical shaft is a building enclosure with large height-to-span ratio (Laws of Hong Kong 1997), passing through floors vertically with openings to different levels. Vertical shafts such as lift shafts, ventilation shafts, light wells, refuse tubes, pipe ducts and cable ducts are commonly found in high-rise buildings in Hong Kong. Problems on fire safety are commonly encountered with vertical shafts. Heat and smoke would spread rapidly to the other levels from the fire floor through the shafts.

A highrise building in Hong Kong constructed before 1973 are classified as old highrise buildings and they can be found everywhere even in the Central District (Chow et al. 1999). About 40% of the 50,000 private buildings can be classified as old buildings as announced by the SAR government (Hong Kong Buildings Department 1997). Since they were constructed at least 30 years ago when the requirements on fire services installations were not so strict as today (Hong Kong Fire Services Departments 1998; Hong Kong Buildings Department 1995, 1996 a, b; Hong Kong Fire Safety Ordinance 1997; Lo 1995), there could be problems on fire safety design, fire services system installed and the fire safety management.

People did not pay much attention to the fire safety aspects for those buildings until a very big fire happened in an old highrise building (South China Morning Post 1996;

Ming Pao 1996; Hong Kong Standard 1997). For that large fire happened in an old high-rise building in 1996, the lift shaft under refurbishment was proposed to be a key element of concern (Woo 1997; Chow 1997, 1998). That fire was suspected to start from a lift shaft which was under refurbishment. Because of the construction work, all the lift doors in that lift shaft were removed with the vertical openings sheltered by temporary plywood partitions. The fire would be started from the lift shaft with nobody paying attention to it at the early stage. Reports pointed out that workers had tried to extinguish the fire but failed. They then reported to the Fire Services Department (FSD) (Fire Daily News 1996) when the fire size grew to quite big and started spreading to the other levels. Combustible materials were ignited at the lower and upper levels to develop fires in those areas and give a very large post-flashover fire that lasted for more than 20 hours. There were arguments (Drysdale 1999) on the location where the fire started. All these required further in-depth scientific investigation for the Authority to judge. The lift shaft under refurbishment without fire protection does certainly cause fire safety problems in transferring heat and smoke and is a key element of concern (Fire Daily News 1996; Chow 1997, 1998). Citizens are now very concerned about the fire safety in those old highrise buildings.

At least 2 key factors on fire safety must be considered: the amount of combustibles described by the fire load density; and the number of people staying inside the building expressed in terms of the occupancy levels (Wong et al. 2000; Wong 2003). As a result of probable high fire load density and high population density, a list of fire safety provisions is required for new highrise commercial buildings (Hong Kong Fire Services Department 1998; Hong Kong Fire Safety Ordinance 1997). The key areas are building structures and fire safety measures (Wong et al. 2000).

Requirements are clearly described in the fire safety (Commercial Premises) Ordinance (1997) for new commercial buildings. However, only fire hydrant and hose reel systems are required in old highrise buildings. Sprinkler systems and smoke control systems are not commonly found in those old highrise buildings (Chow et al. 1999). There could be problems in locating means of escape and fire safety management. Fire safety measures such as smoke door was not properly maintained in some old buildings (Chow et al. 1999). Furthermore, it could be difficult to identify the fire resisting construction elements, because of unreported refurnishing works carried out in the past 30 years.

Smoke spreading is therefore of the primary concern for the fire safety of the old highrise buildings, as smoke is potentially lethal that could rapidly spread to other parts of the buildings (Kolte and Milke 2002; Chew and Liew 2000). Casualties due to fire smoke could be found in reported fire accidents (e.g., South China Morning Post 1997; Singtao Daily 1997; Hong Kong Standard 1998). Studying the motion of hot gases through the lift shaft is very important in understanding how smoke is spread through the building. Both the stack effect and the turbulent mixing process of a lower hot layer of smoke and an initial upper cool layer of air (Cooper 1998) related to the Rayleigh-Taylor mixing process (Zukoski 1995) should be considered.

The fire environment in the old highrise building was studied preliminarily using a two-layer zone model (Friedman 1992, Cooper 1998). Several scenarios were considered by taking the building as multi-level and multi-compartment structures including a lift shaft. The description of a traditional 2-layer zone type compartment fire modelling for a room is not valid for a shaft-like compartment (Cooper 1998). Within the lift shaft, the smoke layer was assumed to start descending from the

ceiling, no matter where the locations of the fire were. However, smoke would take time to travel upward before forming a smoke layer, if a fire started from a lower level (Fujita et al. 1998). The time taken for the smoke to move up to the ceiling is quite significant for a high lift shaft (Tanaka 2000). Therefore, the time for the smoke layer to fill up the stair shaft would be longer than those values predicted by a two-layer zone model. The time taken for the smoke to travel in a vertical shaft is very important and should be studied carefully.

Apart from the numerical simulations of the fire environment using computer models (e.g., Chow and Wong 1993, Chow 1995), experimental studies on the smoke movement and smoke filling process were reported in literatures (e.g. Chow and Lo 1995, Chow *et. al.* 1998). Studies on a full size building with hot smoke are good as the actual picture of the smoke filling process can be obtained (Chow *et. al.* 1998, De Smedt and Morgan 1998, Williams *et. al.* 1998). However, it is very expensive and time consuming to get a wide range of tests in full-size buildings. On-site measurement in a vertical shaft of an occupied building could not be practical. It could be constrained if using 'cold smoke'. Experimental studies with physical scale-down models are alternative to the full-scale tests and have been used in studying smoke movement in indoor spaces (e.g. Thomas *et. al.* 1961, Quintiere *et. al.* 1978, Chow and Lo 1995). It is relatively economical to have a wide-range of experimental results in terms of time, space and cost although, there are some difficulties in preserving all the dimensional groups for scale modelling studies with convenient fluids. Studies (e.g., Fujita et. al. 1998, Chow and Lo 1995, Chow et. al. 1998) showed that reasonable accuracy could be obtained with scale modelling studies when compared with those obtained from full scale burning tests.

Therefore, a study on the smoke spreading in vertical shafts of old highrise buildings with scale modelling technique is proposed so that the probable smoke travelling time in the vertical shaft could be specified. The objectives of this study are:

1. To study the smoke spreading through a vertical shaft with fire at different levels.

2. To study the smoke travel time through the vertical shaft.

3. To develop mathematical models to determine the smoke travel time.

4. To apply the mathematical models to typical vertical shaft in buildings.

Chapter 2 Scale Modelling

Experimental studies with physical scale-down models require the preservation of many parameters. Comprehensive reviews on scaling techniques for fire research was conducted by Williams (1969), Heskestad (1975) and Quintiere (1989). Scaling laws with Froude number modelling technique are available in literature for studying pre-flashover fires (Quintiere 1989). At the early stage of a fire, heat is mainly transferred from the burning object to the upper level by convection. Buoyancy is the driving force for smoke movement in the natural ventilated space. Scaling factors are important in using scale models and reviewed in this chapter.

The governing differential conservation equation for mass, momentum and energy describing one dimensional vertical fluid (in y-direction) are,

Mass,

$$\frac{\partial \rho}{\partial t} + \frac{\partial (\rho v)}{\partial y} = 0 \qquad \ldots (2.1)$$

Momentum (Vertical),

$$\rho \frac{\partial v}{\partial t} + \rho v \frac{\partial v}{\partial y} = -\frac{\partial p'}{\partial y} + g(\rho_a - \rho) + \frac{4}{3}\mu \frac{\partial^2 v}{\partial y^2} \qquad \ldots (2.2)$$

Energy,

$$\rho c_p \left(\frac{\partial T}{\partial t} + v \frac{\partial T}{\partial y} \right) = k \frac{\partial^2 T}{\partial y^2} + \frac{\partial p}{\partial t} + Q \qquad \ldots (2.3)$$

where,

$$p' = p - p_a \quad \ldots (2.4)$$

$$\frac{dp_a}{dy} = -\rho_a g \quad \ldots (2.5)$$

Follow the arguments by Quintiere (1989), the above equations can be made dimensionless by introducing the normalizing parameters. They are the characteristic length L^* (m), the characteristic velocity v^* (m s^{-1}), the characteristic time t^* (s) and the characteristic pressure p^* (Pa). With the initial ambient pressure p_0 (Pa), density ρ_0 (kg m^{-3}) and temperature T_0 (K), the normalized density $\hat{\rho}$, velocity $\hat{u}$, time $\hat{t}$ and length $\hat{x}$ are given by,

$$\hat{\rho} = \frac{\rho}{\rho_0} \quad \ldots (2.6)$$

$$\hat{v} = \frac{v}{v^*} \quad \ldots (2.7)$$

$$\hat{t} = \frac{t}{t^*} \quad \ldots (2.8)$$

$$\hat{y} = \frac{y}{L^*} \quad \ldots (2.9)$$

Taking,

$$\rho_a = \rho_0 \quad \ldots (2.10)$$

$$p' = \hat{p}' p^* \quad \ldots (2.11)$$

$$p = \hat{p}\, p_0 \quad \ldots (2.12)$$

$$T = \hat{T}\,T_0 \qquad \ldots (2.13)$$

The conservation equation for mass, momentum and energy equations (2.1) to (2.3) can be written as,

$$\pi_1 \frac{\partial \hat{\rho}}{\partial \hat{t}} + \frac{\partial(\hat{\rho}\hat{v})}{\partial \hat{y}} = 0 \qquad \ldots (2.14)$$

$$\hat{\rho}\left(\pi_1 \frac{\partial \hat{v}}{\partial \hat{t}} + \hat{v}\frac{\partial \hat{v}}{\partial \hat{y}}\right) = -\pi_2 \frac{\partial \hat{p}'}{\partial \hat{y}} + \frac{4}{3}\pi_3 \frac{\partial^2 \hat{v}}{\partial \hat{y}^2} + \pi_4(1-\hat{\rho}) \qquad \ldots (2.15)$$

$$\hat{\rho}\left(\pi_1 \frac{\partial \hat{T}}{\partial \hat{t}} + \hat{v}\frac{\partial \hat{T}}{\partial \hat{y}}\right) = \pi_3\pi_5 \frac{\partial^2 \hat{T}}{\partial \hat{y}^2} + \pi_6 \frac{\partial \hat{\rho}}{\partial \hat{t}} + \hat{Q} \qquad \ldots (2.16)$$

where the dimensionless groups,

$$\pi_1 = \frac{L^*}{v^* t^*} \qquad \ldots (2.17)$$

$$\pi_2 = \frac{p^*}{v^{*2}\rho_0} \qquad \ldots (2.18)$$

$$\pi_3 = \frac{\mu}{v^* L^* \rho_0} = \frac{1}{Re} \qquad \ldots (2.19)$$

$$\pi_4 = \frac{gL^*}{v^{*2}} = \frac{1}{Fr} \qquad \ldots (2.20)$$

$$\pi_5 = \frac{k}{\mu c_p} = \frac{1}{Pr} \qquad \ldots (2.21)$$

$$\pi_6 = \frac{L^* p^*}{\rho_0 v^* c_p T_0 t^*} = \frac{L^* \rho_0 v^{*2}}{\rho_0 v^* c_p T_0 \frac{L^*}{v^*}} = \frac{v^{*2}}{c_p T_0} \quad \ldots (2.22)$$

$$\hat{Q} = \frac{L^* Q}{\rho_0 v^* c_p T_0} \quad \ldots (2.23)$$

where Re, Fr and Pr are the Reynolds number, Froude number and the Prandtl number respectively.

Taking,

$$t^* = \frac{L^*}{v^*} \quad \ldots (2.24)$$

$$p^* = \rho_0 v^{*2} \quad \ldots (2.25)$$

$$\pi_1 = \pi_2 = 1 \quad \ldots (2.26)$$

With constant temperature and pressure from scale to scale, constancy of both Froude number and Reynolds number cannot be satisfied simultaneously, as required for strict modelling (Heskestad 1975). The requirement of constant Reynolds number is relaxed that is equivalent to ignoring flow effects dependent on viscosity. The experiments would be performed in air at normal ambient conditions for convenience with π_4 the primary group preserved. For natural convection π_4 is set equal to 1. The solid boundary effects are assumed nonexistent or unimportant for a large volume, π_3 (or Reynolds number) therefore would be ignored in the Froude number modelling. The concerned region is far away from the combustion region.

However, the boundary effect could be significant in studying the smoke movement in a long vertical shaft and cannot be ignored.

A point source representation would be used with the chemical energy production rate Q. By Bousinnesq assumption,

$$1-\hat{\rho}=\hat{T}-1 \qquad \ldots (2.27)$$

A normalized temperature is derived by Quintiere (1989),

$$\pi_4(1-\hat{\rho})=(\pi_4\zeta)\left(\frac{\hat{T}-1}{\zeta}\right)=\left(\frac{\hat{T}-1}{\zeta}\right) \qquad \ldots (2.28)$$

Hence,

$$\pi_4\zeta=1 \qquad \ldots (2.29)$$

$$\zeta=\frac{v^{*2}}{gL^*} \qquad \ldots (2.30)$$

Let,

$$\frac{\hat{Q}}{\zeta}=1 \qquad \ldots (2.31)$$

with equation (2.23), equation (2.31) can be written as,

$$\frac{\hat{Q}}{\zeta}=\frac{L^*Q/L^{*3}}{\rho_0 v^* c_p T_0}\frac{gL^*}{v^{*2}}=1 \qquad \ldots (2.32)$$

$$v^* = \left(\sqrt[3]{\frac{g}{\rho_0 c_p T_0}}\right)\left(\frac{Q}{L^*}\right)^{\frac{1}{3}} \quad \ldots (2.33)$$

For scaling studies with preservation of the Froude number of the scale model and the real size building (denoted with subscript M and R respectively),

$$\pi_4|_M = \pi_4|_R \quad \ldots (2.34)$$

$$\frac{gL^*_M}{v^{*2}_M} = \frac{gL^*_R}{v^{*2}_R} \quad \ldots (2.35)$$

The scaling law for the velocity and length of the scale model and real size building is,

$$\left(\frac{L^*_M}{L^*_R}\right)^{\frac{1}{2}} = \frac{v^*_M}{v^*_R} \quad \ldots (2.36)$$

Time in the scale model and the real size building can be related by,

$$t^*_R = \frac{L^*_R}{v^*_R} \quad \ldots (2.37)$$

$$t^*_M = \frac{L^*_M}{v^*_M} \quad \ldots (2.38)$$

The scaling law for the time and length of the scale model and real size building can be written as,

$$\frac{t^*_M}{t^*_R} = \frac{\frac{L^*_M}{v^*_M}}{\frac{L^*_R}{v^*_R}} = \frac{L^*_M}{L^*_R}\frac{v^*_R}{v^*_M} = \frac{L^*_M}{L^*_R}\left(\frac{L^*_M}{L^*_R}\right)^{-\frac{1}{2}} \quad \ldots (2.39)$$

$$\frac{t^{\bullet}_{M}}{t^{\bullet}_{R}} = \left(\frac{L^{\bullet}_{M}}{L^{\bullet}_{R}}\right)^{\frac{1}{2}} \quad \ldots (2.40)$$

Assume g, ρ_o, c_p, T_o are constant for the scale model studies, equation (2.33) can be written as,

$$v^{\bullet} = C \times \left(\frac{Q}{L^{\bullet}}\right)^{\frac{1}{3}} \quad \ldots (2.41)$$

$$\frac{v^{\bullet}_{M}}{v^{\bullet}_{R}} = \left(\frac{Q_M}{L^{\bullet}_{M}}\right)^{\frac{1}{3}} \left(\frac{L^{\bullet}_{R}}{Q_R}\right)^{\frac{1}{3}} \quad \ldots (2.42)$$

$$\left(\frac{L^{\bullet}_{M}}{L^{\bullet}_{R}}\right)^{\frac{1}{2}} = \left(\frac{Q_M}{L^{\bullet}_{M}}\right)^{\frac{1}{3}} \left(\frac{L^{\bullet}_{R}}{Q_R}\right)^{\frac{1}{3}} \quad \ldots (2.43)$$

The scaling law for the heat release rate and length of the scale model and real size building can be written as,

$$\frac{Q_M}{Q_R} = \left(\frac{L^{\bullet}_{M}}{L^{\bullet}_{R}}\right)^{\frac{5}{2}} \quad \ldots (2.44)$$

The equations (2.36), (2.40) and (2.44) are scaling laws with preservation of the Froude number. However, the assumption of neglecting the boundary effect would be inappropriate for this study. The viscous force due to the solid boundary of the vertical shaft might be significant. Therefore, the Froude number modeling was not adopted for this study.

For a fire located at the floor of a lift shaft, the height y (m) that smoke moved up in time t (s) measured experimentally is expressed in terms of the non-dimensional

height $\hat{y}$ and the non-dimensional time $\hat{t}$, through the characteristic length scale of the model D^* (m), and the non-dimensional heat release rate of the fire $\hat{Q}$ expressed in terms of the heat release rate of the fire Q (kW) (Fujita et al. 1998):

$$\hat{y} = \frac{y}{D^*} \quad \ldots (2.45)$$

and

$$\hat{t} = t\sqrt{\frac{g}{D^*}}\hat{Q}^{\frac{1}{3}} \quad \ldots (2.46)$$

with

$$\hat{Q} = \frac{Q}{c_p \cdot \rho \cdot T_a \cdot D^{*\frac{5}{2}}\sqrt{g}} \quad \ldots (2.47)$$

where g (9.81 m s^{-2}) is the acceleration due to gravity, c_p (kJ kg^{-1} K^{-1}) is the specific heat of air at constant pressure, ρ (kg m^{-3}) is smoke density and T_a (K) is ambient temperature.

Following the argument of Fujita et al. (1998) and Tanaka et al. (2000) on the smoke plume induced by a fire of heat release rate Q (kW) placed at the shaft floor, an equation on the temperature rise ΔT (K), upward plume velocity v (m s^{-1}), cross-sectional area of the plume A (m^2) and density ρ (kg m^{-3}) can be set up by conservation of enthalpy:

$$Q \propto c_p \cdot \rho \cdot \Delta T \cdot A \cdot v \quad \ldots (2.48)$$

The upward velocity v (m s^{-1}) is due to buoyancy and so is given by the density difference $\Delta\rho$ (kg m^{-3}), and by the temperature difference ΔT (K) between the plume and the ambient air at temperature T_a (K) as:

$$v \propto \sqrt{g\frac{\Delta\rho}{\rho}\,y} = \sqrt{g\frac{\Delta T}{T_a}\,y} \qquad \ldots (2.49)$$

Combining equations (2.48) and (2.49) gives:

$$\left(\frac{\Delta T}{T_a}\right) \propto \left(\frac{Q}{c_p \cdot \rho \cdot T_a \sqrt{g}}\right)^{\frac{2}{3}} \left(\frac{1}{A\sqrt{y}}\right)^{\frac{2}{3}} \qquad \ldots (2.50)$$

Putting equation (2.50) into (2.49) gives:

$$v \propto \sqrt{g}\left(\frac{Q}{c_p \cdot \rho \cdot T_a \sqrt{g}}\right)^{\frac{1}{3}} \left(\frac{y}{A}\right)^{\frac{1}{3}} \qquad \ldots (2.51)$$

Dividing both sides by $\sqrt{gD^*}$ gives a non-dimensional velocity V:

$$\hat{v} = \frac{v}{\sqrt{g \cdot D^*}} \qquad \ldots (2.52)$$

which can be rewritten as:

$$\hat{v} = \frac{v}{\sqrt{g \cdot D^*}} = \frac{\sqrt{g}}{\sqrt{gD^*}} \left(\frac{Q}{c_p \cdot \rho \cdot T_a \sqrt{g}}\right)^{\frac{1}{3}} \left(\frac{y}{A}\right)^{\frac{1}{3}} \qquad \ldots (2.53)$$

and

$$\frac{v}{\sqrt{g \cdot D^*}} = \left(\frac{Q}{c_p \cdot \rho \cdot T_a \cdot D^{*\frac{5}{2}} \sqrt{g}} \right)^{\frac{1}{3}} \left(\frac{y \cdot D^*}{A} \right)^{\frac{1}{3}} \quad \ldots (2.54)$$

An important point is to assume $\rho = \rho_a$, Q (kW) is now expressed in terms of $\hat{Q}$ as:

$$\frac{v}{\sqrt{g \cdot D^*}} = \hat{Q}^{\frac{1}{3}} \left(\frac{y \cdot D^*}{A} \right)^{\frac{1}{3}} \quad \ldots (2.55)$$

The travel time t (s) of a smoke front from the source to a given height y (m) can be calculated by:

$$t \propto \int_0^y \frac{dy}{v} = \sqrt{\frac{D^*}{g}} \int_0^y \left(\frac{\sqrt{gD^*}}{v} \right) \frac{dy}{D^*} \quad \ldots (2.56)$$

For a fire of constant heat release rate and taken density ρ (kg m^{-3}) as a constant value along y (m), equation (2.56) can be written as:

$$t \propto Q^{-\frac{1}{3}} \int_0^y \left(\frac{A}{y} \right)^{\frac{1}{3}} dy \quad \ldots (2.57)$$

Expressing t (s) in terms of $\hat{t}$:

$$\hat{t} \propto \sqrt{\frac{D^*}{g}} \int_0^y \left(\frac{v}{\sqrt{g \cdot D^*}} \right)^{-1} \left[\sqrt{\frac{g}{D^*}} \left(\frac{v}{\sqrt{g \cdot D^*}} \right) \left(\frac{y \cdot D^*}{A} \right)^{-\frac{1}{3}} \right] \frac{dy}{D^*} \quad \ldots (2.58)$$

or

$$\hat{t} \propto \int_0^y \left(\frac{A}{y \cdot D^*}\right)^{\frac{1}{3}} d\left(\frac{y}{D^*}\right) \qquad \ldots (2.59)$$

There are at least two cases to consider. First, for a tall lift shaft with large height to length ratio, the upward smoke movement is restricted by the vertical shaft and so A (m^2) is taken as a constant. The travel time t given by equation (2.57) can be written as:

$$t \propto Q^{-\frac{1}{3}} \cdot y^{\frac{2}{3}} \qquad \ldots (2.60)$$

or,

$$\hat{t} \propto \hat{y}^{\frac{2}{3}} \qquad \ldots (2.61)$$

Second, for a free plume, there is no physical constraint on the upward movement; A (m^2) is proportional to the square of the plume radius at height y (m), which is proportional to y^2:

$$t \propto Q^{-1/3} \cdot y^{4/3} \qquad \ldots (2.62)$$

or,

$$\hat{t} \propto \hat{y}^{\frac{4}{3}} \qquad \ldots (2.63)$$

The characteristic length scale of the model D^* (m) could be as the hydraulic diameter of the shaft, expressed in terms of the shaft base length L (m) and width W (m) as:

$$D^* = \frac{2 \cdot L \cdot W}{L + W} \qquad \text{... (2.64)}$$

Experimental studies on the travel time of buoyant fire plume fronts in vertical closed shafts induced by a heat source were carried out (Fujita et al. 1998) in a scale model of size 0.8 m by 0.8 m and height 3.22 m; and in a full-size vertical shaft of size 2.8 m by 3 m and height 24 m. The following correlation equations were derived for closed shafts:

$$\hat{t} = \begin{cases} 0.56\hat{y}^{4/3} & ; \quad \hat{y} \le 2.5 \\ 0.30\hat{y}^{2} & ; \quad \hat{y} > 2.5 \end{cases} \qquad \text{... (2.65)}$$

Chapter 3 Experimental set-up

Experiments were carried out in a scale-down model of vertical shaft to simulate the smoke spreading process caused by an actual fire at a vertical shaft. The experiments were carried out inside the laboratory in The Hong Kong Polytechnic University (Fire Services Engineering Laboratory, Department of Building Services Engineering Laboratory). The scale-down model of the vertical shaft was constructed by clear glass as shown in Figure 3.1 to facilitate the smoke movement visualization. It was placed on a reserved area inside the laboratory with a dark footing. A town-gas fire acted as the heat source and a smoke pellet was placed over the fire to generate visible smoke for the scale modeling study. Smoke movements inside the scale-down model illuminated by an in-house developed light source and captured by a camera. The experiments were carried out in different fire sizes in terms of heat release rates with fire placed at different locations as shown in table 3.1 and table 3.2.

For each heat release rates, numbers of test had been repeated and photographs of transient smoke movement in the scale-down model were recorded and studied. The smoke spreading processes were presented in different graphs, and the results obtained were further studied in the next chapters.

This chapter presents the experimental set-up for the experiments and the major experimental equipments.

The major experimental equipments for the experiments are as follows:

1. A scale-down model of vertical shaft consists of: Glass tube model and glass made compartment model

2. A fire chamber

3. Light sources

4. Town-gas burner with gas regulator

5. Smoke pellets

6. Camera with shutter control

Scale-down model

A scale-down glass tube model was constructed for simulating the vertical shafts found in buildings. The main reason for choosing glass is that it is transparent in color which gave a good visualization and ease of cleaning after each experiment conducted. The glass is 0.006 metre in thickness, and the model dimension is 0.076 metre in width, 0.076 metre in length and 1.4 metre in height as shown in Figure 3.1. It has five openings on one side of the vertical surface. The five openings are located at the model base, 0.4 metre, 0.7 metre, 1 metre and 1.3 metre above the model base respectively. The opening's dimensions are 0.05 metre in length and 0.1 metre in height. A room compartment model of size 0.29 metre in length, 0.076 metre in width and 0.11 metre in height was constructed and placed adjacent to the openings of the vertical glass tube model for performing different experiments. The thickness of glass of the room compartment model was same as the shaft model. The configuration, dimensions and the arrangement for the glass tube model and the room compartment model were shown in the Figure 3.1 and Figure 3.2.

Fire Chamber

The experiments were conducted in an enclosed fire chamber, the Fire Services Engineering Laboratory, Department of Building Services Engineering. The location for carrying out the experiments was reserved that the setup was kept no change throughout all experiments. The size of the fire chamber is 6.5 metre in length, 4.5 metre in width and 3 metre in height. The chamber could be ventilated by the exhausted fans. The laboratory were provided with proper electrical power supply, lighting system, plumbing and drainage system, ventilation system, town gas supply, fire extinguishing system and smoke extraction system. There were a footing made of flat wood in black color located at the centre of the reserved area for placing the scale-down model. There were thermometer and relative humidity sensor in the laboratory for monitoring of temperature and relative humidity.

Light Sources

In order to have a clear image on smoke movement, the tungsten lamps were used as localized light sources and only the part of smoke movement was illuminated. The arrangement of tungsten lamps was shown in the Figure 3.3. It was placed at right angled at both sides to the scale-down model. There were three tungsten lamps at one side and totally six tungsten lamps were used. The lamps were placed at levels of 0.4 metre, 0.7 metre and 1 metre at both sides above the flat wood footing. Apart from the specific light sources, all the lightings inside the laboratory were turned off. No flash light was used in taking photographs of the smoke movement.

Camera

Experiments were carried out inside the scale-down model to visualize the smoke spreading patterns for different heat release rates. The photographs of the smoke movement were taken by a 135-film camera on the scale models at right angle in front of the model. The configuration of the camera and the scale model were shown on Figure 3.3. The time intervals for taking photographs were set at one seconds and 0.56 seconds. Therefore, the shutter speed was manual controllable type with a shutter time controller. In order to take photographs in dark environment, the aperture of the camera should also controllable. The camera used with a 35 mm lens.

Smoke pellets

The smoke pellets were used in the experiments for visible smoke generation. They were manufactured by pH products Ltd. (UK). The smoke generated were milky white in color. The smoke viscosity would directly affect its visibility. The smoke pellets were 13 g each. The smoke generated was claimed to be non-toxic but should be stored in dry place.

Chapter 4 Experimental Studies

The experimental equipments and the experimental set-up were presented in the last chapter. This chapter presents the experimental studies including the procedures and the requirements on carrying out the experiments.

Experiments were carried out with the scale-down model of vertical shaft as stated in the last chapter. Experiments were carried out at the reserved area with appropriated experimental equipments, The arrangement of the experimental equipments were shown on Figure 4.1. The scale-down model's dimension was constructed in a scaling factor of 36, in comparing with an actual lift shaft of dimensions 2.3 metre in length, 2.3 metre in width and 48 in metre height. The scale-down model was constructed with openings in five different levels on one side of it's vertical surface for studying smoke movement due to different fire locations. For the ease of presentation, a parameter height ratio H_R is defined.

Height ratio

A parameter height ratio H_R described the relative height of the adjacent fire compartment to the model height H (m) is given by:

$$H_R = \frac{H_c}{H} \qquad \ldots (4.1)$$

where H_C (m) is the height of the compartment base above the scale-down model base.

The height ratio H_R of the compartment at five different levels for the experiments were 0, 0.29, 0.5, 0.71 and 0.93 respectively as shown in Figure 3.2..

Fire location

The smoke movements inside the vertical shaft due to different fire locations were investigated. The six cases of studies were considered with fire happened at different locations, namely case A to case F, which were defined as follows:

Case A – Fire at the room adjacent to the shaft base at H_R=0

This case simulates the smoke movement inside the vertical shaft due to the fire at the lowest compartment of the building. Smoke generated by the fire and spread upward to upper levels of the buildings through the lowest opening of the shaft.

Case B – Fire at the bottom of the vertical shaft

In this case, fire was started at the bottom of the scale-down model as shown in Figure 3.2. It simulated a fire happened at the bottom part of a vertical shaft. In real case, a fire would cause by the ignition of combustibles, flammable liquid such as gear oil/rubbishes/waste left in the bottom of vertical shaft. The smoke generated and spread through the vertical shaft to different level of the building.

Case C – Fire at a room model adjacent to the shaft at height ratio H_R=0.29

This case simulates the smoke movement inside the vertical shaft due to the fire happened in a compartment located at the lower part of the building. Smoke generated and spread upward to upper levels of the buildings and downward to lower levels of the buildings through the opening of the shaft.

Case D – Fire at a room model adjacent to the shaft at height ratio H_R=0.5

This case simulates the smoke movement inside the vertical shaft due to the fire in a compartment located at height ratio H_R=0.5 of the building. Smoke generated and spread upward to upper levels of the buildings and downward to lower levels of the buildings through the opening of the shaft.

Case E – Fire at a room model adjacent to the shaft at height ratio H_R=0.71

This case simulates the smoke movement inside the vertical shaft due to the fire happened in a compartment located at the upper part of the building. Smoke generated and spread upward to upper levels of the buildings and downward to lower levels of the buildings through the opening of the shaft.

Case F – Fire at a room model adjacent to the shaft at height ratio H_R=0.93

This case simulates the smoke movement inside the vertical shaft due to the fire happened in a compartment located at the top most part of the building. Smoke could be generated and spread downward to lower levels of the buildings through the highest opening of the shaft.

Fire Size

For each case, smoke movement was studied with different fire size in terms of heat release rates. In the experiments, five different heat release rates were considered, they were 8.6 W, 28.7 W, 43.1 W, 57.5 W and 86.2 W as shown in Table 3.1. With equation (2.47), the corresponding heat release rates in the full size vertical shaft were 43 kW, 145 kW, 217 kW, 290 kW and 433 kW, respectively as shown in table

4.1. The appropriated heat release rates were kept constant throughout each experiment by constant supply flow rate of the town-gas.

Different heat release rates were achieved by regulating the supply flow rate of town-gas with fuel controller. For the limitation of gas supply from the laboratory, town gas was the fuel for starting a fire. The calorific value of town gas is 17.27 MJm^{-3} (information from HKTGC). Steady burning was achieved by regulating the town gas supply flow rate of values 0.0005 L/s to 0.005 L/s through a 2 mm diameter supply nozzle. Complete combustion was assumed for calculating the heat release rate. With the known calorific value, the heat release rate could be determined. Table 4.1 shows the different heat release rates corresponding to the different town-gas supply flow rates.

Since the town-gas would give a clean fire, smoke pellets were used to generate visible smoke. A smoke pellet was placed on a wire hanger above the gas burner and ignited by the gas burner with the appropriated gas flow rate. A smoke pellet of weight 3.5 g was used in each experiment. When the smoke pellet was ignited, visible smoke generated and started to spread inside the scale-down model at the same time. For each experiment, the transient smoke movement were recorded with the camera in the appropriated time intervals.

The background of the fire chamber was kept dark in order to minimize the chance of any reflection. The walls were covered by black clothes and the footing for placing the scale-down model was also painted in black. The smoke extraction system, ventilation system and air conditioning system of the fire chamber and adjacent areas were stopped during the experiments and the smoke movement could be free from influence. After each experiment, the chamber was purged by fresh air,

the exhaust air fans operated so that the chamber environment could resume "normal" in terms of visibility and temperature. The indoor air temperature and relative humidity were measured for each experiment.

The scale-down model and the room compartment model were clean after each test, tap water was used to clean the scale down model and the room compartment model until all the surfaces of the glass were free from combustion products. The waste water was drained out. The model was dried and cooled down for 30 minutes after each cleaning process. Another experiment could be start again after resetting the scale-down model and experimental equipments to the appropriated and required conditions.

Safety issue

The experiments were carried out with safety officer monitoring throughout process in order to ensure the laboratory safety. Safety procedures in Building Services Engineering laboratory were referred all the time. Investigators and helpers wore mask during the experiment. When fire were made during the experiment, the town gas supply was ensured and safety operation procedures were followed. The main town gas supply shut-off valve was kept on open position to ensure no gas supply between two experiments. Fire extinguishers were available in the chamber and kept in good condition.

Record of smoke movement

The smoke movement in the vertical model were recorded by taking photographs using the camera in appropriated settings. The most suitable settings of the camera were determined before the experiments were carried out in the appropriate light

source, film speed, speed of smoke movement and shutter speed. A range of settings of the camera were determined in order to capture high quality photographs of the smoke movement with a series of trial run of the experiments. A 135-film camera installed with a 35 mm lens were used. The aperture and shutter speed were set at f/5.6 and 1/125 s (+0, -0.45 ms) respectively with shooting frequency of 0.56 seconds for case of fire placed at the bottom of the scale model (Case B); and f/4 and 1/60 s respectively with shooting frequency of one seconds for the case A, case C to case F. The images were recorded on 35 mm x 24 mm films of speed ISO400 with resolving power 125 $llmm^{-1}$ for contrast 1/1000 and 40 $llmm^{-1}$ for contrast 1/1.6.

The shutter frequency was controlled by a timer relay circuit, in which it could select different time intervals for taking the photographs and the time intervals were under control and monitoring. The shooting frequency was adjustable to suit the different speed of smoke movement inside the shaft.

A roll of film could take 38 individual photographs and good for the recording purpose of the smoke movement inside the shaft. The time required for smoke generated from smoke pellet to fill up the scale down model was determined by trial run of experiments. The time spent was confirmed with experiment when the trial run have done thereafter.

The photographs were taken when smoke generated from the smoke pellet was subject to a flame in each experiment. It was observed that the smoke generated from the smoke pellets spread from the fire origin and fill up the shaft. For the case the fire in the compartment adjacent to the shaft, smoke spread through the opening to the shaft and filled up the shaft. The results from the unsuccessful ignition of the smoke pellet were rejected in the subsequent analysis.

For each fire size of each case, repeated experiments have been done and average position of the transient plume front was evaluated. For the case A, case C, case D, case E and case F, the experiments were repeated for three times for each heat release rate; for case B, experiments were repeated for four times for each heat release rate. There were totally over hundred of experiments have been done for this research. All the results obtained for this research were taken from the success experiments.

The images of the smoke movement were printed out and scanned into computer files for further studies. The quality image showed the scale-down model part with visible smoke spread inside it. In determining the levels that the smoke reached, the computer program photoshop version number six were used.

Evaluation of plume front

The images were converted to black and white color by the computer software, and the level of smoke reached were determined if the grey scale = 50% of the images is found. For each photograph, a normal value should be found individually for comparison to minimize the error happened. The typical smoke movement patterns in the scale-down model for different cases at different time intervals were shown in the Figures 4.2 to 4.7. The transient position of the plume front were determined from the images assisted with computer software, and the results at different heat release rates were shown at Figures 4.8 to 4.13 for different cases respectively.

Important points for the experiments

During the experiments, many important points need to pay attention to. There were things to do in preparing to perform the experiments, during the experiments and

after the experiments. Important things to be reminded for the experiments could be summarized in the following points. In order to ensure the experiments could be carried out successfully, the following steps could be helped and acted as a guideline in performing each experiment.

1. Make sure that all the experimental equipments for the experiment were well prepared in the laboratory.

2. The scale-down model (glass tube and room compartment model) should be cleaned with fresh water before each experiment. The surface of the scale-down model must keep dry, clean and clear.

3. The tungsten lamps were arranged in proper positions at both sides of the scale-down model so that no glare would be created on the camera lens or images. The lamps should be checked in proper working conditions before each experiment.

4. Ensure the camera was in proper position in front of the scale down model. The settings of the camera should be checked before each experiment to ensure the quality images. The time intervals of the timer for the shutter control should be checked in correct settings before each experiment.

5. The smoke pellets should be weighted before each experiment, the smoke pellets were cut with cutter and weighted to ensure the same weighted smoke pellets were used in each experiment.

6. Ensure the town gas supply was available at suitable pressure inside the laboratory. The town gas control valve should be opened during each experiment and closed after each experiment. The gas flow rate should be

checked with the gas flow rate regulator for each experiment to ensure it is in proper settings.

7. Ensure the walls inside the laboratory were covered with black clothes and the environment of the laboratory was free from reflected surfaces.

8. Ensure the extraction fans for the laboratory were available and in standby condition. All the ventilation system, air conditioning system, smoke extraction system and any system would induce air moments inside the laboratory should be turn off during the experiment. The extraction fans should be turned on whenever each experiment was completed to ensure the smoke from accumulating inside the laboratory.

9. When all the experimental equipments were available, the equipments should be placed in proper positions. The scale-down model should be placed at the flat wood footing in black colored. The smoke pellet was placed above the gas burner inside the room compartment model fixed at the appropriate height for carrying out the experiments. The camera was in standby conditions. The scale-model should be ensured to seal well to prevent any leakage of smoke.

10. The general lighting system for the laboratory should be turned off. The specific light sources turned on. The town gas control valve turn on with the preset town gas flow rate. The fire would then be made by a spark.

11. When smoke generated from the smoke pellets, camera started to take photographs until the end of the experiments with suitable time intervals.

12. During the experiments, no people can be accessed to the reserved area in order to minimize any influence to the experiments. Investigators must wear mask to perform the experiments to fulfill the laboratory safety regulations.

13. Turn off the town gas control valve immediately when the experiment completed. Turn on the lighting system and smoke extraction fans to provide sufficient illumination and extract the smoke from the laboratory. Allow the scale-down model to cool down before cleaning for the model was performed. People should be kept away from the laboratory when the smoke generated were still inside the laboratory.

14. Turn off the tungsten lamps, take off the film from the camera for recorded and cleaning for the scale-down model when it is cool-down. Ensure all the inner surface and the outer surface were clean with fresh water and dry naturally. The scale down model was then ready for the next experiments.

15. Repeated experiments would be done to get an average values.

16. In performing each experiment, laboratory safety officer must be standby in the laboratory to ensure the experiment was performed in safe condition.

Chapter 5 Experimental Results

This chapter presents the experimental results obtained from the experiments of smoke movement in the scale down vertical shaft. The first part of this chapter presents the observation of different experiments. The second part of this chapter reports the investigation results of transient plume front for the cases concerned and the third part of this chapter presents the proposed correlation equations developed from the experimental results to determine the position of the transient plume front in a vertical shaft.

Smoke spreading pattern

Smoke spreading pattern were recorded with photographs taken by camera in proper settings. The settings and the procedures of taking photographs were presented in the Chapter 4. The scanned images were analyzed with aided by computer software. For different cases, typical photographs on the smoke patterns in the scale model were shown in Figure 4.2 to 4.7. The smoke spreading patterns for different cases were observed. The rate of smoke rise and sink were recorded and the position of the plume front inside the closed scale-down model in different height ratios studied. The smoke were found rise and also sink in vertical motion as shown in the figures.

The smoke generated was found accumulated first and then spread in descending rate or ascending rate at the vertical direction throughout the scale-down model. The smoke spreading patterns for different cases were described in the following paragraphs.

Case A

In this case, the smoke started spreading through the scale-down model from a room compartment model through the vertical opening, where the opening base at the height ratio H_R=0. The smoke generated from the smoke pellet firstly accumulated in the room compartment model, the smoke then spread inside the scale-down model from the room compartment to the lowest part of the scale-down vertical shaft through the opening between these two compartments. The smoke spread rapidly at the first few seconds and then rose in a quite steady rate. When the scale-down model was about 70% filled up, the rate of smoke rise slowed down. The smoke accumulated horizontally first and then rose slowly. The visibilities of smoke were found similar throughout the vertical shaft during the experiment.

Samples of the smoke spreading patterns were captured form the photographs and shown in the Figure 4.2.

Case B

As shown in Figure 4.3, the fire were started at the bottom of the scale model. The smoke was generated from the smoke pellet when it was ignited. The smoke spreading patterns were similar to case A. The smoke spread from the smoke pellet to upward direction to fill up the vertical shaft. At the beginning, it rose at a rapid rate. The visibility of the smoke was not significant as compared with the later stage of the smoke filling process. A few seconds after the smoke was generated, the rate of smoke rise slowed down. This reflected the decrease in velocity of smoke run. The visibility of the smoke became significant as smoke accumulated. The color of smoke was changed from diluted milky white color to milky white color.

The smoke tended to accumulate in horizontal position first and then rose slowly in the upward direction in vertical position. When the smoke was near to fill up the whole vertical shaft, the smoke spreading rate slowed down.

Case C

In this case, the smoke started spreading to the scale down model from the room compartment at the height ratio H_R=0.29. The smoke filling process could be described in two stages. The smoke generated from the smoke pellet was accumulated in the room compartment model first, and then it started to spread through the scale down model from the room compartment model, through the vertical opening between the two compartments. The smoke rose and filled up the upper part of the scale-down model and also sank to fill up the lower part of the scale-down model. The smoke rose up in a steady filling rate. On the other hand, the smoke started to sink in a slow filling rate. At the first few seconds, the smoke was found rise but the rate of smoke sink was not significant. As time goes on, the smoke keep on rising and sinking to fill up the upper part and the lower part of the scale-down model.

From the observations, the time for smoke to fill up the upper part of the vertical shaft and the time for smoke to fill up the lower part of the vertical shaft were nearly the same although it is in small values of height ratio. It was observed that the smoke traveling speed for smoke move upward was much faster that the smoke move downward. Especially in the very beginning of the experiment, the smoke sank in a very slow filling rate. Until the smoke rose and filled up the scale-down model at a certain percentage, the rate of smoke sink became significant.

Samples of the smoke spreading patterns were captured from the photographs and shown in the Figure 4.4.

Case D

The fire were made in a room compartment model adjacent to the vertical shaft at a height ratio H_R=0.5. The smoke spread from the room compartment model to the scale-down model through the vertical opening. The smoke spreading pattern inside the scale-down vertical shaft could be mentioned in two stages. The smoke generated from the smoke pellet and accumulated the room compartment model at first.

When the smoke spread through the opening to the vertical shaft, it rose and filled up the upper part of the scale down model and sank to fill up the lower part of the scale down mode at a slow filling rate.

It was observed that in the first few seconds, the smoke rose in a significant filling rate. The rate of smoke rise in the upward direction was fast at that time. At the same time, the smoke sank to the lower part of the scale model in a comparatively slower filling rate. The velocity of smoke in downward direction was comparatively slower.

Few seconds later, the upper part of the scale-down model was totally filled up by the smoke. The visibility of smoke became significant and the smoke inside the vertical shaft seem to be accumulated. At that time, the smoke keep on sinking to the lower part of the scale down model and the filling rate became more significant. It was observed that the smoke accumulated at the upper part of the closed shaft, and the smoke keep on generated from the smoke pellet inside the room compartment.

The rate of smoke sink in downward was found significant. The smoke filling process completed until the whole vertical shaft was filled up with smoke.

Samples of the smoke spreading patterns were captured from the photographs and shown in the Figure 4.5.

Case E

In case E, the smoke spread throughout the scale-down model from the fire made at the room compartment to the vertical shaft at a height ratio H_R=0.71. In this case, the smoke rose and filled up the upper part of the scale-down model in few seconds only. The velocity of smoke rise was observed very fast. After the smoke accumulated the upper part of the scale down model, the smoke spreading movement towards the lower part of the scale down model became significant. The reason is that the upper part of the scale down model was filled up with smoke. The smoke generated from the room model sank to the lower part of the scale down model. The smoke sank in a slow filling rate at first, and the rate of smoke sink became steady when the upper part of the scale-down model was filled up with smoke. As time goes on, the rate of smoke sink slowed down. The smoke filling process completed until the whole vertical shaft was filled up.

In this case, it can be observed that the filling process of the upward moment of the smoke is more significant than the downward moment of the smoke. The smoke accumulated at the upper part of the scale-down model would help to accelerate the downward moment of the smoke inside the scale-down model.

Samples of the smoke spreading patterns of this case were captured from the photographs and shown in the Figure 4.6.

Case F

In case F, the smoke started spreading to the scale-down model from the highest most opening at H_R=0.93. The smoke started spreading in the downward direction just after the smoke was spread into the scale-down vertical shaft from the room compartment model.

The smoke generated from the smoke pellet accumulated the room compartment at first, the smoke then spread inside the scale-down model from the room compartment to the highest part of the scale-down vertical shaft and started spreading through it. The smoke spread rapidly at the first few seconds and then spreading rate slowed down. And it was happened when the scale-down model was about 70% filled up. The smoke accumulated horizontally first and then sank slowly. Finally, it spread through the scale-down model and filled it up. The visibilities of smoke were found similar throughout the vertical shaft during the experiment.

Samples of the smoke spreading pattern for this case were captured from the photographs and shown in the Figure 4.7.

The observation of the experiments was presented in the above paragraphs. The recorded positions of plume front as in photographs taken were plotted graphically for subsequent analysis. For each case, five heat release rates of fire were plotted. For each of the heat release rates, results of the repeated experiments were shown in figures. The average values of the plume front position were measured and plotted graphically and described on the following sections.

In general, the transient plume fronts were spread in two directions. The first part was the upward movement of the smoke and the second part was the downward

movement of the smoke. In case A and case B, smoke spread in the upward movement only. For case C, case D and case E, smoke spread in the upward movement and also in downward movement. In case F, The smoke spread in the downward movement only.

Upward movement of smoke

The upward movement of smoke inside the scale-down model for different cases were studies in this section. They were happened in case A to case E.

Case A

The heights of transient smoke fronts were plotted against time for case A were shown in the Figure 4.8. The heights of transient smoke fronts for the first three seconds were not shown in graph as the smoke generated from the bottom of the scale-down model at the first few seconds was unable to determine, as the position of the plume front was unclear. The height of transient smoke front after the third second were plotted against time and shown in the figure.

As shown in the figure, the heights of the transient smoke front increased corresponding to time. Results from scale modelling studies by Fujita et. al. (1998) with verifications using full scale experimental data were shown for comparison. A good agreement was found between the studies. This confirmed the validity of the experimental techniques adopted for the current study. In comparing with different heat release rates for the first fifteen seconds, the smoke filling rate was found similar especially for the heat release rates of 28.7 W, 43.1 W and 86.2 W. The time required for smoke to fill up the scale-down model was found inversely proportional to the heat release rates from 8.6 W to 43.1 W.

The shortest time needed to fill up the whole scale-down model was recorded in heat release rate of 8.6 W where the time needed to fill up the whole scale-down model in heat release rate 43.1 W was the longest.

Case B

As shown in Figure 4.9, the heights of transient plume front for this case were plotted graphically from the second second of ignition.

For different heat release rates of fire, the trends of smoke rise were similar. The time for the smoke to fill up the scale down model was found to be inversely proportional to the heat release rates, except the case with heat release rate of 43.1 W. It found that the gradient for time from the fifth second to the thirteenth second for heat release rates of 8.6 W, 28.7 W, 43.1 W, 57.5 W and 86.2 W were 0.0475 m/s, 0.0436 ms^{-1}, 0.0413 ms^{-1}, 0.0563 ms^{-1} and 0.06 ms^{-1} respectively. It shown that the velocity of small heat release rate were similar. When heat release rate increase, the velocity of smoke also increase in this time interval.

In general, the time for smoke to fill up the whole scale-down model was fast, it takes twenty-two seconds for smoke to fill up the shaft for the heat release rate of 86.2W. The longest smoke filling time was thirty-two seconds for the heat release rate of 8.6 W.

In comparing with case A, the smoke spreading patterns were generally similar. The time required for smoke to fill up the scale-down model for case A was shorter in comparing with this case.

Case C

The heights of transient plume front were plotted against time as shown in Figure 4.10. The transient smoke fronts could be divided into two parts. The first part is the smoke rising part where the second part is the smoke sinking part. The smoke spread from a room compartment model at height ratio H_R=0.29 and then spread to the vertical shaft through the vertical opening. The opening in which connected to the room model and the vertical shaft was 0.1 metre in height. The heights of transient smoke front started from 0.5 metre height was shown in the figure.

For the rising part of the smoke movement, the rate of smoke rise for different heat release rates were similar. As shown in the figure, for the first ten seconds, the rate of smoke rise were nearly the same for different heat release rates. For the next ten seconds, different in rate of smoke rises were found. In general, the smoke filling time for different heat release rats were similar. It took twenty one seconds to fill up the vertical shaft for heat release rate of 86.2 W and twenty four seconds to the case for heat release rate of 8.6 W.

Case D

In this case, the smoke spread from the room compartment to the scale-down vertical shaft at a height ratio H_R=0.5 as shown in Figure 4.11. The smoke filling process were divided into two parts. The rising part and the sinking part in which the division line is on H_R=0.5 as shown in the figure. The time for smoke rise was much shorter in comparing with the sinking time.

For the case of heat release rate 86.2 W, it took ten seconds to fill up the upper part of the scale-down vertical shaft. The time to fill up the upper part of the scale-down

vertical shaft was inversely proportional to the heat release rates, except the case for heat release rate 43.1 W as shown on the figure. In general, the smoke traveling times for filling up the upper part of the scale-down model were fast compared with the filling time for the lower part. It only took ten seconds for fire of heat release rate 86.2 W to fill up the whole upper part of the vertical shaft, and fourteen seconds for heat release rate 8.6 W to fill the same position of the vertical shaft.

Case E

The smoke spread from the room compartment model to the scale-down vertical shaft through the vertical opening at height ratio H_R=0.71 in this case as shown in Figure 4.12. The smoke rose to fill up the upper part of the scale down vertical shaft and also sank to fill up the lower part of the scale-down vertical shaft. The time for smoke rose up was much faster than that the smoke sank.

In general, the smoke rising rates for different heat release rates were found similar. The smoke filling up time for different heat release rates were similar too. It took seven to eight seconds for the smoke to fill up the upper part of the scale-down vertical shaft of different heat release rates. As the smoke filling time for different heat release rates were similar, there were no significant different observed in filling processes between different heat release rates.

Observations of upward movement of smoke

Upward movement of smoke were found in case A, case B, case C, case D and case E. General speaking, for the five different heat release rates, the time required for the smoke to fill up the upper part of the vertical shaft were found inversely

proportional to the heat release rates. It can be fond in case A, case B, case C and case D.

It was observed that the rate of smoke rise for the filling up process were decreasing. That means the velocity of the smoke filling decreased as time goes on throughout the filling process. It can be found in case B, case C and case D.

It was observed that the smoke start to rise inside the vertical shaft just after the smoke spread through the compartment openings to the vertical shaft for all cases. The smoke filling process for the first few seconds were found rapid for all cases.

Downward movement of smoke

The downward movements of plume front inside the scale-down model for different cases are presented in this section. Generally speaking, the downward movements of smoke for different cases were not significant at the beginning of the experiments. The downward movements were significant for different fire sizes as the smoke spread further. The following section present the downward movement of smoke for different cases.

Case C

The transient smoke front for downward moment of smoke were plotted and shown in the Figure 4.10. The rate of smoke sink was inversely proportional to the heat release rates. The downward movement at the first few seconds was not of experimental significance. At the time of the eighth second, the velocity became faster for different heat release rates as shown in the figure. The rate of smoke sink

increased until the whole scale-down model was filled up for different heat release rates.

It took seventeen seconds for smoke to fill up the lower part of the scale-down vertical shaft for the case of heat release rate 86.2 W, and twenty one seconds to fill it up for the case of heat release rate 8.6 W.

Case D

The transient smoke front for downward moment of smoke were plotted and shown in figure 4.11 for this case. The downward moment of smoke to fill up the lower part of the scale-down model took longer time than the upward moment of smoke to fill up the upper part of the scale-down model.

The time to fill up the lower part of the scale-down vertical shaft was inversely proportional to the heat release rates except the case of heat release rate 43.1 W. For the case of heat release rate 86.2 W, it took twenty five seconds to fill up the lower part of the scale-down vertical shaft and twenty nine seconds to fill it up for the case of heat release rate 8.6 W.

The rates of smoke sink at the beginning for different heat release rates were found not significant. Few seconds later, the rate of smoke sink increased. The filling processes completed until the lower part of the vertical shaft were filled up.

Case E

The transient smoke front for downward moment of smoke were plotted and shown in figure 4.12. In general, it took much longer time for smoke to fill up the lower

part of the scale-down model than that the upward moment of smoke to fill up the upper part of the scale-down model.

The smoke spreading rate in the downward moment for the first few seconds was not significant. At about the ninth seconds, the rate of smoke sink increased. It happened in all heat release rates. The rate of smoke sink became steady as time goes on and the filling processes completed until the whole vertical shaft were filled up with smoke. The times needed for the different heat release rates to fill up the scale-down model were found similar. It took thirty one seconds for case of heat release rate 86.2 W to fill up the lower part of the scale-down vertical shaft and thirty four seconds for case of heat release rate 8.6 W to fill it up.

- ***Case F***

In this case, the smoke spread from the room compartment to the scale-down vertical shaft form at height ratio H_R=0.93. The smoke spread from the upper most position inside the scale-down vertical shaft to the lower part of the scale-down vertical shaft. As shown in the figure 4.13, the time for smoke to fill up the whole scale-down model were inversely proportional to the heat release rates except the case for heat release rate 43.1 W.

In this case, the smoke spread into the scale-down vertical shaft was found significant at the beginning. The smoke filling rates were quite steady throughout the experiment for different cases. It took thirty seconds to fill up the whole scale-down vertical shaft for the case of heat release rate 86.2 Wand thirty five seconds to fill it up for the case of heat release rate 8.6 W.

Observations of downward movement of smoke

Downward movement of smoke were found in case C, case D, case E and case F. In general, the followings observations were found for those cases.

It was observed that the times required for smoke to fill up the lower part of the vertical shaft were found inversely proportional to the heat release rates. It can be found in case C, case D and case F.

It was observed that the downward movement of smoke were not significant at the beginning of the experiments for all cases as shown on different figures.

It was observed that the rate of smoke sink were quite steady. It can be found in case E and case F.

Non-dimensional height

In the experiments, five constant heat release rates were used in each case. By equation (2.46), $\hat{t}$ was found to be 1.91 t, 2.85 t, 3.27 t, 3.60 t and 4.12 t respectively for the five heat release rates.

A parameter $\hat{y}_1$ is defined for presenting the plume front moving upward inside the scale-down vertical shaft, the compartment height H_C (m) is used to evaluated the non-dimensional distance, i.e.,

$$\hat{y}_1 = \frac{(y - H_c)}{D} \qquad \ldots (5.1)$$

Another parameter $\hat{y}_2$ is proposed for presenting the plume front moving downward inside the scale-down vertical shaft, the compartment height H_C (m) is used to evaluated the non-dimensional distance, i.e.,

$$\hat{y}_2 = \frac{(H_c - y)}{D} \qquad \ldots (5.2)$$

where D is the hydraulic mean depth of the model base and given in equation (2.64)

Position of plume height

Correlation relationships for the smoke traveling time were determined with the experimental results. This section presents the mathematic model proposed.

The values of $\hat{t}$ were plotted against $\hat{y}$ for case A and shown in Figure 5.1. The results of Fujita et al. (1998) given by equation (2.65) were also plotted. A correlation equation with correlation coefficient 0.85 found:

$$\hat{t} = 8.66\ \hat{y}^{2/3} \qquad \ldots (5.3)$$

For case B, the results of $\hat{t}$ were plotted against $\hat{y}$ in Figure 5.2. Correlation equations for $\hat{t}$ and $\hat{y}$ were found with correlation coefficients of 0.85 and 0.88 respectively:

$$\hat{t} = \begin{cases} 7.9\ \hat{y}^{2/3} & ; \quad \hat{y} < 2.5 \\ 4.3\ \hat{y}^{7/6} & ; \quad \hat{y} \geq 2.5 \end{cases} \qquad \ldots (5.4)$$

For case C, case D and case E, the values of $\hat{t}$ were plotted against $\hat{y}_1$ for smoke front moving upward inside the shaft model as shown in Figure 5.3, Figure 5.4 and

Figure 5.5. Correlation equations were derived from the measured results for H_R of 0.29, 0.5 and 0.71 with correlation coefficients 0.88, 0.79 and 0.84 respectively.

$$\hat{t} = \begin{cases} 0.943\hat{y}_1^{1.64} & ; \quad H_R = 0.29 \\ 1.81\hat{y}_1^{1.35} & ; \quad H_R = 0.50 \\ 2.63\hat{y}_1^{1.23} & ; \quad H_R = 0.71 \end{cases} \quad \ldots (5.5)$$

The results of case A were plotted together with the three cases in the Figure 5.6 for comparison. The traveling time for the smoke front moving upward inside the scale-down shaft model could be significantly increased with higher height ratio H_R. It is observed that the non-dimensional time $\hat{t}$ is about three times longer for H_R=0.71 than for H_R=0 at the early stage of smoke movement.

For the smoke front moving downward inside the scale-down shaft model, the values of $\hat{t}$ were plotted against $\hat{y}_2$ as shown in Figure 5.7, Figure 5.8 and Figure 5.9 for case C, case D and case E. Correction equations were derived form the measured results for H_R of 0.29, 0.5 and 0.71 with correction coefficients 0.78, 0.76 and 0.73 respectively.

$$\hat{t} = \begin{cases} 30.4\hat{y}_2^{0.4} & ; \quad H_R = 0.29 \\ 27.4\hat{y}_2^{0.5} & ; \quad H_R = 0.50 \\ 21.0\hat{y}_2^{0.58} & ; \quad H_R = 0.71 \end{cases} \quad \ldots (5.6)$$

Correlation equations was derived from the measured results for H_R of 0.93 with correlation coefficient 0.91.

$$\hat{t} = 8.93\ \hat{y}^{0.82} \qquad \ldots (5.7)$$

The results of case F were plotted in the Figure 5.10 and also plotted together with the three cases in the Figure 5.11 for comparison.

The traveling time for the smoke front moving downward inside the vertical shaft model could be significantly increased with lower height ratios H_R. It is observed that the non-dimensional traveling time $\hat{t}$ for H_R=0.93 is half of that for H_R=0.29 at the early stage of smoke movement.

The correlation equations (5.3) to equations (5.7) are proposed to determine the transient plume front position in vertical shaft in case of fire.

Chapter 6 Discussion

The correlation relationships of the non-dimensional time and the non-dimensional smoke front heights were found for different cases in the Chapter 5. They are applicable to the smoke filling process in vertical shafts in highrise buildings in real case and would be demonstrated in this chapter. Six cases were considered in the experiments, they are the fire happened at the bottom of vertical shaft, fire happened in a room adjacent to the vertical shaft at three height ratios, and fire happened in a room adjacent to the top most level of the vertical shaft.

General speaking, the smoke filling processes were due to the vertical motions of smoke inside the vertical shaft. The equations (5.3) to (5.7) developed in last chapter can be applied to determine the transient position of plume front in vertical shaft at different fire sizes at the designated fire locations. Examples on applying the equations in buildings are discussed in this chapter.

In this chapter, different configurations of vertical shaft are demonstrated. Figure 6.1 shows the different configurations of vertical shaft concerned. Through the demonstrations, the time for the smoke front to fill up the vertical shaft in different dimensions, different height ratios and different configurations can be determined easily with the proposed mathematical expressions developed.

Example cases

Different cases were considered in developing the empirical correlations as described in the last chapter. Example cases were selected to demonstrate here to show the application of the mathematic expressions. They are applicable to various types of vertical shafts inside buildings such as lift shafts, ventilation shafts, light wells,

refuse tubes, pipe ducts and cable ducts, those are common features in highrise buildings in Hong Kong. As an example, a lift shaft having a single lift car would have a vertical lift shaft with a square base. Example of smoke spreading inside an individual lift shaft were demonstrated in case 1. In addition, for the cases that having more than one service lifts with a common lift shaft, it could be formed in other shape. Therefore, cases for doubling and tripling the base length of the lift shafts were considered in other examples.

Different in height of building also reflected to different in height of vertical shafts inside the building. Taking lift shaft as an example, it is highly dependent on where the building levels served by the lift car. In general, the vertical lift shaft for high zone lifts would have a similar height to the building if the service lift served from the ground floor level to the top most floor. And the buildings of increasing height are recently reported in Hong Kong. Cases of different shaft heights were also considered. In modern buildings, vertical shafts with larger area could also be found. The vertical shafts with variations area of shaft base were considered in the later part of this chapter as well.

The cases demonstrated were summarized in Figure 6.1 and Table 6.1.

For the different cases concerned as stated in the above paragraphs, results have been obtained in applying the proper correlation equations. Table 6.1 shows the different cases concerned with the relative non-dimensional heights at different height ratios. The non-dimensional height and the non-dimensional time for different cases are determined and shown on Table 6.2. Tables 6.3 and 6.4 show the result of smoke traveling time for different cases at different height ratio for a designed fire of 5MW and 10MW.

Case 1: H_R=0

Example case 1 is referred in this section. For a large fire happened in an old highrise building in late 1997 (South China Morning Post 1996; Ming Pao 1996; Hong Kong Standard 1997), the fire was suspected to start from a lift shaft which was under refurbishment. Because of the construction work, all the lift doors in that lift shaft were removed with the vertical openings sheltered by temporary plywood partitions. The fire started from the lift shaft with nobody paying attention to it at the early stage. For this large fire, case B was believed to be one of the possible scenarios. Equation (5.4) derived in this study is applicable to determine the probable smoke traveling time. The dimension of the lift shaft is 2.3 m (length) x 2.3 m (width) x 48 m (height). Therefore, with the application of Equation (2.64), the hydraulic diameter D^* of the shaft is,

$$D^* = 2.3m \quad \ldots (6.1)$$

Applying equation (2.45), The non-dimensional height $\hat{y}$ of the shaft:

$$\hat{y} = 20.9 \quad \ldots (6.2)$$

Applying the Equation (5.4)

$$\hat{t} = 149\text{s} \quad \ldots (6.3)$$

The non-dimensional time $\hat{t}$ of 149 seconds for the smoke front to travel from the bottom to the top of the lift shaft is determined. For a design fire of 5 MW, with Equation (2.46) and Equation (2.47),

$$\hat{t} = 1.68\ \text{t} \quad \ldots (6.4)$$

This means that smoke supported by a 5 MW fire in a compartment adjacent to the shaft base could take 88 seconds to reach the top. Smoke could then spread to the adjacent levels if the doors are opened to the lift shaft. The example case showed the smoke traveling time for smoke from the fire to the top of the shaft with applying the experimental results.

Case 2: H_R=0.5

Last section presented an real case example for smoke traveling time with known fire size happened at the bottom of the lift shaft. The equations derived can also be applied to other case with different height ratios. The Equation (5.5) and Equation (5.6) can be applied to a fire happened at a height ratio H_R=0.5. The smoke movement can be considered in two parts: The first part is the rising part and the second part is the sinking part. For the same design fire in the last example happens in a compartment at height ratio H_R=0.5, the applications of the derived equations are detailed. The dimension of the lift shaft was 2.3 m (length) x 2.3 m (width) x 48 m (height). Therefore, the hydraulic diameter D^* of the shaft:

$$D^* = 2.3m \quad \ldots (6.5)$$

The non-dimensional height $\hat{y}_1$ and $\hat{y}_2$ of the shaft:

$$\hat{y}_1 = \hat{y}_2 = 10.4 \quad \ldots (6.6)$$

and

Applying the Equation (5.5) and Equation (5.6),

$$\hat{t} = 1.81\ \hat{y}_1^{1.35} \quad ,H_R=0.5 \quad \ldots (6.7)$$

and

$$\hat{t} = 27.4\ \hat{y}_2^{0.5} \quad ,H_R=0.5 \qquad \ldots (6.8)$$

therefore,

$$\hat{t} = 42.7 \text{ s (upward movement of smoke)} \qquad \ldots (6.9)$$

and

$$\hat{t} = 88.4 \text{ s (downward movement of smoke)} \qquad \ldots (6.10)$$

That means, it would take non-dimensional time τ of 42.7 seconds for the smoke front to travel from H_R=0.5 to the top of the lift shaft and 88.4 seconds for the smoke front to travel from H_R=0.5 to the bottom of the lift shaft. For a design fire of 5 MW, applying Equation (2.46) and Equation (2.47),

$$\hat{t} = 1.68\ t \qquad \ldots (6.11)$$

This means that smoke generated from the 5 MW fire in a compartment at a height ratio H_R=0.5 could take 25.4 seconds to reach the top and 52.6 seconds to reach the bottom.

Further cases

A summary of results for different cases in Table 6.1 is tabulated in Table 6.3 and Table 6.4. Shaft configuration is found to be a parameter to determine the smoke traveling time. The results are demonstrated in the following sections.

Length of the vertical shaft

The vertical shafts concerned in case 1, case 5, case 9 and case 13 are of square base where the other cases are of rectangular base. For case 1, the length and width of the vertical shaft are 2.3 metre and in height 48 metre. The traveling time for upward smoke to fill up the vertical shaft at H_R=0 is 88 seconds. If the length of lift shaft changes to 4.6 metre, with the same width and height, the traveling time for upward smoke to fill up the vertical shaft become 92 seconds, i.e. 4 seconds more. If shaft length is tripled, the corresponding smoke filling time is 94 seconds.

For the downward movement of smoke, the traveling time of smoke to fill up the vertical shaft is 63 seconds, 74 seconds and 78 seconds corresponding to 2.3 metre, 4.6 metre and 6.9 metre in length of the vertical shaft, respectively.

The results showed that the time for smoke to fill up the vertical shaft is directly proportional to length of vertical shaft both in upward smoke movement and downward smoke movement. For the upward smoke movement, there were 4.5% and 6.8% percentage difference for doubling and tripling the length of vertical shaft. On the other hand, the percentage different were 17.5% and 23.8% for doubling and tripling the length of vertical shaft in downward moment of smoke. It shows that the downward movement of the smoke inside the vertical shaft is influenced by the length of vertical shaft much more than the upward smoke movement inside the vertical shaft.

Height of the vertical shaft

In case 1, case 5 and case 9, the width and the length of the vertical shaft are kept no change. But the height of the vertical shafts are doubled and tripled in height. The

upward traveling time of smoke in H_R=0 are 88 seconds, 207 seconds and 333 seconds corresponding to 48 metre, 96 metre and 144 metre in height. The percentage changes are 135% and 278% for case of doubling and tripling the height.

The downward traveling time of smoke in H_R=0.93 were 64 seconds, 113 seconds and 157 seconds corresponding to 48 metre, 96 metre and 144 metre in height. The percentage changes are 76% and 145% for case of doubling and tripling the height. It is observed that the time required for smoke to travel in upward and downward direction to fill up the vertical shaft is directly proportional to the height of vertical shafts. The rate of increase of the percentage change in upward movement of smoke are found significant than that of downward movement of smoke.

Area of the vertical shaft

For case 4 and 13, the areas of the vertical shaft are the same with the same smoke traveling height, they are also 21.2 metre square in area and 48 metre in height. The results obtain for the case of upward traveling time of smoke in H_R=0 are 95 seconds and 99 seconds. And for case 8 and 14, the vertical shafts also have the same areas and same smoke traveling height. The results obtain for the case of smoke traveling time in H_R=0 are 214 seconds and 222 seconds. For case 12 and 15, the results obtain for case of smoke traveling time in H_R=0 are 343 seconds and 356 seconds.

On the other hand, the results obtain for the case of smoke traveling in H_R=0.93 are 81 seconds and 91 seconds in case 4 and case 13; 143 seconds and 161 seconds in case 8 and case 14; and 200 seconds and 224 seconds in case 12 and case 15.

It is observed that the time for smoke travel in square sized vertical shaft could have a slower fill up times of smoke. The downward movement of smoke are found more significant in compare with the upward movement of smoke in different cases.

Applications of the proposed mathematical expressions in determine the smoke filling time were demonstrated in this chapter. The time needed for upward movement and the downward movement of smoke to fill up a vertical shaft could be determined. The following points are concluded from the demonstrations.

1. The time for smoke to fill up the vertical shaft is directly proportional to length of vertical shaft both in upward movement of smoke and downward movement of smoke.

2. The time required for smoke to travel in upward and downward direction to fill up the vertical shaft is directly proportional to the height of vertical shafts. The increase rate in upward smoke movement is more significant than that of downward smoke movement.

3. The smoke traveling time inside a vertical shaft with square base could have a slower filling up time. The downward movements of smoke are shown to be more significant in comparing with the upward movement of smoke.

Chapter 7 Conclusion

Smoke movement in vertical shafts of highrise buildings was studied experimentally with a physical scale model using scale modelling technique. As stated in Chapter 1, there are large numbers of private building in Hong Kong which can be classified as old highrise buildings. There could be problems on fire safety design, fire services system installed and the fire safety managements inside those building as the requirements on fire services installation were not so strict at 30 years ago. When a fire happened, heat and smoke would spread rapidly to other levels from the fire floor through the vertical shafts inside those buildings. Study of smoke movement in vertical shafts is of the primary concern for the fire safety of the old highrise building in Hong Kong.

Scale modelling techniques for fire research were reviewed and presented in Chapter 2. Scaling factors are important in performing scale models studies. For the experimental studies of smoke movement in vertical shafts, the assumption of neglecting the boundary effect would be inappropriate and cannot be ignored. The Froude number modelling and the Reynolds number modelling techniques cannot be considered in this study. As a result, the scaling parameters with considering the conservation of enthalpy were selected for the experimental study in this research.

Experiments were carried out with fire in a room compartment at different levels adjacent to the vertical shaft. The smoke spreading patterns for different cases were studied in Chapter 5. It was pointed out that the location of the fire would be important in determining the smoke travelling time in vertical shafts. The upward moment and downward moment of smoke inside the closed vertical shaft were studied too. Empirical correlations on the smoke travelling time were derived from

the results. For the correlations derived in case A of this study, a good agreement was found in comparing with the results of Fujita et al. (1998). Practically, these equations could be easily applied for predicting the time of smoke spread inside vertical shafts. They are useful informations for understanding the smoke filling process in vertical shafts.

Applications on different cases were demonstrated in Chapter 6 and different cases of applying the derived empirical correlations were carried out. For the big fire in an old highrise building, Case B was believed to be one of the possible scenarios. Employing the correlations derived in Chapter 5, the non-dimensional time for the smoke to travel from the bottom to the top of the lift shaft was 149 seconds. This means that smoke emitted from a 5 MW fire in a compartment at the bottom would take 88 seconds to reach the top. The information obtained provided a possible smoke travelling time in real case when a probable fire located at a room adjacent to the vertical shaft. The correlations derived can also be applied to any other vertical shafts when the information of that shaft was known.

This study showed that the smoke travelling time in the building vertical shaft is an important concern for fire safety designs. It is recommended that building designers, fire safety engineers and authorities account for the probable smoke travelling time required in the vertical shaft in planning the building evacuation. Proper fire safety management procedures may be adopted by building owners and building management in building maintenance involving the vertical shafts.

In addition, the study could be continued as further higher degree projects. The experimental studies can be continued with more cases in consideration. For example, the cases with different scale-down vertical shaft model, with different heat

release rates and experiments in other height ratios. Further verifications with full scale burning tests for smoke from the adjacent room of a vertical shaft are recommended. More repeated experiments would also be suggested in extended application range of fire sizes. It is possible to introduce other methods of data collection such as video recording in order not to limit the data recorded by the time intervals of taking photographs. For minimizing the error caused by ambient environment, serious experiments with the same settings could be done at the same time if it have enough materials for the experiments. As a conclusion, it would be widen the studies if there are more empirical correlations derived from the experimental results.

List of symbols

A	area (m^2)
C	Constant
c_p	specific heat of air at constant pressure (kJ kg^{-1} K^{-1})
D^*	characteristic length scale of the shaft model (m)
G	acceleration due to gravity (9.81 m s^{-2})
K	thermal conductivity ($kJs^{-1}m^{-1}K^{-1}$)
L	shaft base length (m)
$\hat{Q}$	non-dimensional heat release rate of the fire
Q	heat release rate of the fire (kW)
T	ambient temperature (K)
t	time (s)
V	volume (m^3)
$\hat{v}$	non-dimensional velocity
V	velocity (m s^{-1})
W	shaft base width (m)
$\hat{y}$	non-dimensional height

y	height of smoke moved up (m)
$\hat{t}$	non-dimensional time
μ	viscosity ($kgm^{-1}s^{-1}$)
π	dimensional group
ρ	smoke density ($kg\ m^{-3}$)
ζ	parameter defined in equation (2.30)
Δ	change of

Subscripts

0	initial condition
1, 2, ...	conditions 1, 2, ...
A	of ambient air
M	of scale model
P	of plume
R	of full size building

Superscripts

*	characteristic quantity
^	normalized quantity

References

1. Buildings Ordinance, Chapter 123, Laws of Hong Kong, Hong Kong (1997).

2. Chow, W. K. and Lo, C.W.A. Scale modelling studies on atrium smoke movement and the smoke filling process. Journal of Fire Protection Engineering Vol. 7, No. 2, pp. 55-64 (1995).

3. Chow, W. K. and Wong, W. K. On the simulation of atrium fire environment in Hong Kong using zone models. Journal of Fire Sciences, Vol. 11, No. 1, pp. 3-51 (1993).

4. Chow, W. K. Use of computational fluid dynamics for simulating enclosure fire. Journal of Fire Sciences, Vol. 13, No. 4, pp. 300-334 (1995).

5. Chow, W. K., Fong, N. K., Cui, E., Ho, P. L., Wong, L. T., Huo, R., Fan, W. C., Li, Y. Z., and Yuan, L. M. PolyU/USTC atrium: a full-scale burning facility – preliminary experiments. Journal of Applied Fire Science, Vol. 8, No. 3, pp. 229-241 (1998).

6. Chow, W.K., Numerical studies on recent large high-rise building fire, ASCE Journal of Architectural Engineering, Vol. 4, No. 2, pp. 65-74 (1998).

7. Chow, W.K., Preliminary studies of a large fire in Hong Kong, Journal of Applied Fire Science, Vol. 6, No. 3, pp. 243-268 (1997).

8. Chow, W.K., Wong, L.T. and Kwan, Eric C.Y., A proposed fire safety ranking system for old highrise buildings in the Hong Kong Special Administrative Region, Fire and Materials, Vol. 23, No. 1, pp. 27-31 (1999).

9. Cooper, L.Y. Simulating smoke movement through long vertical shafts in zone-type compartment fire models, Fire Safety Journal, Vol. 31, No. 2, pp. 85-99, (1998).

10. De Smedt, J. C. and Morgan, H. P. Achieving fire safety where a prescriptive code of practice could not be applied. Proceedings of the First International Symposium on Engineering Performance-Based Fire Codes. 8 September 1998. Ed. Chow WK, The Hong Kong Polytechnic University, Hong Kong (1998).

11. Drysdale, D.D., Interpretation of evidence at the fire scene: The importance of fire dynamics, Proceedings of the Interflam '99 Conference, Edinburgh Conference Centre, Scotland, 29 June – 1 July 1999, Edited by Grayson, S., Interscience Communications Limited, London, UK, p. 233-244 (1999).

12. Fire Daily News, Report from the Fire Services Department on the preliminary investigation of the Garley Building, 14 December (1996).

13. Friedman, R., An international survey of computer models for fire and smoke, Journal of Fire Protection Engineering, Vol. 4, No. 3, pp. 81-92 (1992).

14. Fujita, T., Yamaguchi, J. and Tanaka, T., Investigation into travel time of buoyant fire plume fronts, Proceedings of the First International Symposium on Engineering Performance-Based Fire Codes, Ed. Chow, W. K., Department of Building Services Engineering, The Hong Kong Polytechnic University, Hong Kong, China, 8 September 1998, pp. 220-228 (1998).

15. Heskestad, G. Physical modelling of fire. Journal of fire and Flammability Vol. 6, pp. 253- 273 (1975).

16. Hong Kong Buildings Department, An introduction to the building safety inspection scheme (1997).

17. Hong Kong Buildings Department, Code of practice for fire resisting construction (1996b).

18. Hong Kong Buildings Department, Code of practice for means of access for firefighting and rescue (1995).

19. Hong Kong Buildings Department, Code of practice for the provision of means of escape in case of fire (1996a).

20. Hong Kong Fire Safety (Commercial Premises) Ordinance, Laws of Hong Kong (1997).

21. Hong Kong Fire Services Department, Codes of practice for minimum fire service installations and equipment and inspection (1998).

22. Hong Kong Standard, 17 January (1997).

23. Hong Kong Standard, 7 January (1998).

24. Lo, S.M., Fire safety design in buildings of Hong Kong: a preliminary view. Asia Pacific Building and Construction Management Journal, Vol. 1 No. 1 pp. 41-50 (1995).

25. Ming Pao, 22 November (1996).

26. Quintiere, J. G. Scaling applications in fire research. Fire Safety Journal, Vol. 15, No. 1, pp. 3-29 (1989).

27. Quintiere, J. G., McCaffrey, B. J. and Rinkinen, W. Visualization of room fire induced smoke movement and flow in a corridor. Fire and Materials, Vol. 2, No. 1, pp. 18-24 (1978).

28. Singtao Daily, 11 December (1997).

29. South China Morning Post, 21 November (1996).

30. South China Morning Post, 9 April (1997).

31. Tanaka, T., Fujita, T. and Yamaguchi, J., Investigation into rise time of buoyant fire plume fronts, International Journal on Engineering Performance-Based Fire Codes, Vol. 2, No. 1, pp. 14-25 (2000).

32. Thomas, P. H., Hinkley, P. L., Theobald, C. R. and Simms, D. L. Investigations into the flow of hot gases in roof venting. Fire research technical paper no. 7, Her Majesty's Stationary Office (HMSO), London, UK (1961).

33. Williams, C., Harrison, R., Morgan, H., Shipp, M. and De Smedt, J. C. In situ acceptance testing of smoke ventilation systems using real fires in the European parliament building. Paper presented in the 2-Day Short Course in An Introduction to Performance-Based Design Procedures for Smoke Control, 9-10 September 1998, Hong Kong. The Hong Kong Polytechnic University, Hong Kong, FRS/IFSET (Asia) Ltd./Fire Research Station, Building Research Establishment, UK (1998).

34. Williams, F. A. Scaling mass fires. Fire Research Abstract and Review, pp. 1-22 (1969).

35. Wong, L.T. Occupant load assessment for old residential high-rise buildings, Architectural Science Review, accepted for publication (2003).

36. Wong, L.T., Chow, W.K. and Kwan, Eric C.Y., A brief review on fire regulations for old highrise commercial buildings in Hong Kong. International Journal on Engineering Performance-Based Fire Codes, Vol. 2, No. 4, pp. 153-160 (2000).

37. Woo, K.W., Final Report of the inquiry into the Garley Building fire on 20 November 1996. Printing Department, Hong Kong (1997).

38. Zukoski, E.E., A review of flows driven by natural convection in adiabatic shafts NIST-GCR-95-679 National Institute of Standards and Technology, U.S. Department of Commence, U.S.A. (1995).

39. Chew, M.Y.L. and Liew, P.H., Smoke movement in atrium buildings. International Journal on Engineering Performance-Based Fire Codes, Vol. 2, No. 2, pp. 68-76 (2000).

40. Klote, J.H. and Milke, J.A., Principles of smoke management. ASHRAE (Atlanata, GA) and SFPE (Boston, MA), U.S.A. (2002).

List of Tables

List of Figures

Table 3.1 Experiment carried out in different heat release rates

Experiments	Heat release rates (W)
Case 1	8.6
Case 2	28.7
Case 3	43.1
Case 4	57.5
Case 5	86.2

Table 3.2 Experiment carried out with different fire locations

Experiments	Fire locations
Case A	In a room compartment placed at the lowest level
Case B	At the bottom of the scale-down model
Case C	In a room compartment placed at height ratio 0.29
Case D	In a room compartment placed at height ratio 0.5
Case E	In a room compartment placed at height ratio 0.71
Case F	In a room compartment placed at height ratio 0.93

Table 3.3 Experiments carried out in different heat release rates and locations

Experiment Number	Heat release rates (W)	Fire locations	Experiment number	Heat release rates (W)	Fire locations
1	case 1	case A	16	case 1	case D
2	case 2		17	case 2	
3	case 3		18	case 3	
4	case 4		19	case 4	
5	case 5		20	case 5	
6	case 1	case B	21	case 1	case E
7	case 2		22	case 2	
8	case 3		23	case 3	
9	case 4		24	case 4	
10	case 5		25	case 5	
11	case 1	case C	26	case 1	case F
12	case 2		27	case 2	
13	case 3		28	case 3	
14	case 4		29	case 4	
15	case 5		30	case 5	

Notes: For case A, case C, case D, case E and case F, the experiments were repeated for three times for each heat release rates.

For case B, the experiments were repeated for four times for each heat release rates.

Table 4.1 The town gas flow rate for different heat release rates

Town gas flowrate (L/s)	Heat release rates $\hat{Q}$ (scale-down) (W)	Heat release rates Q (full-scale) (kW)
0.0005	8.6	43
0.0017	28.7	145
0.0025	43.1	217
0.0042	57.5	290
0.005	86.2	433

Notes: The conversion of heat release rates were based on the Equation (2.47)
The calorific value of town gas is 17.27 MJ/cu. M

Table 6.1 Table of non-dimensional height in different height ratio with different cases

Case nos.	Dimension of the vertical shaft (m)			Hydralic diameter (m)	non-dimensional height (upward)				non-dimensional height (downward)			
	L	W	H		HR=0	HR=0.29	HR=0.5	HR=0.71	HR=0.29	HR=0.5	HR=0.71	HR=0.93
1	2.3	2.3	48	2.3	20.9	14.8	10.4	6.1	6.1	10.4	14.8	20.9
2	4.6	2.3	48	3.1	15.7	11.1	7.8	4.5	4.5	7.8	11.1	15.7
3	6.9	2.3	48	3.5	13.9	9.9	7.0	4.0	4.0	7.0	9.9	13.9
4	9.2	2.3	48	3.7	13.0	9.3	6.5	3.8	3.8	6.5	9.3	13.0
5	2.3	2.3	96	2.3	41.7	29.6	20.9	12.1	12.1	20.9	29.6	41.7
6	4.6	2.3	96	3.1	31.3	22.2	15.7	9.1	9.1	15.7	22.2	31.3
7	6.9	2.3	96	3.5	27.8	19.8	13.9	8.1	8.1	13.9	19.8	27.8
8	9.2	2.3	96	3.7	26.1	18.5	13.0	7.6	7.6	13.0	18.5	26.1
9	2.3	2.3	144	2.3	62.6	44.5	31.3	18.2	18.2	31.3	44.5	62.6
10	4.6	2.3	144	3.1	47.0	33.3	23.5	13.6	13.6	23.5	33.3	47.0
11	6.9	2.3	144	3.5	41.7	29.6	20.9	12.1	12.1	20.9	29.6	41.7
12	9.2	2.3	144	3.7	39.1	27.8	19.6	11.3	11.3	19.6	27.8	39.1
13	4.6	4.6	48	4.6	10.4	7.4	5.2	3.0	3.0	5.2	7.4	10.4
14	4.6	4.6	96	4.6	20.9	14.8	10.4	6.1	6.1	10.4	14.8	20.9
15	4.6	4.6	144	4.6	31.3	22.2	15.7	9.1	9.1	15.7	22.2	31.3

Table 6.2 Table of non-dimensional time in different height ratio with different cases

Case nos.	non-dimensional time (upward) (s)				non-dimensional time (downward) (s)			
	HR=0	HR=0.29	HR=0.5	HR=0.71	HR=0.29	HR=0.5	HR=0.71	HR=0.93
1	149.1	78.4	42.9	24.1	62.5	88.5	100.3	107.9
2	106.5	48.9	29.1	16.9	55.7	76.7	84.9	85.2
3	92.9	40.3	24.8	14.6	53.1	72.3	79.3	77.3
4	86.1	36.3	22.8	13.5	51.8	70.0	76.4	73.4
5	334.7	244.5	109.4	56.5	82.4	125.2	149.9	190.4
6	239.2	152.5	74.2	39.7	73.5	108.4	126.9	150.4
7	208.5	125.7	63.3	34.3	70.1	102.2	118.5	136.6
8	193.4	113.1	58.0	31.7	68.3	99.0	114.1	129.5
9	537.2	475.4	189.1	93.0	96.9	153.3	189.7	265.5
10	384.0	296.6	128.3	65.3	86.4	132.8	160.5	209.7
11	334.7	244.5	109.4	56.5	82.4	125.2	149.9	190.4
12	310.4	219.9	100.3	52.2	80.3	121.2	144.4	180.6
13	66.4	25.2	16.8	10.3	47.3	62.6	67.1	61.1
14	149.1	78.4	42.9	24.1	62.5	88.5	100.3	107.9
15	239.2	152.5	74.2	39.7	73.5	108.4	126.9	150.4

Table 6.3 Table of actual traveling for smoke with different height ratio in fire size=5MW

Case nos.	Dimension of the vertical shaft (m)			actual traveling time* (upward) (s)				actual traveling time*(downward) (s)			
	L	W	H	HR=0	HR=0.29	HR=0.5	HR=0.71	HR=0.29	HR=0.5	HR=0.71	HR=0.93
1	2.3	2.3	48	88.2	46.4	25.4	14.3	37.0	52.4	59.4	63.8
2	4.6	2.3	48	92.5	42.5	25.3	14.7	48.3	66.6	73.7	74.0
3	6.9	2.3	48	94.3	41.0	25.2	14.9	54.0	73.4	80.5	78.6
4	9.2	2.3	48	95.4	40.2	25.2	15.0	57.3	77.5	84.6	81.2
5	2.3	2.3	96	198.1	144.7	64.7	33.4	48.8	74.1	88.7	112.7
6	4.6	2.3	96	207.8	132.5	64.4	34.4	63.8	94.1	110.2	130.6
7	6.9	2.3	96	211.9	127.8	64.3	34.9	71.2	103.8	120.4	138.7
8	9.2	2.3	96	214.1	125.2	64.2	35.1	75.6	109.6	126.4	143.4
9	2.3	2.3	144	317.9	281.3	111.9	55.0	57.4	90.7	112.2	157.1
10	4.6	2.3	144	333.5	257.6	111.4	56.7	75.0	115.3	139.4	182.1
11	6.9	2.3	144	340.0	248.4	111.2	57.4	83.7	127.2	152.3	193.5
12	9.2	2.3	144	343.7	243.5	111.0	57.8	88.9	134.2	159.9	200.0
13	4.6	4.6	48	99.0	37.5	25.1	15.3	70.6	93.3	100.0	91.1
14	4.6	4.6	96	222.2	117.0	64.0	35.9	93.1	132.0	149.5	160.8
15	4.6	4.6	144	356.7	227.4	110.6	59.1	109.5	161.6	189.2	224.2

Table 6.4 Table of actual traveling for smoke with different height ratio in fire size=10MW

Case nos.	actual traveling time* (upward) (s)				actual traveling time*(downward) (s)			
	HR=0	HR=0.29	HR=0.5	HR=0.71	HR=0.29	HR=0.5	HR=0.71	HR=0.93
1	70.0	36.8	20.2	11.3	29.3	41.6	47.1	50.7
2	73.4	33.7	20.1	11.7	38.4	52.8	58.5	58.7
3	74.9	32.5	20.0	11.8	42.8	58.3	63.9	62.4
4	75.7	31.9	20.0	11.9	45.5	61.5	67.1	64.5
5	157.2	114.8	51.4	26.5	38.7	58.8	70.4	89.4
6	164.9	105.1	51.1	27.3	50.6	74.7	87.4	103.7
7	168.1	101.4	51.0	27.7	56.5	82.4	95.6	110.1
8	170.0	99.4	51.0	27.8	60.0	87.0	100.3	113.8
9	252.3	223.3	88.8	43.7	45.5	72.0	89.1	124.7
10	264.7	204.4	88.4	45.0	59.5	91.5	110.6	144.5
11	269.9	197.2	88.2	45.6	66.5	100.9	120.9	153.5
12	272.8	193.3	88.1	45.9	70.6	106.5	126.9	158.7
13	78.5	29.8	19.9	12.1	56.0	74.1	79.4	72.3
14	176.4	92.8	50.8	28.5	73.9	104.7	118.7	127.6
15	283.1	180.5	87.8	46.9	86.9	128.3	150.1	178.0

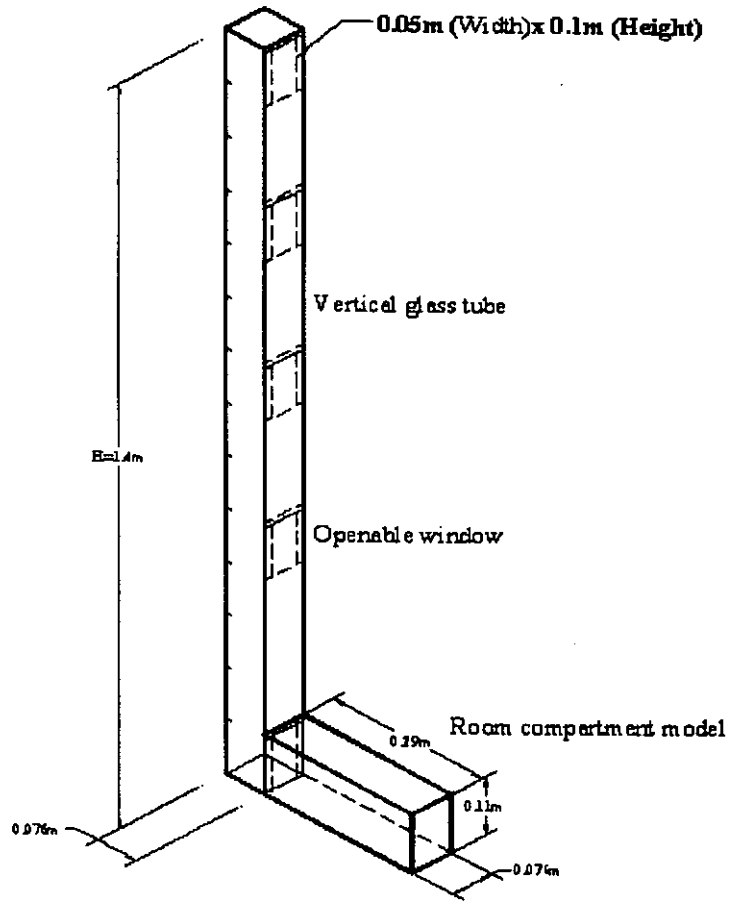

Figure 3.1: Scale-down model

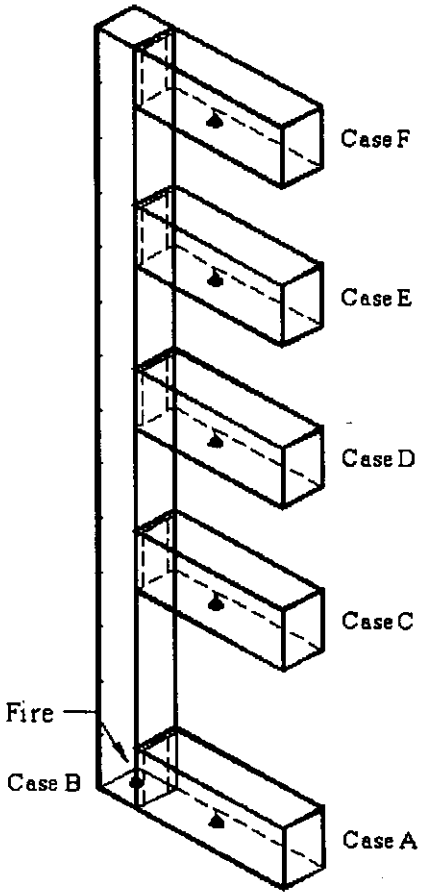

Figure 3.2: Different cases

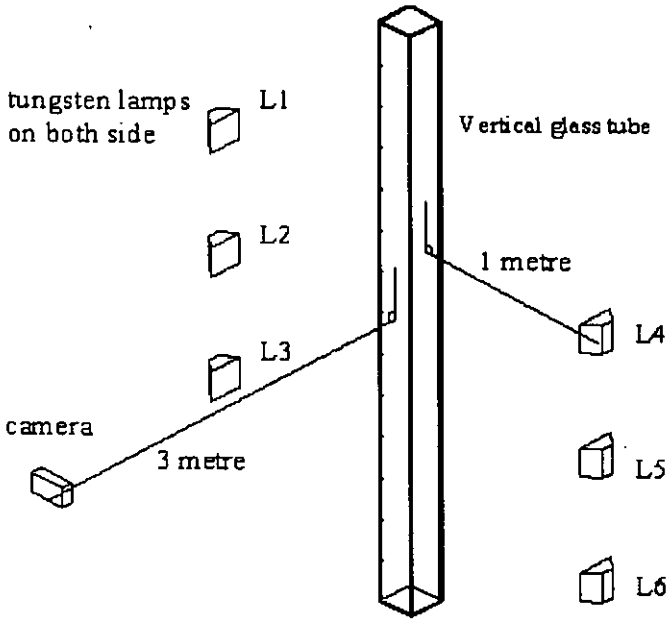

Figure 3.3: Configuration for tungsten lamps and camera

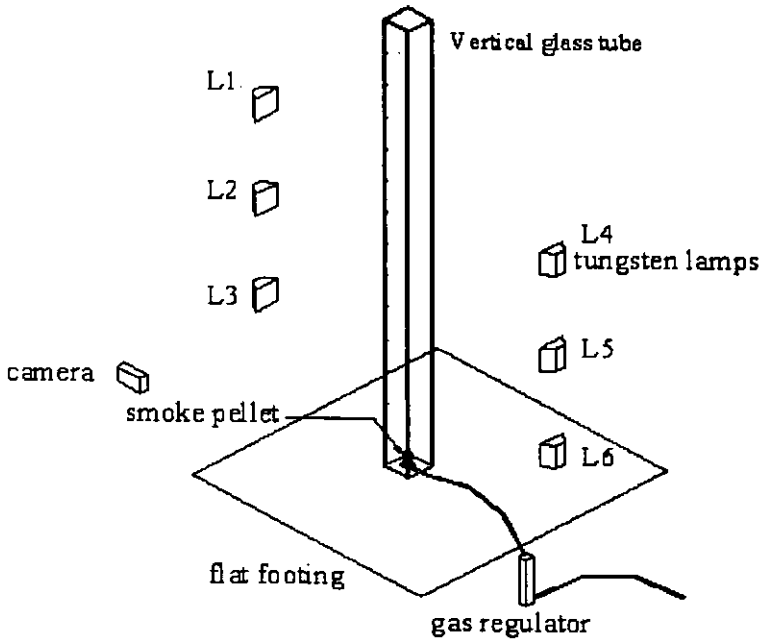

Figure 4.1: Arrangement of experimental equipments

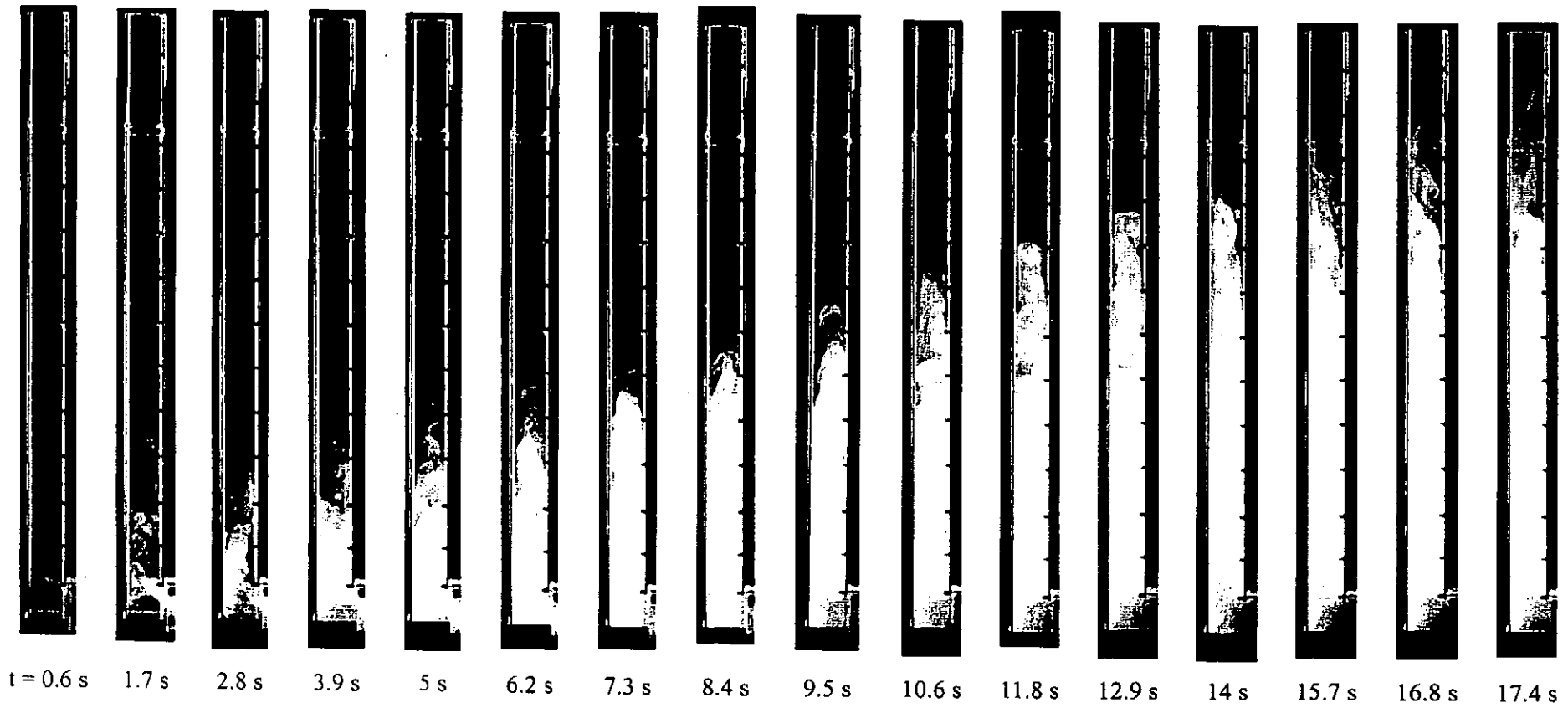

Figure 4.2: Typical photographs of the smoke filling process for case A

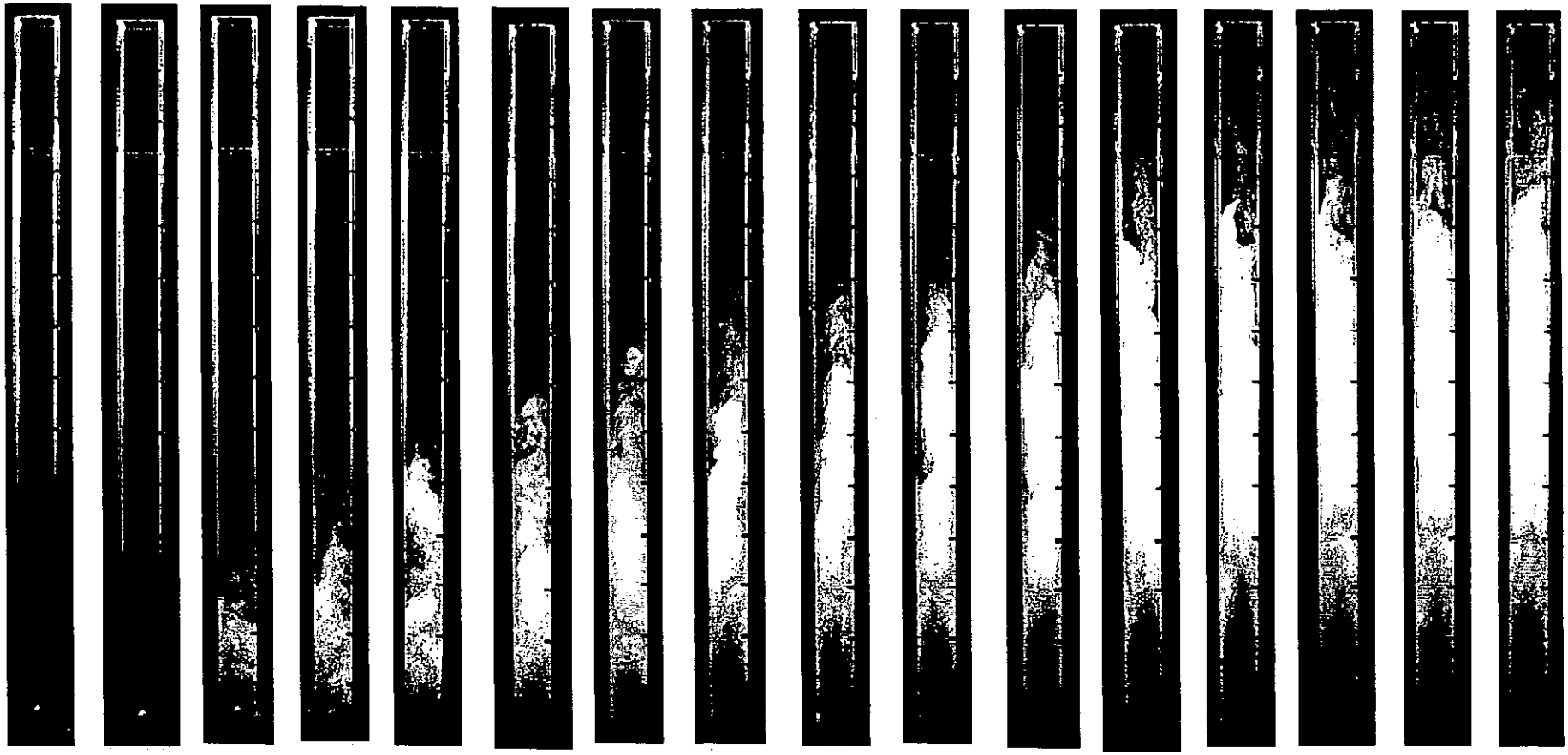

Figure 4.3: Typical photographs of the smoke filling process for case B

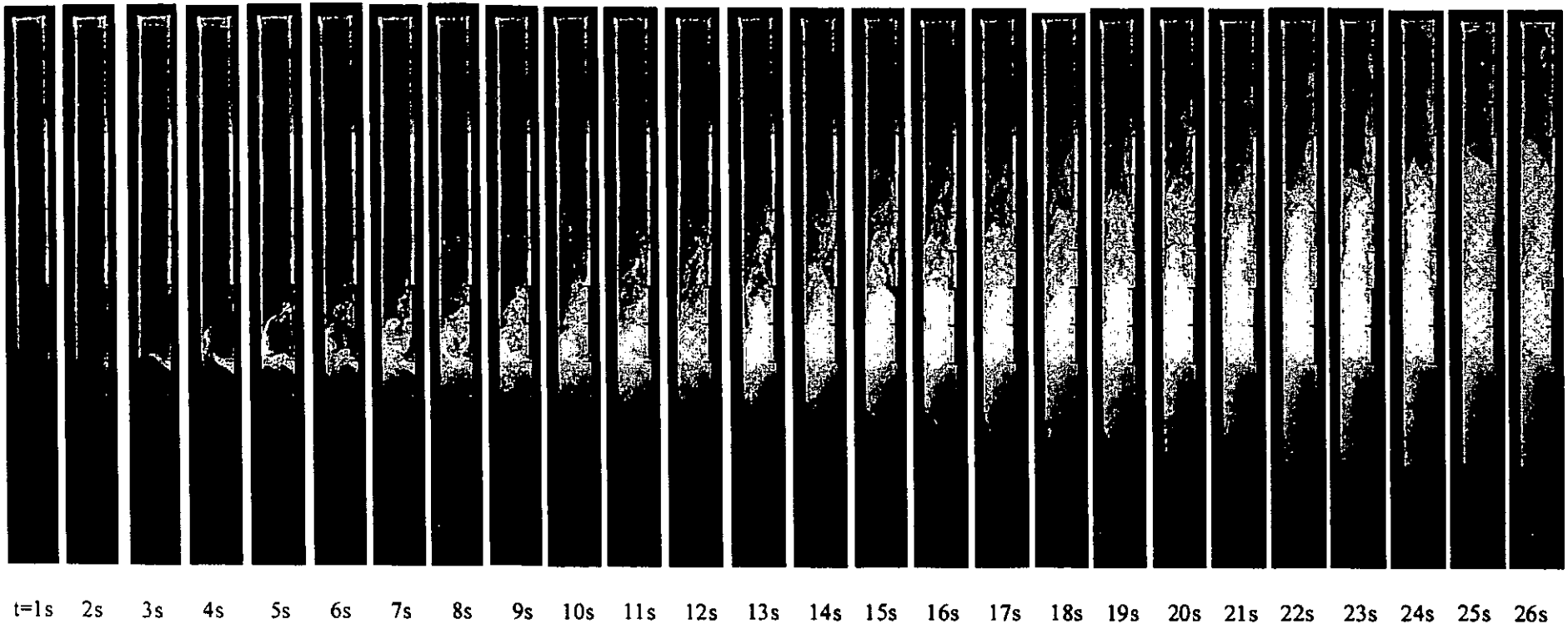

Figure 4.4: Typical photographs of the smoke filling process for case C

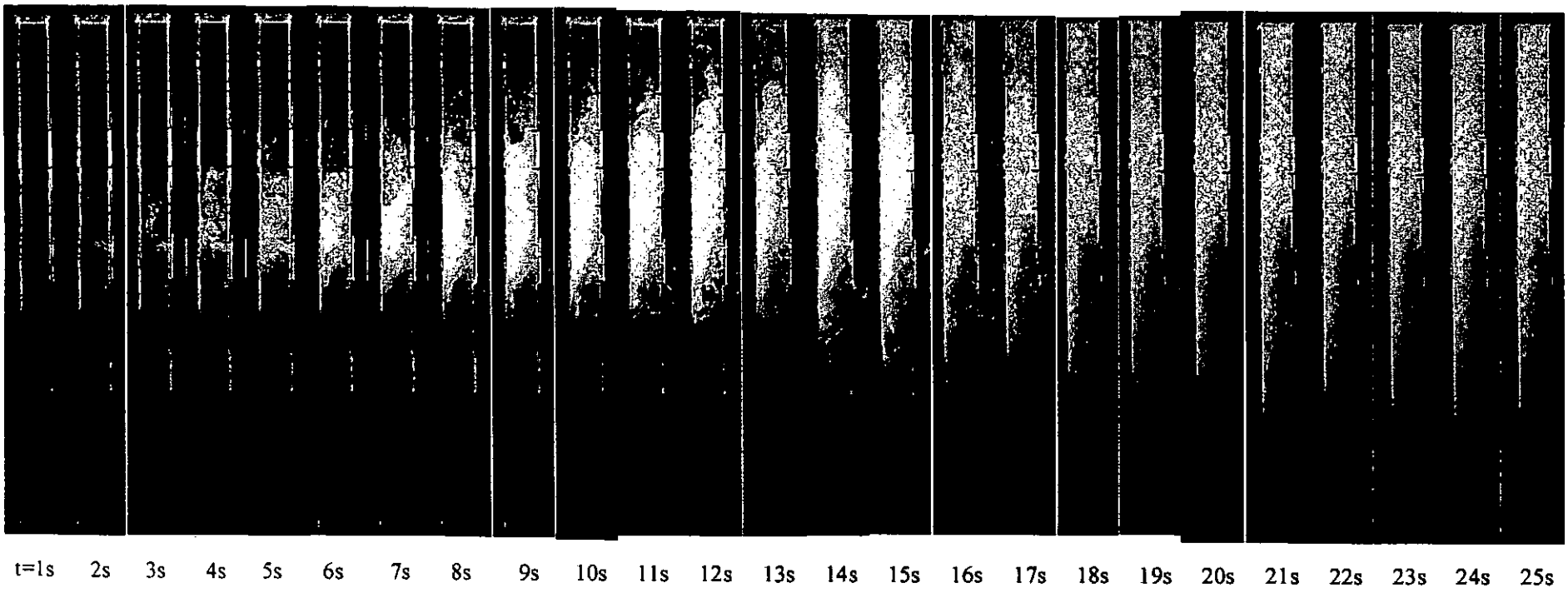

Figure 4.5: Typical photographs of the smoke filling process for case D

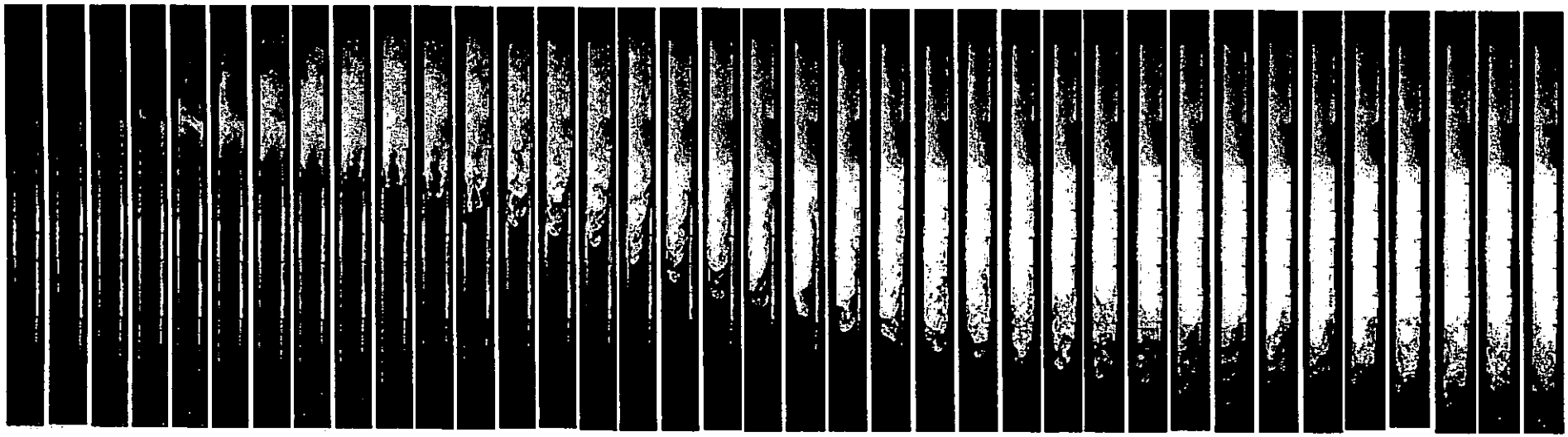

Figure 4.6: Typical photographs of the smoke filling process for case E

Figure 4.7: Typical photographs of the smoke filling process for case F

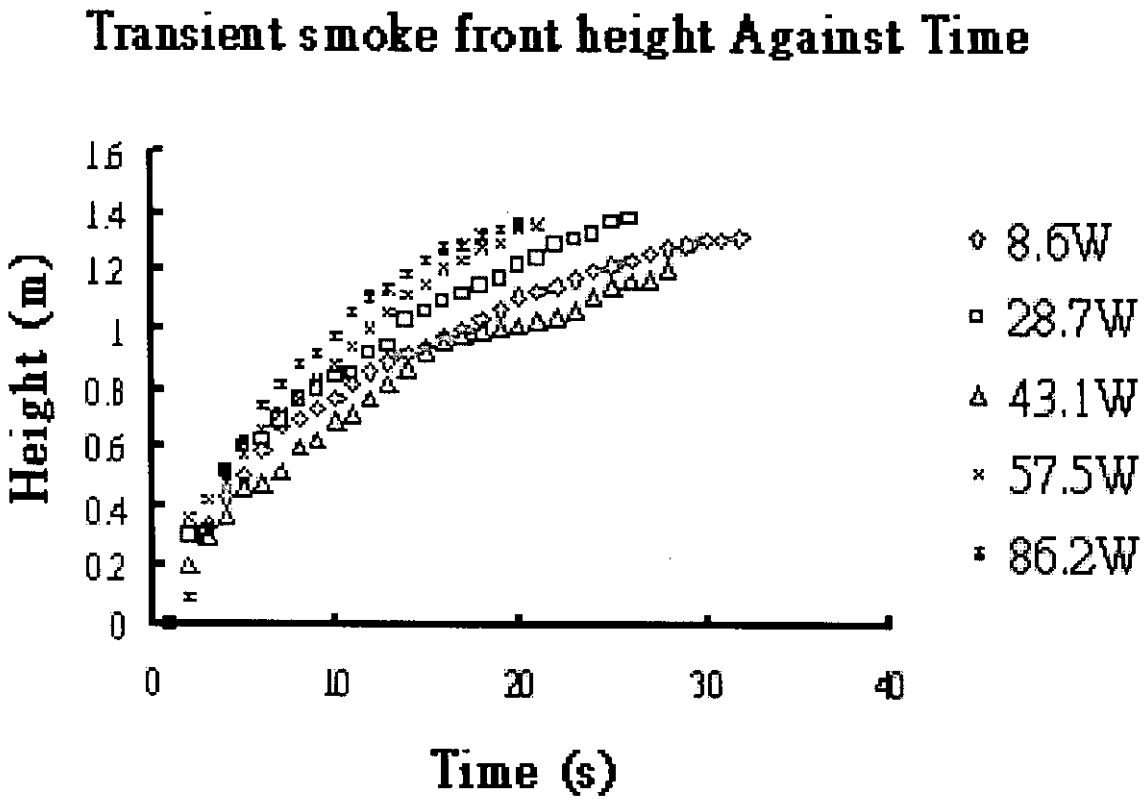

Figure 4.8: Height of transient smoke front for case B

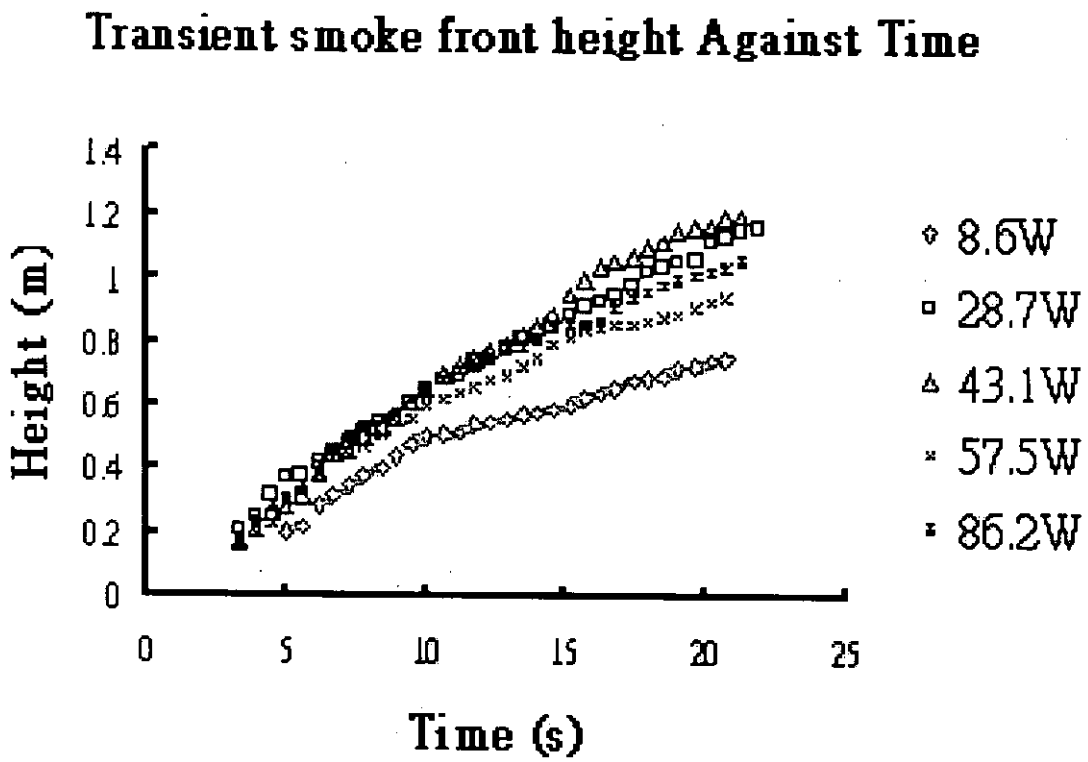

Figure 4.9: Height of transient smoke front for case A

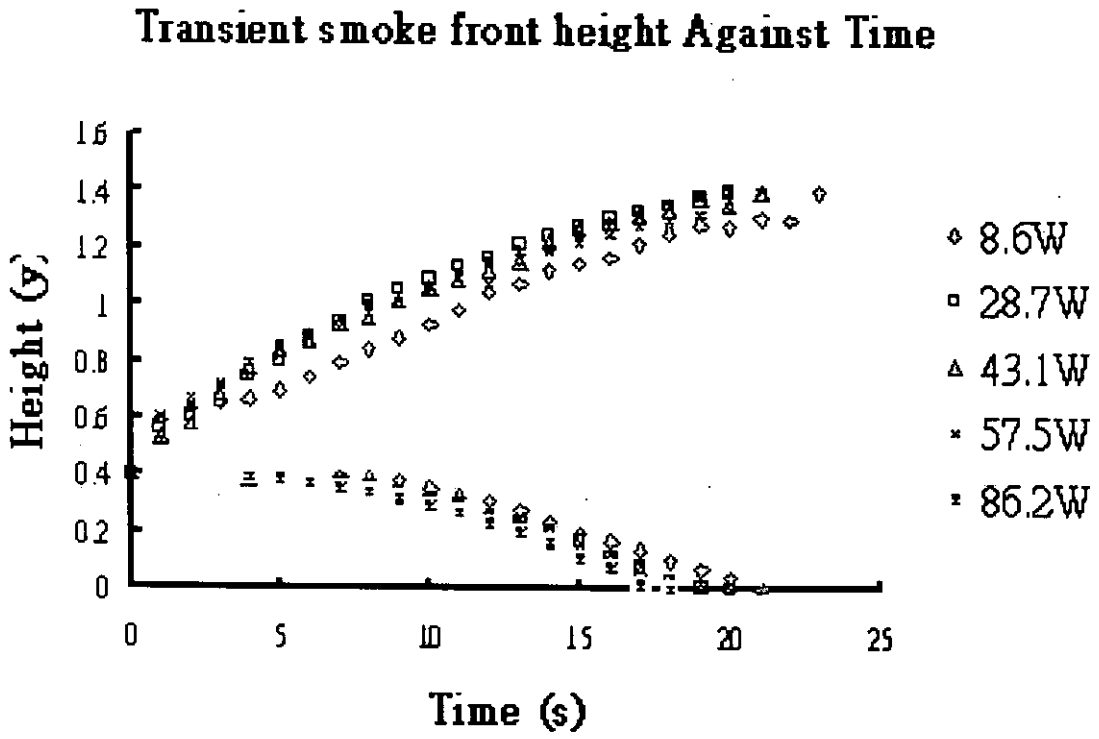

Figure 4.10: Height of transient smoke front for case C

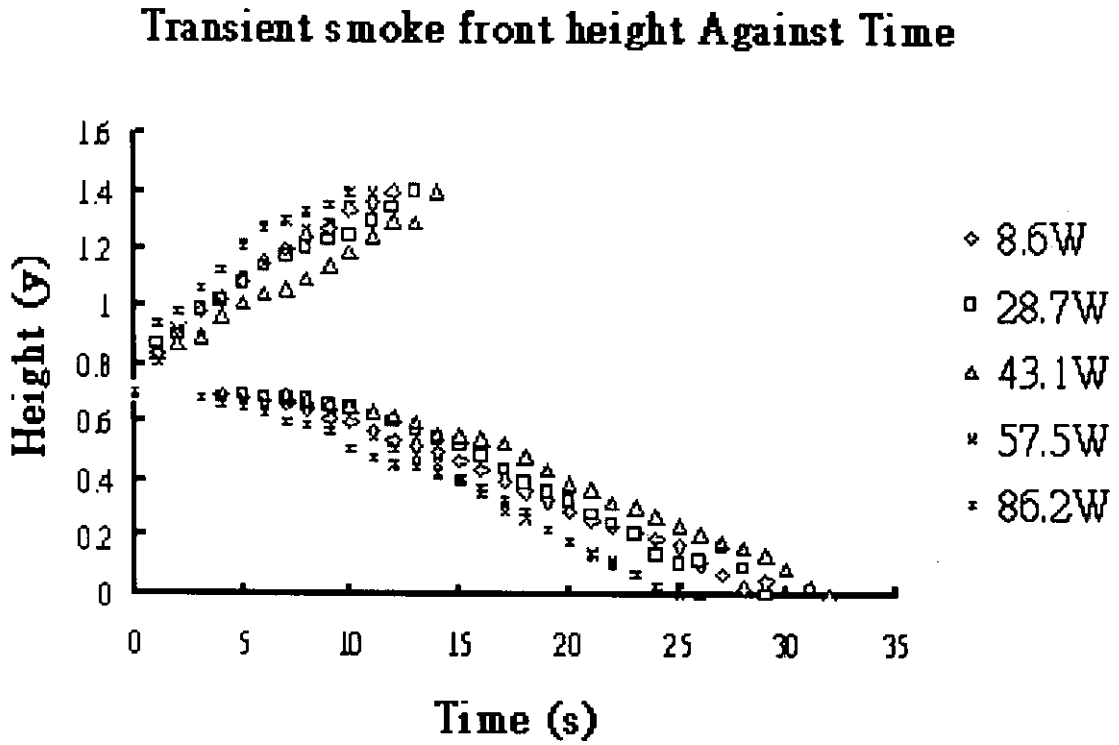

Figure 4.11: Height of transient smoke front for case D

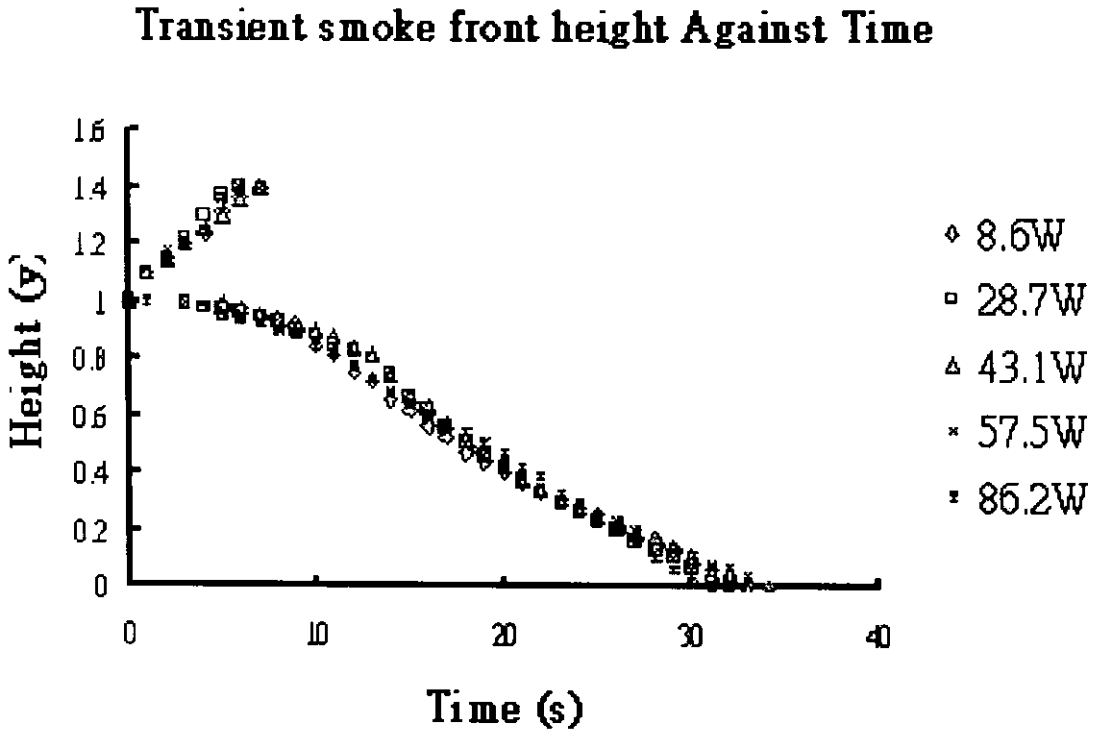

Figure 4.12: Height of transient smoke front for case E

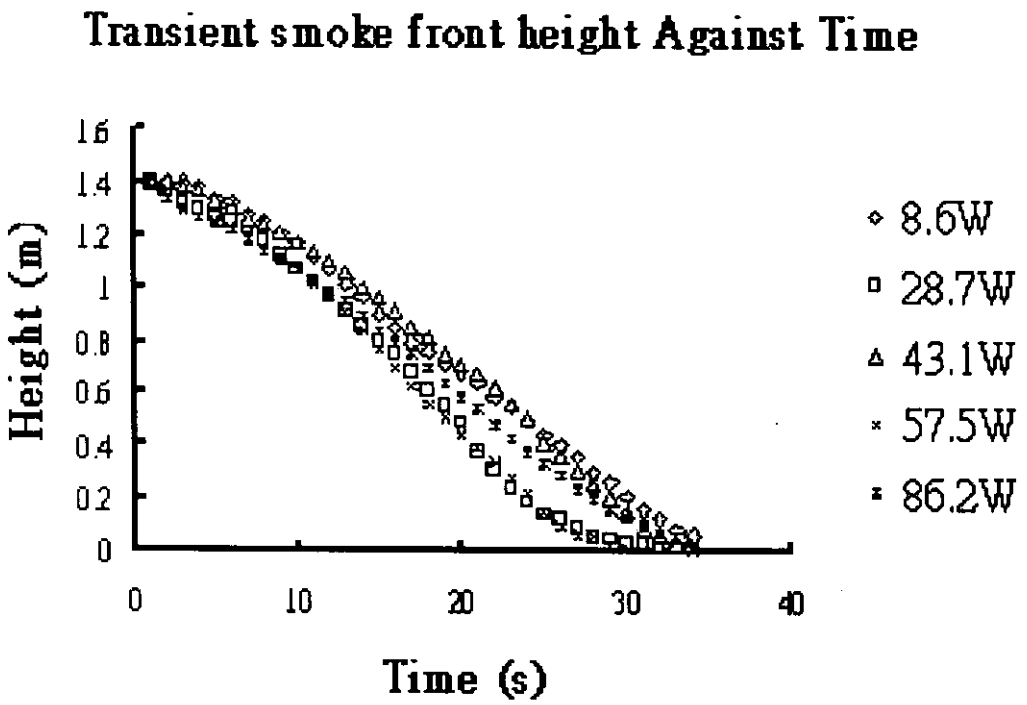

Figure 4.13: Height of transient smoke front for case F

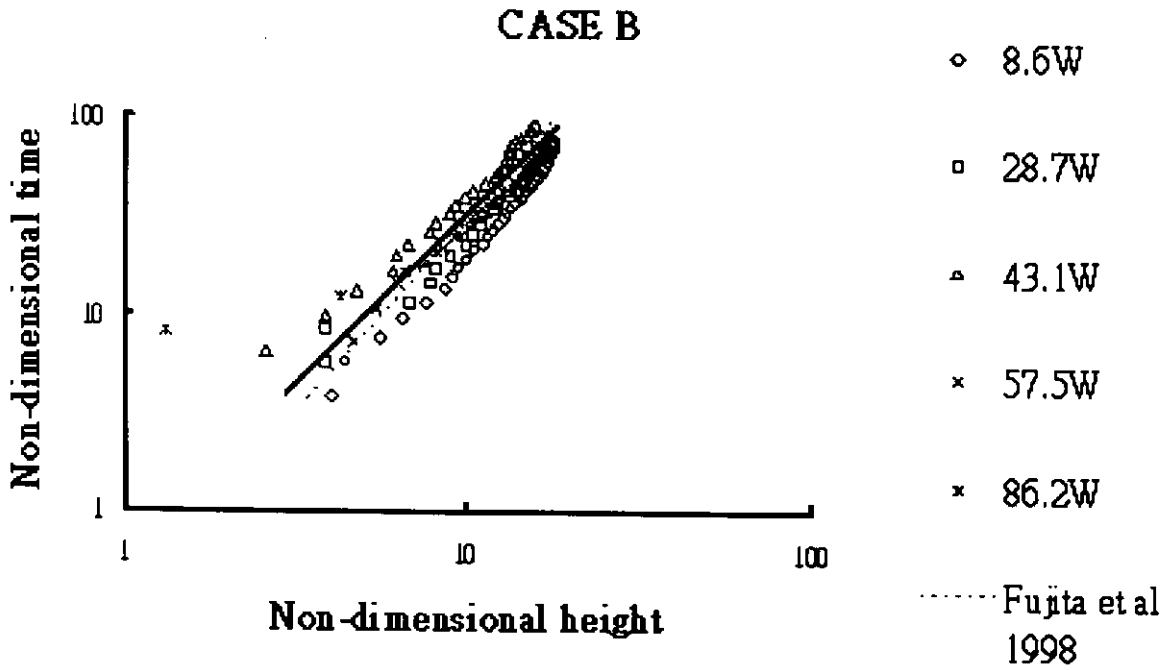

Figure 5.1: Correlation of non-dimensional travel time with non-dimensional height for case B (upward movement of smoke)

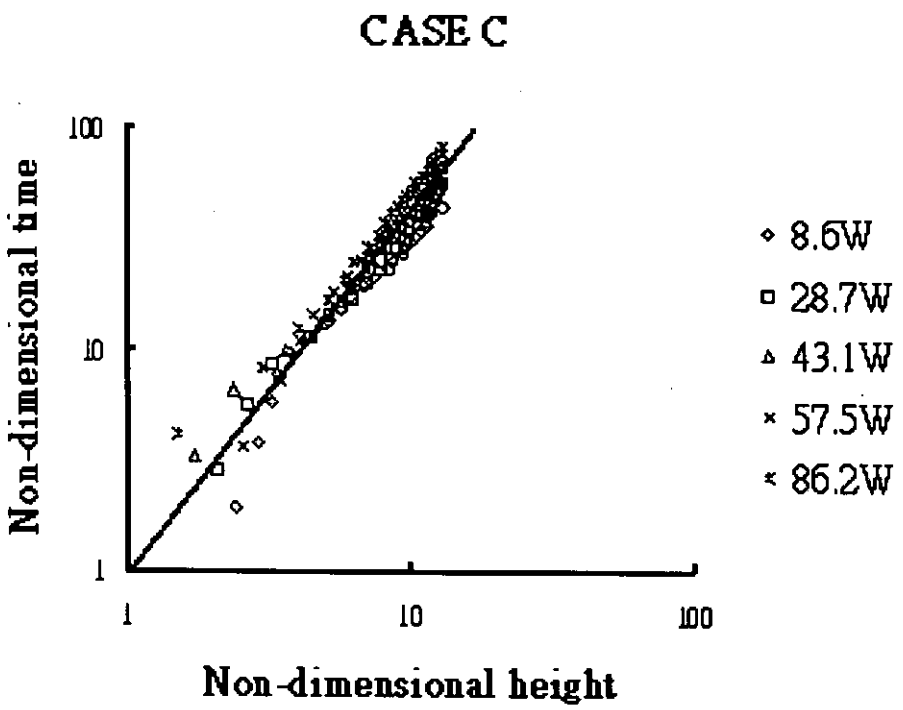

Figure 5.2: Correlation of non-dimensional travel time with non-dimensional height for case C (upward movement of smoke)

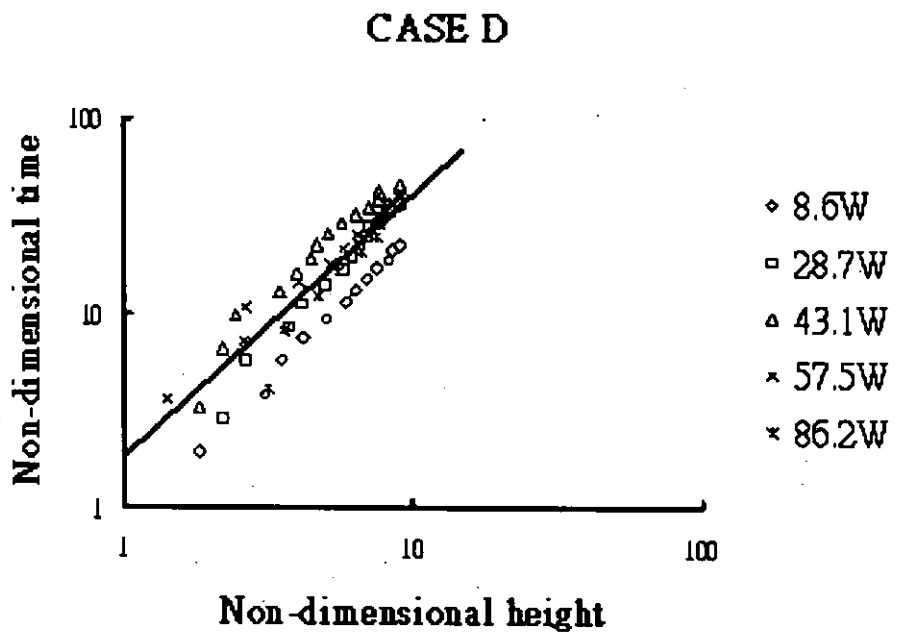

Figure 5.3: Correlation of non-dimensional travel time with non-dimensional height for case D (upward movement of smoke)

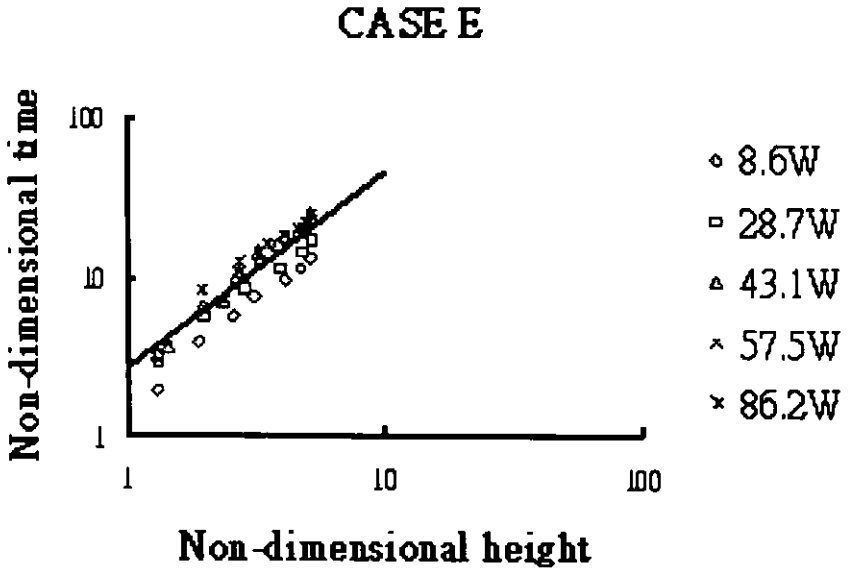

Figure 5.4: Correlation of non-dimensional travel time with non-dimensional height for case E (upward movement of smoke)

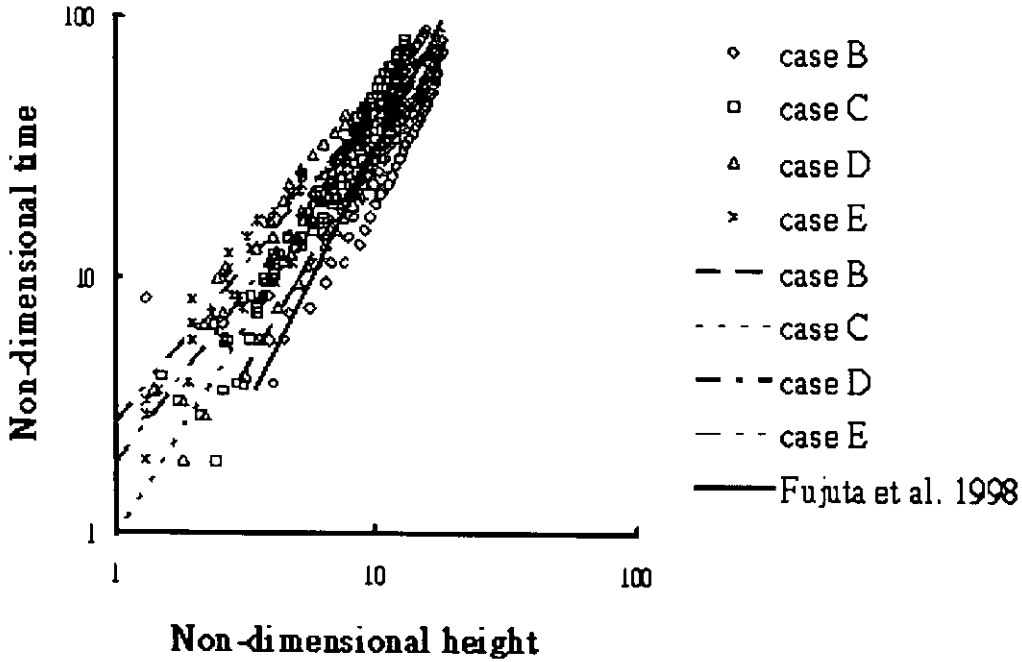

Figure 5.5: Correlation of non-dimensional travel time with non-dimensional height (upward movement of smoke)

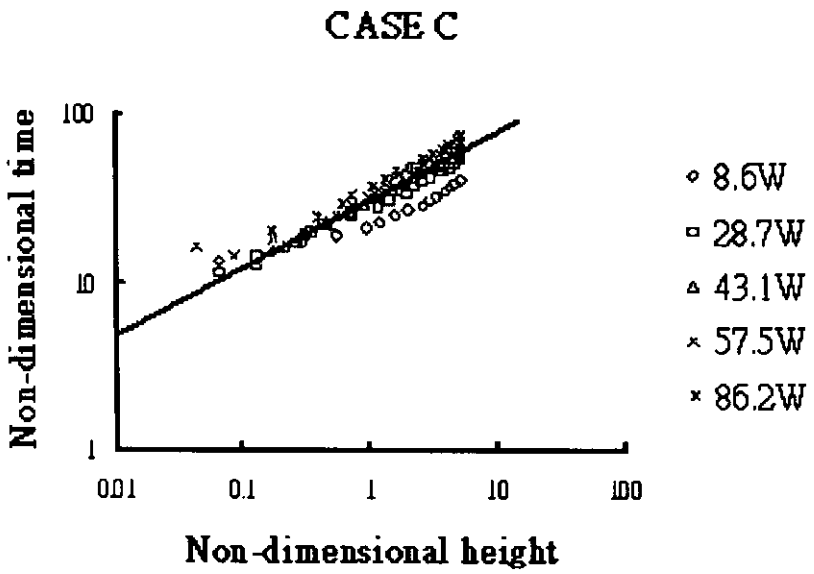

Figure 5.6: Correlation of non-dimensional travel time with non-dimensional height for case C (downward movement of smoke)

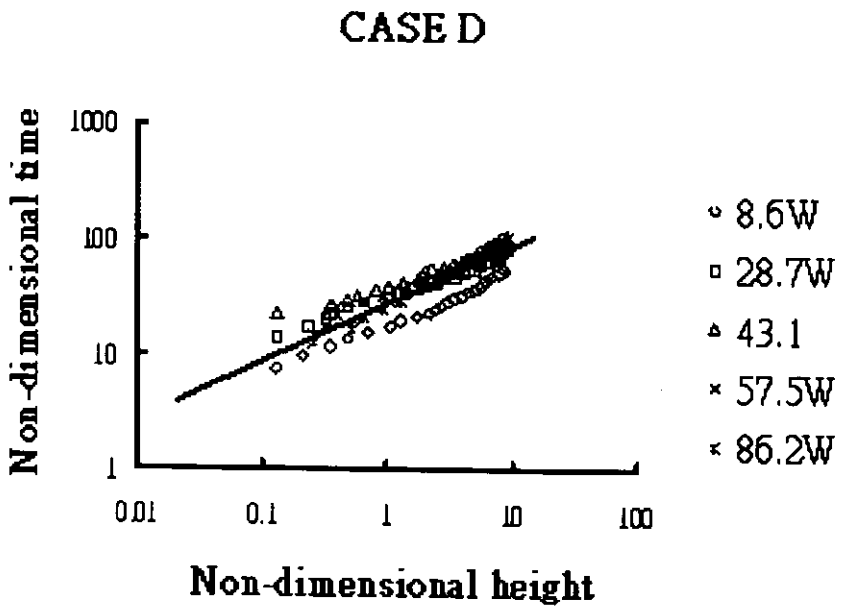

Figure 5.7: Correlation of non-dimensional travel time with non-dimensional height for case D (downward movement of smoke)

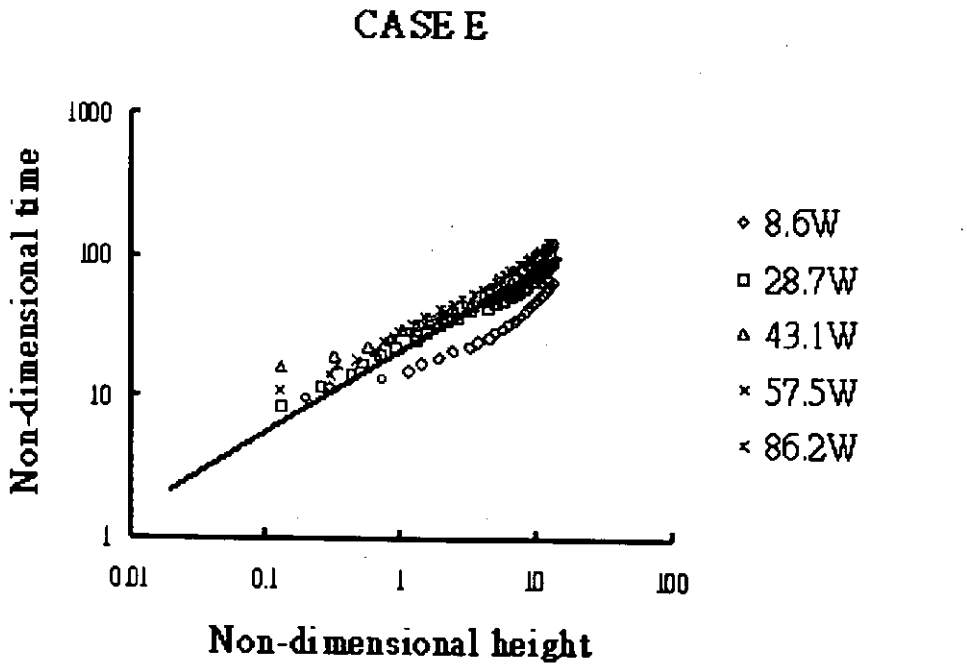

Figure 5.8: Correlation of non-dimensional travel time with non-dimensional height for case E (downward movement of smoke)

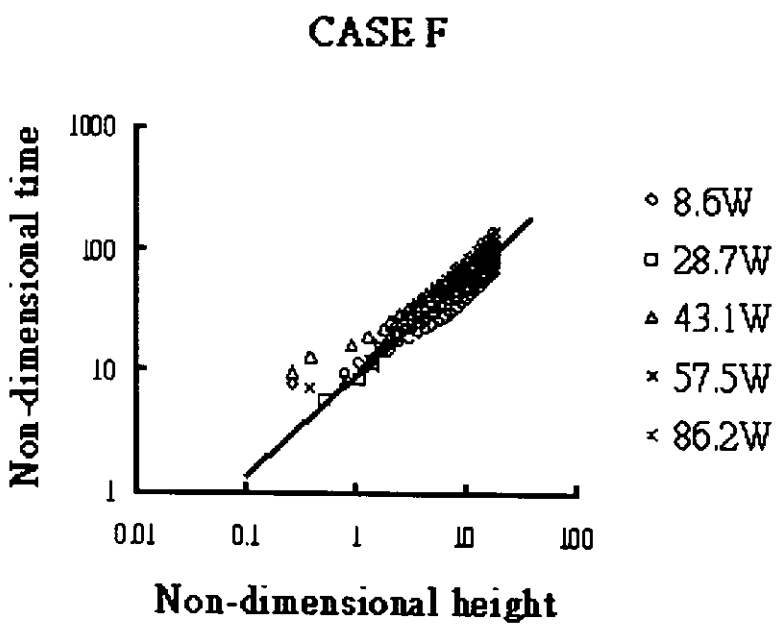

Figure 5.9: Correlation of non-dimensional travel time with non-dimensional height for case F (downward movement of smoke)

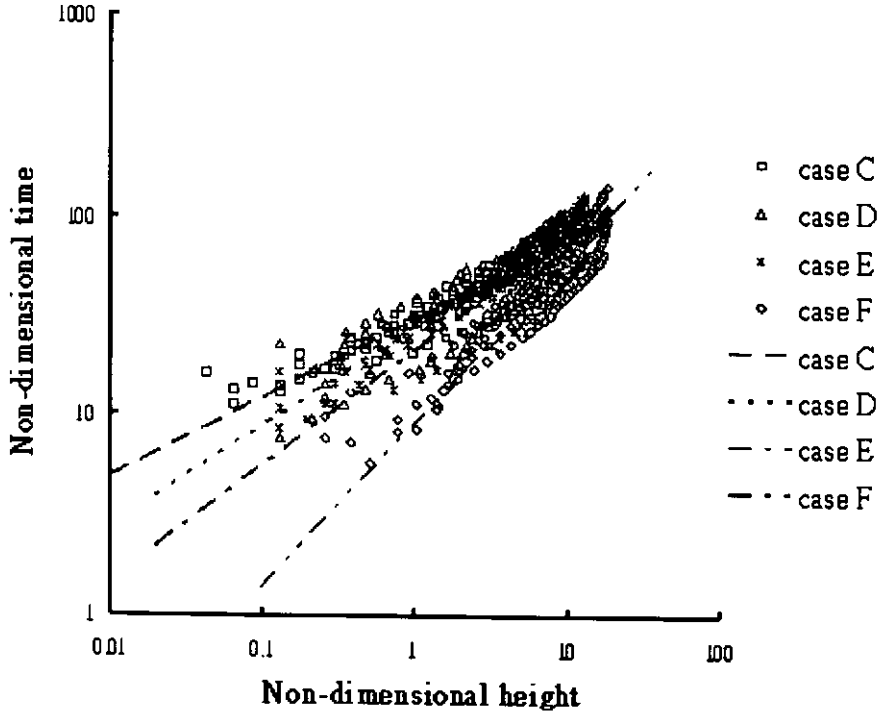

Figure 5.10: Correlation of non-dimensional travel time with non-dimensional height (downward movement of smoke)

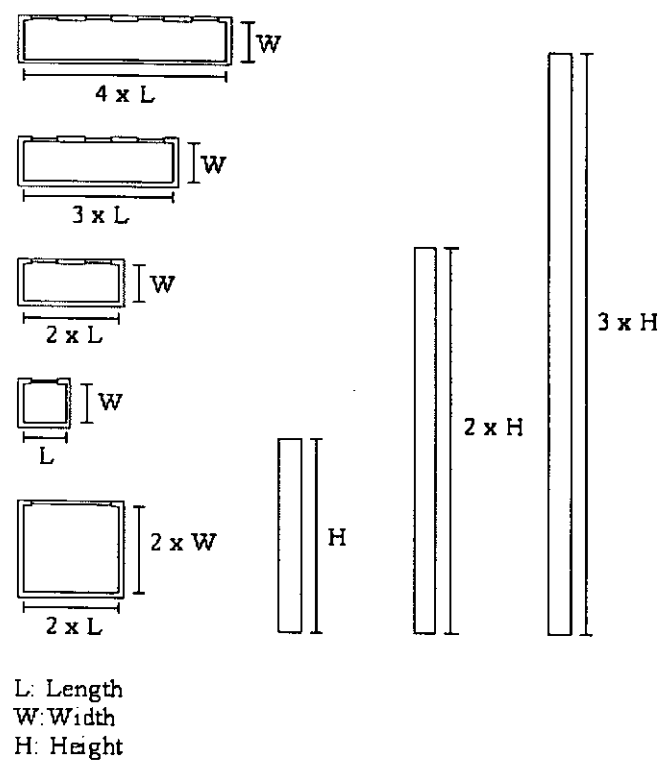

Figure 6.1: Different cases of typical configuration of vertical shafts

Appendix Publication from this study

1. W. K. Chow, L. T. Wong, P. M. Tang and E. C. Y. Kwan, "Scale model studies on smoke filling in the lift shaft of an old highrise building", Journal of Applied Fire Science, Vol. 9, No. 2, pp. 135-151. (1999-2000).
2. P. M. Tang, L. T. Wong and W. K. Chow, "Natural smoke filling in a physical vertical shaft model", Fire and Materials (2003).

J. APPLIED FIRE SCIENCE, Vol. 9(2) 135-151, 1999-2000

SCALE MODEL STUDIES OF SMOKE FILLING IN THE LIFT SHAFT OF AN OLD HIGH-RISE BUILDING*

W. K. CHOW

L. T. WONG

P. M. TANG

ERIC C. Y. KWAN

The Hong Kong Polytechnic University, China

ABSTRACT

Fires safety in older high-rise buildings is of great concern to the general public as a result of a large fire which recently occurred in an existing high-rise building in Hong Kong. Further to the preliminary analysis on three points identified earlier, another key point is the smoke movement in the lift shaft. This information is important as it would affect the fire safety requirements in these class of buildings. The smoke movement pattern in a lift shaft was studied with a scale model. Three cases were considered with the fire at the bottom of the lift shaft; in a compartment next to the lower part of the lift shaft; and in a compartment next to the upper part of the lift shaft. Empirical correlations of smoke travel time were derived from the results reported in this study.

INTRODUCTION

An existing high-rise building in the Hong Kong Special Administrative Region (HKSAR, formerly Hong Kong) refers to a building built twenty years ago

*The project is funded by The Hong Kong Polytechnic University under account number G-V504.

[e.g., 1]. At that time, requirements for fire protection installations were not so strict as they are today. For example, sprinkler systems were not required. Not much attention was paid to fire safety aspects until a very large fire occurred in a high-rise building in late 1997 [e.g., 2-5]. Citizens are now very concerned about the fire safety in those old high-rise buildings.

The noted fire was believed to have started in [e.g., 2-5] a lift shaft which was under reconstruction. Because of the construction work, all the lift doors in that shaft were removed with the vertical openings sheltered by temporary plywood partitions. The fire that started in the lift shaft was not discovered during its early stage. Reports note that workers tried to extinguish the fire but failed. They then reported it to the Fire Services Department (FSD) [4] after the fire had grown significantly and started spreading to the other levels. Combustible materials were ignited at the lower and upper levels of the shaft. As a result, flashover occurred in part of the building, and a post-flashover fire with duration longer than twenty hours ensued.

Three points were studied initially [6, 7]:

- Fire-induced air flow in the lift shaft.
- Likelihood of flashover in the lift shaft.
- Consequences of igniting combustible materials.

The lift shaft under refurbishment was believed to be the key element of concern in this fire [2-5]. Studying the motion of hot gases through the lift shaft is essential to the understanding of the smoke spreading mechanism, which was studied by considering both the stack effect and the turbulent mixing process of a lower hot layer of smoke and an initial upper cool layer of air. As proposed by Zukoski, this is related to the Rayleigh-Taylor mixing process [8]. Further studies were performed using a scale model as described in this article.

SMOKE MOVEMENT IN THE LIFT SHAFT

The building of concern is of length 34 m, width 28 m and height 50 m. There are fifteen levels each of height 3.1 m and a ground story of height 3.5 m. Three lift shafts of average dimensions 2.3 m by 2.3 m by 48 m (i.e., aspect ratio about 1 × 1 × 20) were installed to serve all levels. One of the lift shafts was under refurbishment with all the lift doors having been removed for some time. Vertical openings of width 0.8 m and height 2 m connect this lift shaft to each level.

As the building was constructed before 1987 and was classified as a "commercial and residential" building, only fire hydrant and hosereel (FH/HR) systems were installed. The SAR Government is reviewing the current situation and additional active fire protection systems such as sprinkler systems and fire detection systems might be required in these existing buildings. However, if the sprinkler actuation time is shorter than the egress time, hot steam generated by

the water spray would hurt the firemen and occupants left inside. Also, automatic fire detection would give rise to the problem of false alarms. Therefore, whether those systems are good for fire control or not is to be debated. A more appropriate action to take immediately is to provide better training on fire safety management. In addition, the smoke movement in the lift shaft and the stair shaft as well should be studied carefully.

The fire environment in older high-rise buildings was studied first using a two-layer zone model [9]. Several scenarios were considered by taking the building as multi-level and multi-compartment structures including a lift shaft. Within the lift shaft, the smoke layer was assumed to start descending from the ceiling, no matter where the locations of the fire were. As pointed out by Fujita et al., smoke would take time to travel upward before forming a smoke layer, if a fire started from a lower level [10]. The time taken for the smoke to move up to the ceiling is quite significant for a high lift shaft. Therefore, the time for the smoke layer to fill the stair shaft would be longer than those values predicted by a two-layer zone model.

The time taken for the smoke to travel to the top of a stair shaft is important and should be studied carefully. A scale model was used in this article to have a preliminary understanding of the smoke movement pattern.

SCALE MODELING

Scaling factors are important in using scale models. For a fire located at the floor of a lift shaft, the height y that smoke reaches in time t measured experimentally is expressed in terms of the non-dimensional height Y and the non-dimensional time τ, through the characteristic length scale of the model D, and the non-dimensional heat release rate of the fire $\dot{Q}^*$ expressed in terms of the heat release rate of the fire $\dot{Q}$ [10]:

$$Y = \frac{y}{D} \tag{1}$$

and

$$\tau = t\sqrt{\frac{g}{D}}\dot{Q}^{*\frac{1}{3}} \tag{2}$$

with

$$\dot{Q}^* = \frac{\dot{Q}}{c_p \cdot \rho \cdot T_\infty \cdot D^{\frac{1}{2}}\sqrt{g}} \tag{3}$$

where g is the acceleration due to gravity, c_p is the specific heat of air at constant pressure, ρ is smoke density and T_∞ is the ambient temperature. The derivation of

travel time of smoke front was described by Fujita et al. [10] with a summary listed in Appendix A.

The characteristic length scale of the model D was taken to be the hydraulic diameter of the shaft, expressed in terms of the shaft base length L and width W as:

$$D = \frac{2 \cdot L \cdot W}{L + W} \tag{4}$$

Relationships of the non-dimensional height Y in terms of τ were derived earlier [10] by taking the smoke density ρ to be a constant value which is the ambient air density ρ_∞. This point has to be considered carefully.

Experimental studies on the travel time of buoyant fire plume fronts in vertical closed shafts induced by a heat source were carried out [10] in a scale model of size 0.8 m by 0.8 m and height 3.22 m; and in a full-size vertical shaft of size 2.8 m by 3 m and height 24 m. The following correlation equations were derived for closed shafts:

$$\tau = \begin{cases} 0.56Y^{4/3}; & Y \leq 2.5 \\ 0.30Y^{2}; & Y > 2.5 \end{cases} \tag{5}$$

EXPERIMENTS

Experiments were carried out in a scale model of a lift shaft 0.076 m by 0.076 m and height 1.4 m, giving the aspect ratio 1 × 1 × 18. This gave a scaling factor of 36, in comparing with the lift shaft of the subject high-rise building. The model for studying the smoke movement in a closed vertical shaft was constructed of clear glass, fastened together with adhesive. A room model of size 0.29 m by 0.076 m and height 0.11 m was placed adjacent to the vertical shaft at the floor level, through a vertical opening of width 0.05 m and height 0.1 m. The characteristic length scale D was 1.89 m.

A gas burner was used to simulate the scaled fire. Steady burning was achieved by regulating the gas supply at constant flow rates of values 0.0005 $L \cdot s^{-1}$ to 0.005 $L \cdot s^{-1}$ through a 2 mm diameter supply nozzle. Complete combustion was assumed for calculating the heat release rate, using the calorific value of town gas of 17.27 MJm^{-3}. A smoke pellet of mass 3.5 g was placed above the gas burner to generate visible smoke. Tungsten lamps were used for illumination so that the smoke movement could be visualized.

Three sets of experiments, labeled as cases A, B and C, under atmospheric pressure were performed with geometry shown in Figure 1:

- Case A:
  The fire was placed at the bottom of the lift shaft model, room model was not used.

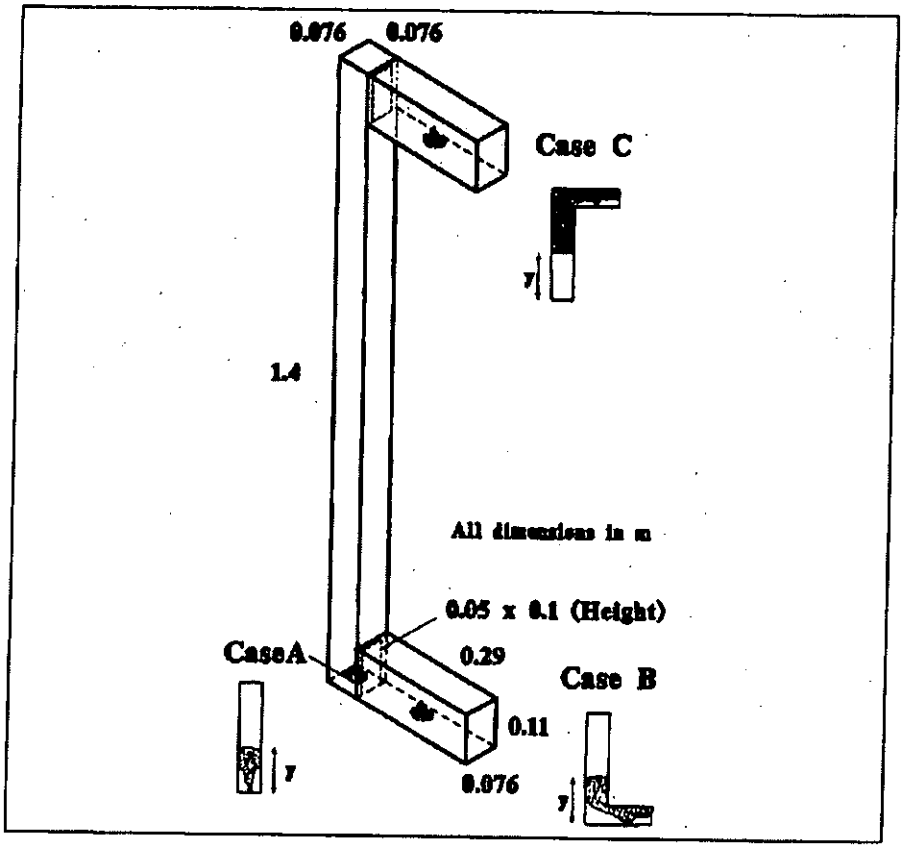

Figure 1. Scale model experiment.

- Case B:
  The room model was placed at the lower level.
- Case C:
  The room model was placed at the upper level.

Five constant heat release rates of 8.6 W, 28.7 W, 43.1 W, 57.5 W, and 86.2 W corresponding to gas flow rates 0.0005 $L \cdot s^{-1}$ to 0.005 $L \cdot s^{-1}$ were used in each set of experiments. In this way, τ was found to be 1.91 t, 2.85 t, 3.27 t, 3.60 t, and 4.12 t, respectively, for the five heat release rates. For cases A and C, three experiments were repeated for each heat release rate and so giving a total of fifteen tests for each case. For case B, four experiments were repeated for each heat release rate, giving a total of twenty tests. Note that the model was cleaned before each test.

For a clear visualization of smoke movement pattern and movement, the experiments were carried out under light sources. Except the specified light sources, the environment of the laboratory was kept dark. Photographs were taken by a camera at a right angle to the light source.

Photographs of the transient smoke movement in the shaft were taken by a camera with a 35 mm lens. The aperture and shutter speed were set at $f/4$ and 1/60 s respectively with shooting frequency of 1 s for cases A and C; and $f/5.6$ and 1/125 s (+0, –0.45 ms) respectively with shooting frequency of 0.56 s for case B. The images were recorded on 35 mm × 24 mm films of speed ISO400 with resolving power 125 $ll \cdot mm^{-1}$ for contrast 1/1000 and 40 $ll \cdot mm^{-1}$ for contrast 1/1.6. The experiments were also recorded by a video camera for further analysis.

RESULTS

Typical photographs of smoke movement patterns in the scale model at different time intervals for the three cases are shown from Figures 2 to 4. The average transient values of y were determined from the photographs, and the results at different heat release rates are shown in Figures 5 to 7 for cases A, B, and C, respectively.

The values of τ were plotted against Y for case A in Figure 8. The results of Fujita et al. [10] given by equation (5) were also plotted. Very good agreement was found. In addition, a simplified equation with correlation coefficient 0.85 can be fitted:

$$\tau = 8.66\, Y^{2/3} \tag{6}$$

For case B, the results of τ were plotted against Y in Figure 9. Correlation equations between τ and Y were found with correlation coefficients of 0.85 and 0.88 respectively:

$$\tau = \begin{cases} 7.9Y^{2/3}; & Y < 2.5 \\ 4.3Y^{7/6}; & Y \geq 2.5 \end{cases} \tag{7}$$

The results are shown in Figure 9 as well.

Further, the times taken for the smoke front to reach the fixed heights y at 0.2 m, 0.4 m, 0.6 m, 0.8 m and 1.0 m were plotted against $\dot{Q}^{1/3}$ in Figure 10. Fairly linear correlation relations are found.

These results of τ against Y for case C are shown in Figure 11. It is difficult to observe any correlation relationship for τ and Y. A new parameter Y_1 is defined:

$$Y_1 = \frac{(H-y)}{D} \tag{8}$$

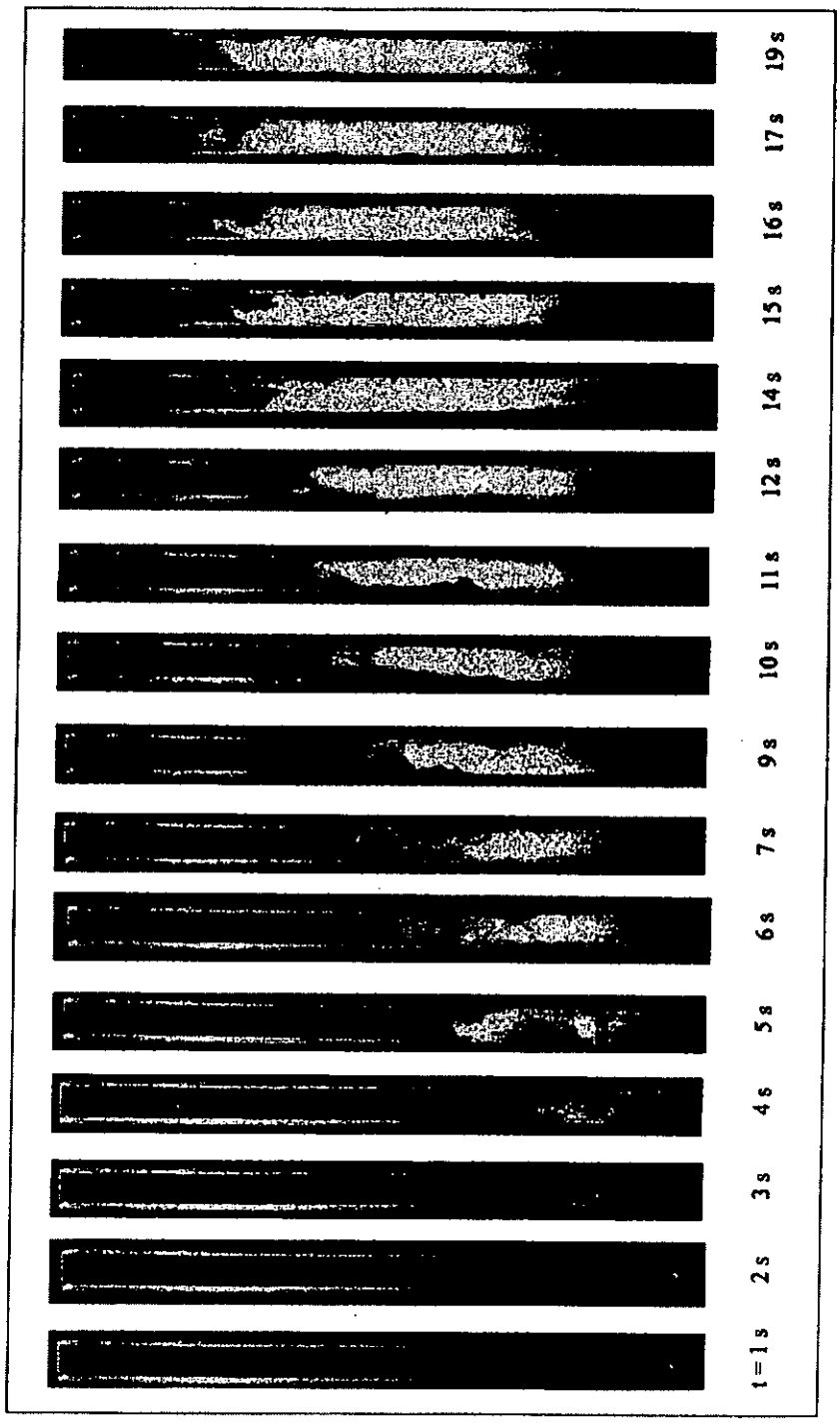

Figure 2. Typical photographs of the smoke filling process for case A.

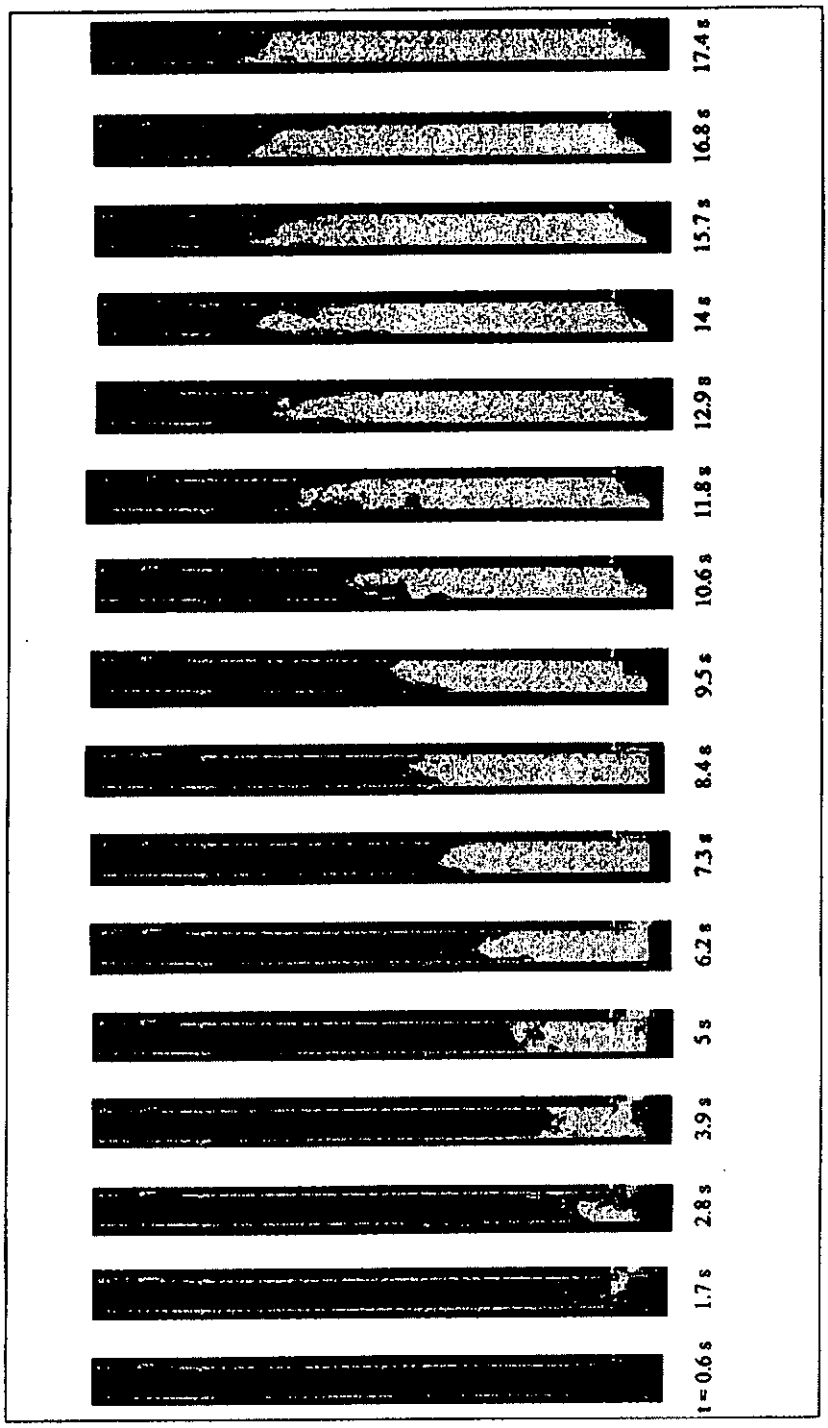

Figure 3. Typical photographs of the smoke filling process for case B.

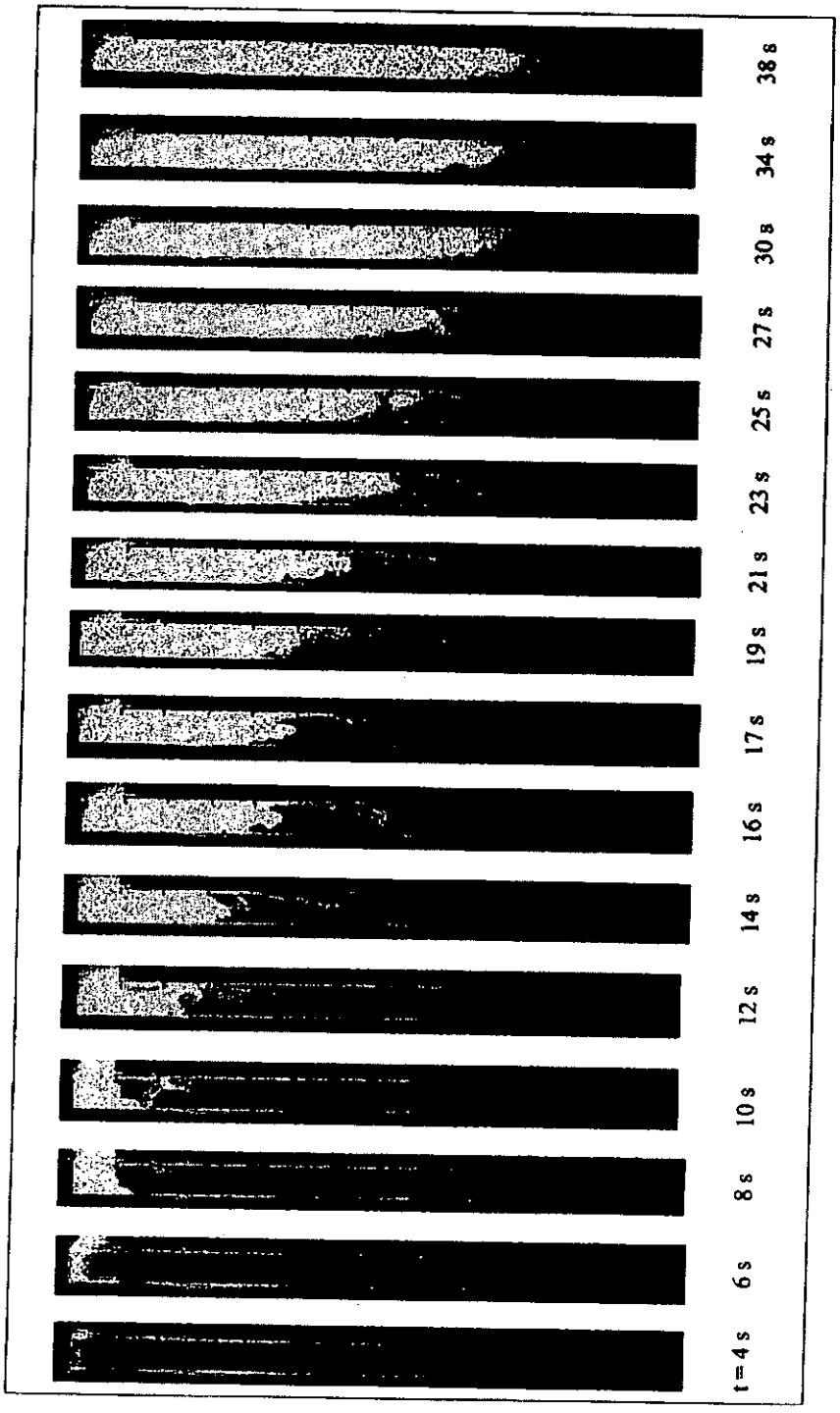

Figure 4. Typical photographs of the smoke filling process for case C.

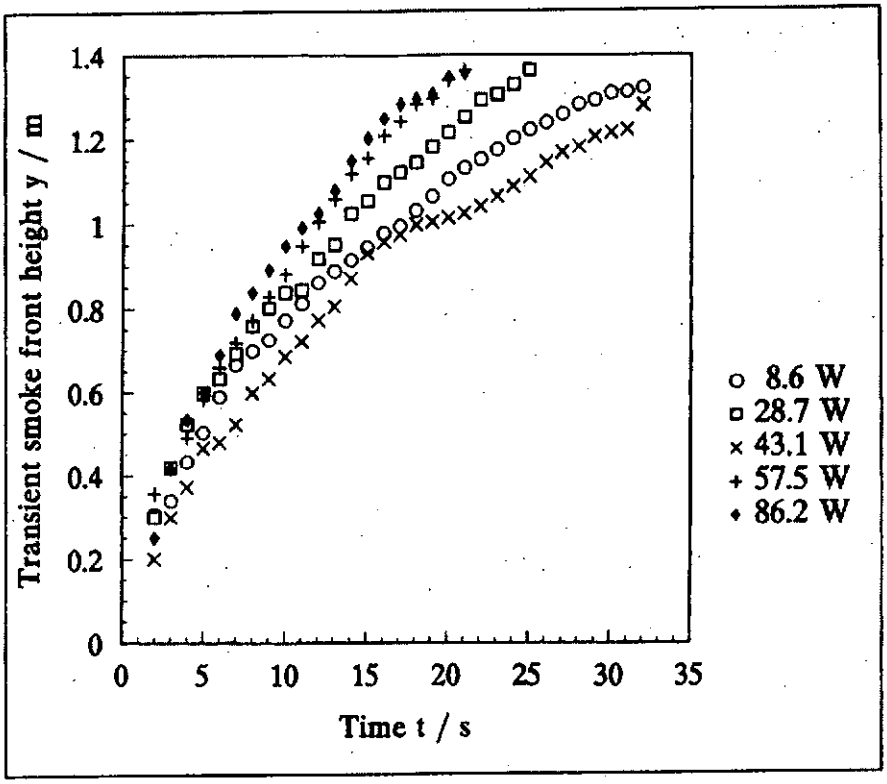

Figure 5. Height of transient smoke front for case A.

The results of τ are plotted against Y_1 in Figure 12. The following equation with a correlation coefficient of 0.91 can be fitted:

$$\tau = 8.93\ Y_1^{0.82} \tag{9}$$

CONCLUSION

The smoke filling process in a vertical lift shaft in a high-rise building was studied using scale modeling techniques. Three cases were considered with a fire at the lift shaft, a fire in a room adjacent to the lift shaft at low level, and a fire in a room adjacent to the lift shaft at high level. Following the concept of Fujita et al. [10], correlation relationships between the smoke and the travel time were developed for the three cases. These equations are useful for understanding the smoke filling process in the lift shaft.

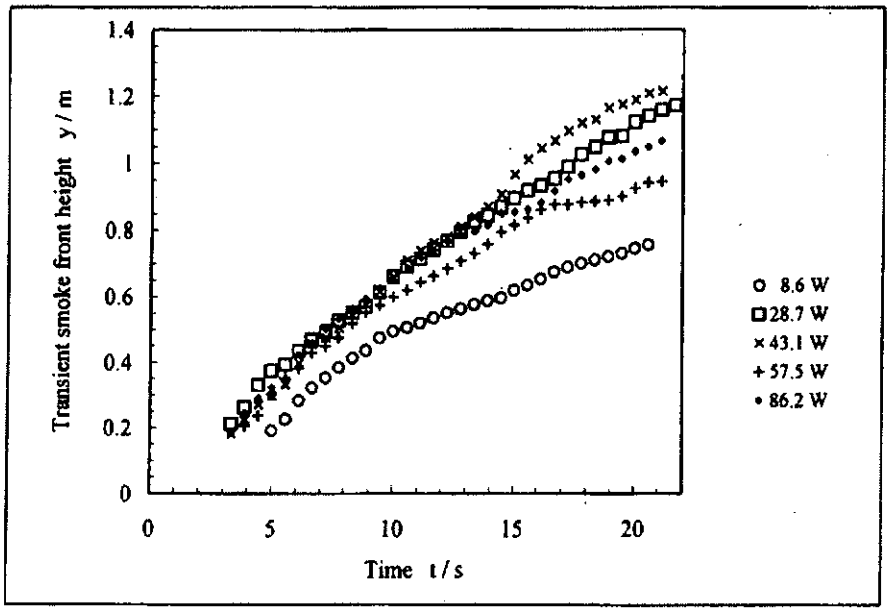

Figure 6. Height of transient smoke front for case B.

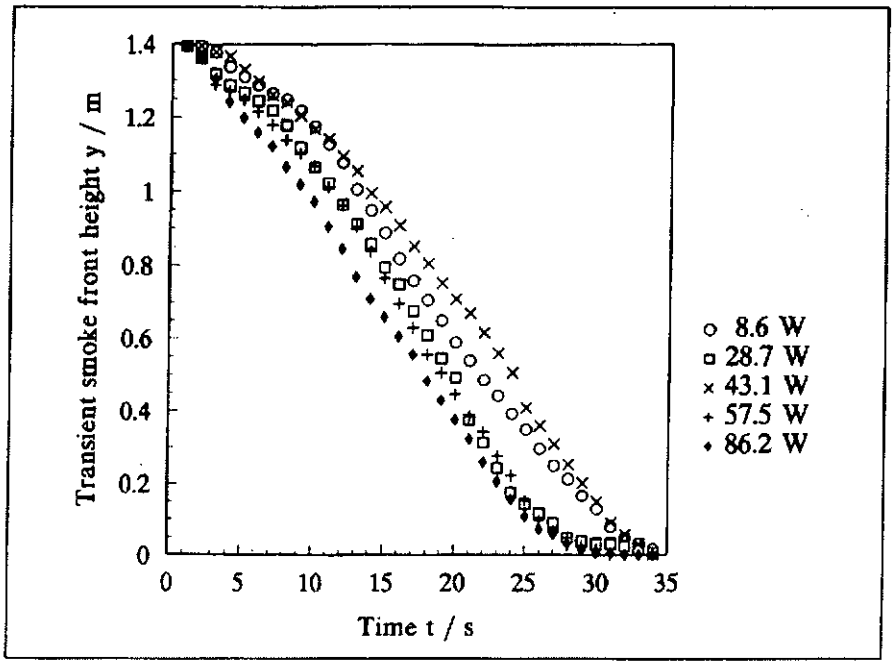

Figure 7. Height of transient smoke front for case C.

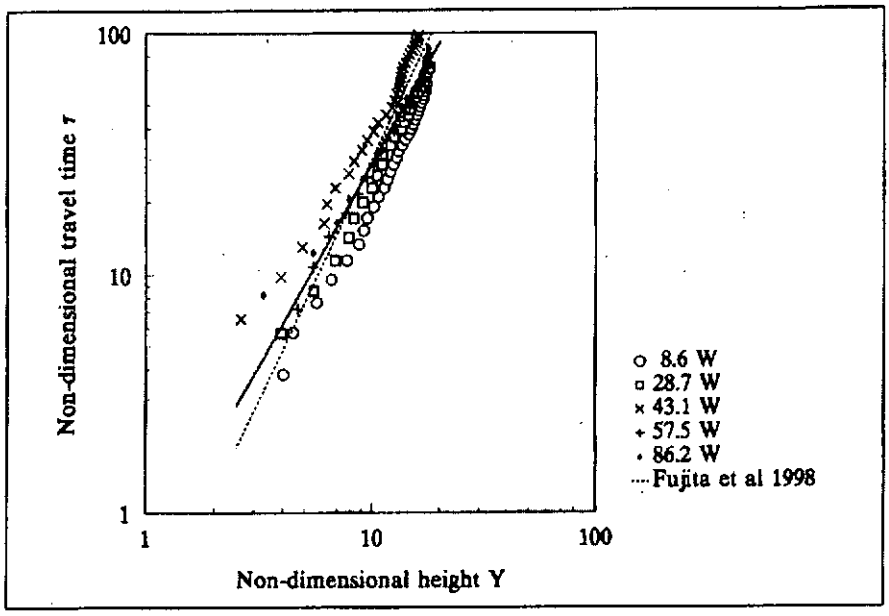

Figure 8. Correlation of non-dimensional travel time with non-dimensional height Y for case A.

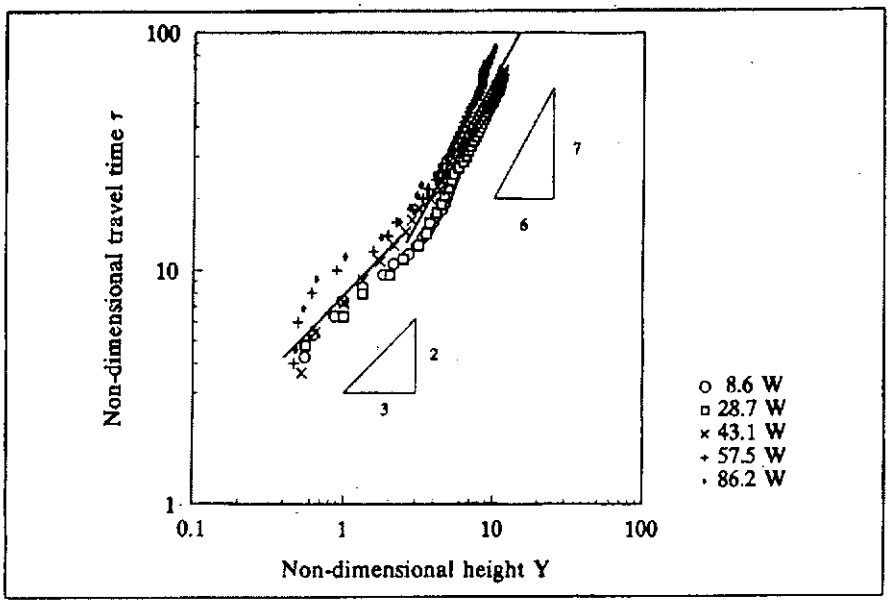

Figure 9. Correlation of non-dimensional travel time with non-dimensional height Y for case B

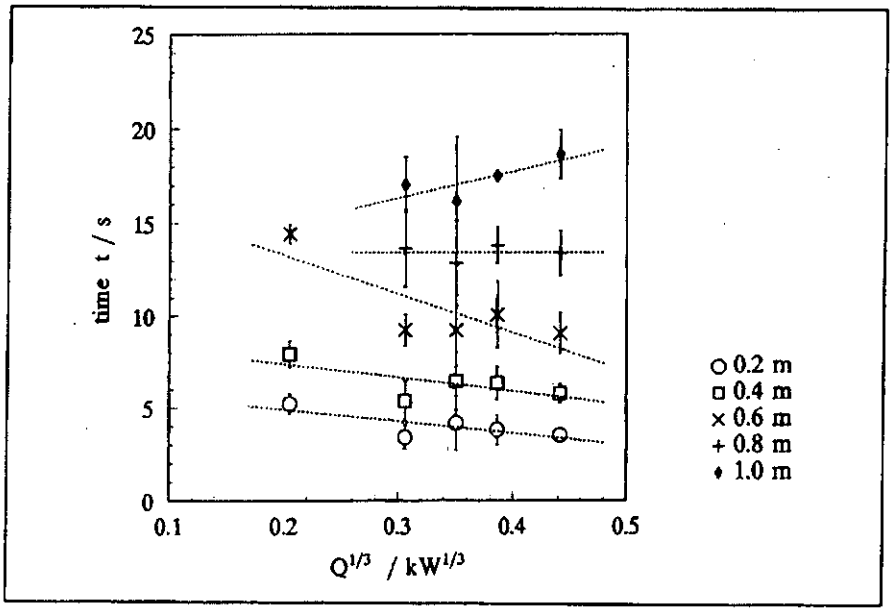

Figure 10. Correlation of time of travel with heat release rate for case B.

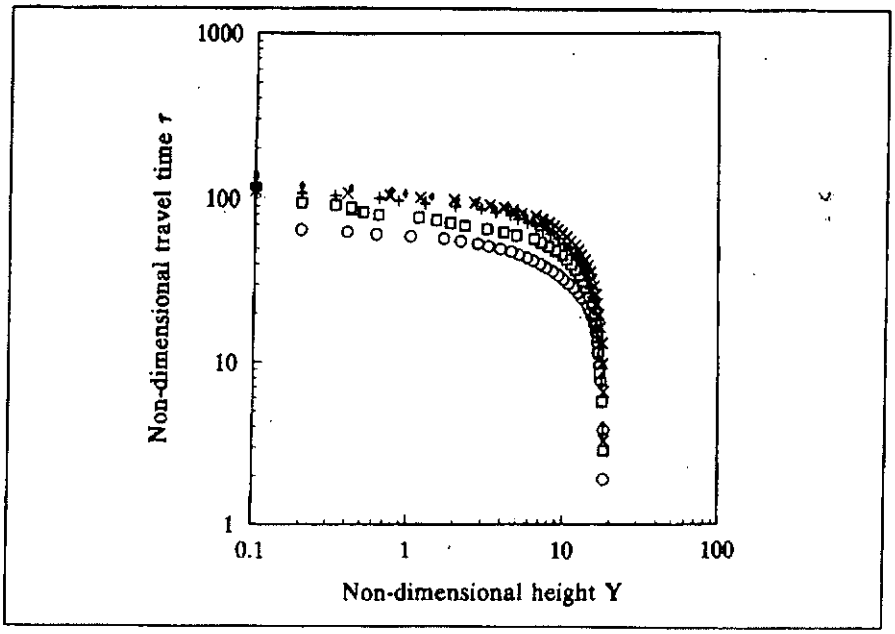

Figure 11. Results of non-dimensional travel time with non-dimensional height Y for case C.

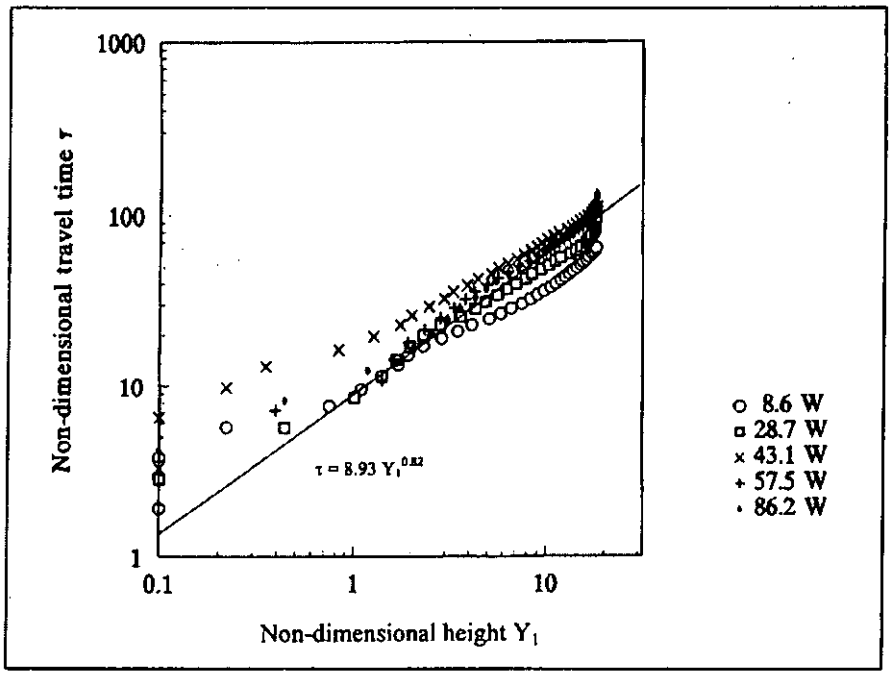

Figure 12. Correlation of non-dimensional time travel with non-dimensional height Y_1 for case C.

For the large fire in a high-rise building mentioned earlier, case B was believed to be one of the possible scenarios. Equation (7) derived in this study would help professionals to consider the possible smoke travel time. The height y of the stair shaft is 48 m and the non-dimensional height Y is 20.9 for that model configuration. It would take non-dimensional time τ of 149 s for the smoke front to travel from the bottom to the top of the lift shaft. This means that smoke emitted from a 5 MW fire in a compartment at the bottom would take 132 s to reach the top. After that, a smoke layer would be formed and then descend to fill the lower part of the shaft. Smoke would then spread to the adjacent levels if the doors are opened to the lift shaft.

APPENDIX A: TRAVEL TIME OF SMOKE FRONT [10]

Following the argument of Fujita et al. [10] on the smoke of plume induced by a fire of heat release rate $\dot{Q}$ placed at the shaft floor, an equation of the temperature rise ΔT, upward plume velocity v, cross-sectional area of the plume A and density ρ can be set up by conservation of enthalpy:

$$\dot{Q} \propto c_p \cdot \rho \cdot \Delta T \cdot A \cdot v \tag{A1}$$

The upward velocity v is due to buoyancy and so is given by the density difference $\Delta\rho$, and by the temperature difference ΔT between the plume and the ambient air at temperature T_∞ as:

$$v \propto \sqrt{g \frac{\Delta\rho}{\rho} y} = \sqrt{g \frac{\Delta T}{T_\infty} y} \tag{A2}$$

Combining equations (A1) and (A2) gives:

$$\left(\frac{\Delta T}{T_\infty}\right) \propto \left(\frac{\dot{Q}}{c_p \cdot \rho \cdot T_\infty \sqrt{g}}\right)^{\frac{2}{3}} \left(\frac{1}{A\sqrt{y}}\right)^{\frac{2}{3}} \tag{A3}$$

Putting equation (A3) into (A2) gives:

$$v \propto \sqrt{g} \left(\frac{\dot{Q}}{c_p \cdot \rho \cdot T_\infty \sqrt{g}}\right)^{\frac{1}{3}} \left(\frac{y}{A}\right)^{\frac{1}{3}} \tag{A4}$$

Dividing both side by $\sqrt{gD}$ gives a non-dimensional velocity V:

$$V = \frac{v}{\sqrt{g \cdot D}} \tag{A5}$$

or

$$V = \frac{v}{\sqrt{g \cdot D}} = \frac{\sqrt{g}}{\sqrt{gD}} \left(\frac{\dot{Q}}{c_p \cdot \rho \cdot T_\infty \sqrt{g}}\right)^{\frac{1}{3}} \left(\frac{y}{A}\right)^{\frac{1}{3}}$$

or

$$\frac{v}{\sqrt{g \cdot D}} = \left(\frac{\dot{Q}}{c_p \cdot \rho \cdot T_\infty \cdot D^{\frac{1}{2}} \sqrt{g}}\right)^{\frac{1}{3}} \left(\frac{y \cdot D}{A}\right)^{\frac{1}{3}}$$

An important point is to assume $\rho = \rho_\infty$, $\dot{Q}$ is now expressed in terms of $\dot{Q}^*$ as:

$$\frac{v}{\sqrt{g \cdot D}} = \dot{Q}^{*\frac{1}{3}} \left(\frac{y \cdot D}{A}\right)^{\frac{1}{3}} \tag{A6}$$

The travel time of a smoke front from the source to a given height y can be calculated by:

$$t \propto \int_0^y \frac{dy}{v} = \sqrt{\frac{D}{g}} \int_0^y \left(\frac{\sqrt{gD}}{v} \right) \frac{dy}{D} \tag{A7}$$

For a fire of constant heat release rate and taking ρ as a constant value along y, equation (A6) can be written as:

$$t \propto \dot{Q}^{-\frac{1}{3}} \int_0^y \left(\frac{A}{y} \right)^{\frac{1}{3}} dy \tag{A8}$$

Expressing t in terms of τ:

$$\tau \propto \sqrt{\frac{D}{g}} \int_0^y \left(\frac{v}{\sqrt{g \cdot D}} \right)^{-1} \left[\sqrt{\frac{g}{D}} \left(\frac{v}{\sqrt{g \cdot D}} \right) \left(\frac{y \cdot D}{A} \right)^{-\frac{1}{3}} \right] \frac{dy}{D}$$

or

$$\tau \propto \int_0^y \left(\frac{A}{y \cdot D} \right)^{\frac{1}{3}} d\left(\frac{y}{D} \right) \tag{A9}$$

There are at least two cases to consider:

1. For a tall lift shaft with large height to length ratio:
   The upward smoke movement is restricted by the vertical shaft and so A is taken as a constant. The travel time t given by equation (A7) can be written as:

$$t \propto \dot{Q}^{-\frac{1}{3}} \cdot y^{\frac{2}{3}} \tag{A10}$$

or

$$\tau \propto Y^{\frac{2}{3}} \tag{A11}$$

2. For a free plume:
   There is no physical constraint on the upward movement, A is proportional to the square of the plume radius at height y, which is proportional to y^2:

$$t \propto \dot{Q}^{1/3} \cdot z^{4/3} \tag{A12}$$

or

$$\tau \propto Y^{4/3} \tag{A13}$$

REFERENCES

1. W. K. Chow, L. T. Wong, and E. C. Y. Kwan, A Proposed Fire Safety Ranking System for Old High-Rise Buildings in the Hong Kong Special Administrative Region, *Fire and Materials, 23*:1, pp. 27-31, 1999.
2. *South China Morning Post,* November 21, 1996.
3. *Ming Pao,* November 22, 1996.
4. Report from the Fire Services Department on the Preliminary Investigation of the Garley Building, *Fire Daily News,* December 14, 1996.
5. *Hong Kong Standard,* January 17, 1997.
6. W. K. Chow, Preliminary Studies of a Large Fire in Hong Kong, *Journal of Applied Fire Science, 6*:3, pp. 243-268, 1997.
7. W. K. Chow, Numerical Studies on Recent Large High-Rise Building Fire, *ASCE Journal of Architectural Engineering, 4*:2, pp. 65-74, 1998.
8. E. E. Zukoski, *A Review of Flows Driven by Natural Convection in Adiabatic Shafts NIST-GCR-95-679 National Institute of Standards and Technology,* U.S. Department of Commerce, U.S.A., 1995.
9. R. Friedman, An International Survey of Computer Models for Fire and Smoke, *Journal of Fire Protection Engineering, 4*:3, pp. 81-92, 1992.
10. T. Fujita, J. Yamaguchi, and T. Tanaka, Investigation into Travel Time of Buoyant Fire Plume Fronts, *Proceedings of the First International Symposium on Engineering Performance-Based Fire Codes,* W. K. Chow (ed.), Department of Building Services Engineering, The Hong Kong Polytechnic University, Hong Kong, China, pp. 220-228, September 8, 1998.

Direct reprint requests to:

Dr. W. K. Chow
Department of Building Services Engineering
The Hong Kong Polytechnic University
HUNG Hom Kowloon
Hong Kong

Natural smoke filling in a physical vertical shaft model

P.M. Tang, L.T. Wong and W.K. Chow
Department of Building Services Engineering
The Hong Kong Polytechnic University
Hong Kong, China

Abstract

Smoke movement in vertical shafts of highrise buildings was studied experimentally with a physical scale model. It was pointed out that the location of fire would be important in determining the smoke travelling time in vertical shafts. Scenarios of a fire in a compartment at three different levels adjacent to the shaft were considered. Empirical correlations on the smoke travelling time were derived from the results reported. Comparison with the previous experimental data was made. The results further confirm that the location of the fire compartment adjacent to the vertical shaft is important in understanding the smoke filling process.

1. Introduction

Vertical shaft is an essential architectural element in high-rise buildings for service installation and transportation. A vertical shaft is a building enclosure with large height-to-span ratio [e.g. 1], passing through floors vertically with openings to different levels. Vertical shafts such as lift shafts, ventilation shafts, light wells, refuse tubes, pipe ducts and cable ducts are commonly found in high-rise buildings in Hong Kong.

Problems on fire safety are commonly encountered with vertical shafts. Heat and smoke would spread rapidly to the other levels from the fire floor through the shafts. For that large fire happened in an old high-rise building in 1996 [e.g. 2-4], the lift shaft under refurbishment was proposed to be a key element of concern [5-7]. Because of the construction work, all the lift doors in that lift shaft were removed with the vertical openings sheltered by temporary plywood partitions. There were arguments [e.g. 8] on the location where the fire started. All these required further in-depth scientific investigation for the Authority to judge. But that lift shaft without fire protection would certainly cause safety problems in transferring heat and smoke. Combustible materials in the lower and upper levels were then ignited to give a very

large post-flashover fire that lasted for more than 20 hours. Note that indoor air motion depends on stack effect, buoyancy of smoke, wind-induced action, and most importantly, the flow induced by mechanical ventilation and air-conditioning system.

Studying the motion of hot gases through the lift shaft is very important in understanding how smoke is spread through the building. Both the stack effect and the turbulent mixing process of a lower hot layer of smoke and an initial upper cool layer of air [9] related to the Rayleigh-Taylor mixing process [10] should be considered. The time taken for the smoke to travel through a lift shaft from the fire floor is also important and should be studied carefully. Smoke would take time [11] to travel upward before forming a smoke layer, if the fire is started at a lower level. The results can then be put into a two-layer zone model for studying the possible fire environment [e.g. 12]. That scale model of the lift shaft was used in this paper to have a preliminary understanding on the smoke movement pattern.

Smoke movement pattern in a lift shaft was studied recently with a scale model [13]. Three fire compartments at three different levels: at the bottom of the lift shaft; at the lower part of the lift shaft; and at the upper part of the lift shaft; were considered. It was proposed that the location of the fire compartment would affect the smoke filling process. Further, experiments on the smoke movement in a lift shaft scale model with the fire in an adjacent compartment at different levels were carried out. Empirical correlations on the smoke travelling time were derived from the results. Comparison with the travelling time derived earlier was made.

2. Smoke Model Studies

The old highrise building where the big fire occurred is of length 34 m, width 28 m and height 50 m. There are 15 levels each of height 3.1 m and a ground level of height 3.5 m. Three lift shafts of average dimensions 2.3 m by 2.3 m by 48 m (i.e. aspect ratio about 1 × 1 × 20) were installed to serve all levels. That lift shaft under refurbishment with all the lift doors removed for some time was considered. Vertical openings of this lift shaft of width 0.8 m and height 2 m were opened to each level.

Experiments were carried out in a scale model of lift shaft with geometry similar to that building. The size of the model was 0.076 m by 0.076 m, with a height of 1.4 m, giving an aspect ratio of 1 × 1 × 18. This gave a scaling factor of 36, in comparing with the lift shaft concerned. The model was constructed of clear glass

sticked together by adhesives for studying the smoke movement in a closed vertical shaft.

Scaling factors are important in using scale models. For a fire located at the floor of a lift shaft, the height y that smoke moved up from the fire base in time t measured experimentally is expressed in terms of the non-dimensional height Y and the non-dimensional time τ, through the characteristic length scale of the model D, and the non-dimensional heat release rate of the fire $\dot{Q}^*$ expressed in terms of the heat release rate of the fire $\dot{Q}$ [11,14]:

$$Y = \frac{y}{D} \qquad \ldots (1)$$

and

$$\tau = t\sqrt{\frac{g}{D}}\dot{Q}^{*\frac{1}{3}} \qquad \ldots (2)$$

with

$$\dot{Q}^* = \frac{\dot{Q}}{c_p \rho T_\infty D^{\frac{5}{2}} \sqrt{g}} \qquad \ldots (3)$$

where g is the acceleration due to gravity, c_p is the specific heat of air at constant pressure, ρ is the smoke density and T_∞ is the ambient temperature. The derivation of travel time of smoke front was described by Fujita et al. [11] and Tanaka et al. [14] and reviewed by Chow et al. [13].

The characteristic length scale of the model D was taken to be the hydraulic diameter of the shaft expressed in terms of the shaft base length L and width W as:

$$D = \frac{2LW}{L+W} \qquad \ldots (4)$$

Relationships of the non-dimensional height Y in terms of τ were derived earlier [11,14] by taking the smoke density ρ to be a constant value which is the ambient air density ρ_∞. This point has to be considered carefully.

3. Review on Previous Results

Experimental studies on the travel time of buoyant fire plume fronts in vertical closed shafts induced by a heat source were carried out [11,14] in a scale model of size 0.8 m by 0.8 m and height 3.22 m; and in a full-size vertical shaft of size 2.8 m by 3 m and height 24 m. The following correlation equations were derived for closed shafts:

$$\tau = \begin{cases} 0.56Y^{4/3} & ; \quad Y \le 2.5 \\ 0.3Y^{2} & ; \quad Y > 2.5 \end{cases} \qquad \ldots (5)$$

Another experimental studies on the travel time of buoyant fire plume fronts in vertical closed shafts by a heat source were carried out [13] in that scale model of size 0.076 m by 0.076 m and height 1.4 m. The characteristic length scale D of the shaft model was 0.076 m. The following correlation equations were derived for closed shafts with a fire placed at the model base:

$$\tau = 0.60\ Y^{1.68} \qquad \ldots (6)$$

Correlations derived for the closed shafts with a fire in a compartment next to the lower part of the shaft are:

$$\tau = \begin{cases} 7.9Y^{2/3} & ; \quad Y < 2.5 \\ 4.3Y^{7/6} & ; \quad Y \ge 2.5 \end{cases} \qquad \ldots (7)$$

For the fire in a compartment next to the upper part of the shaft, the correlations are fitted with experimental data [13]:

$$\tau = 15.82Y_*^{0.65} \qquad \ldots (8)$$

where the non-dimensional distance Y_* is given by:

$$Y_* = \frac{(H_c - y)}{D} \qquad \ldots (9)$$

with H_c being the height of the compartment base above the shaft model base.

4. Current Experiments

A room model of size 0.29 m by 0.076 m and height 0.11 m placed adjacent to the vertical shaft at different levels, through a vertical opening of width 0.05 m and height 0.1 m, was considered. A new parameter height ratio H_R describing the relative height of the adjacent fire compartment to the model height H is given by:

$$H_R = \frac{H_c}{H} \qquad \ldots(10)$$

where H_c is the height of the compartment base above the shaft model base.

The compartment was placed at three different levels at 0.4 m, 0.7 m and 1 m measured from the shaft base to the compartment base, giving the height ratio H_R of 0.29, 0.5 and 0.71 respectively. Three sets of experiments, labelled as cases A, B and C for the fire compartments with H_R of 0.29, 0.50, and 0.71 respectively under atmospheric pressure, were performed with geometry shown in Fig. 1.

A gas burner was used as the scaled fire. Steady burning was achieved by regulating the gas supply at constant flow rates of values 0.0005 Ls^{-1} to 0.005 Ls^{-1} through a 2 mm diameter supply nozzle. Complete combustion was assumed for calculating the heat release rate, using the calorific value of town gas 17.27 MJm^{-3}. A smoke pellet of mass 3.5 g was placed above the gas burner to generate visible smoke. Tungsten lamps were used for illumination so that the smoke movement could be visualized.

Five constant heat release rates 8.6 W, 28.7 W, 43.1 W, 57.5 W and 86.2 W corresponding to the gas flow rates 0.0005 Ls^{-1} to 0.005 Ls^{-1} were used in each set of experiments. These correspond to the heat release rates 43 kW, 145 kW, 217 kW, 290 kW and 433 kW in the full-size model. In this way, τ was found to be 1.91 t, 2.85 t, 3.27 t, 3.60 t and 4.12 t respectively for the five heat release rates. The experiments were repeated three times for each heat release rate and a total of 15 tests were carried out. Note that the model was cleaned before each test.

For a clear visualization of smoke movement pattern, the experiments were carried out under light sources. Except the specified light sources, the environment of the

laboratory was kept dark. Photographs were taken by a camera at right angle to the light source.

Photographs of the transient smoke movement in the shaft were taken by a camera installed with a 35 mm lens. The aperture and shutter speed were set at *f*/4 and 1/60 s respectively with shooting frequency of 1 s. The images were recorded on 35 mm × 24 mm films of speed ISO400 with resolving power 125 *ll*/mm for contrast 1/1000 and 40 *ll*/mm for contrast 1/1.6.

5. Results

Typical photographs on the smoke pattern in the scale model at different time intervals for the three cases are shown in Figs. 2 to 4. The average transient values of y were determined from the pictures, and the results at different heat release rates are shown in Figs. 5 to 7 for cases A, B and C respectively.

For smoke front moving upward inside the vertical shaft model, the compartment height H_c is used to evaluate the non-dimensional distance, i.e.,

$$Y_1 = \frac{(y - H_c)}{D} \qquad \ldots (12)$$

The values of τ were plotted against Y_1 for smoke front moving upward inside the shaft model in Fig. 8. Correlation equations were derived from the measured results for H_R of 0.29, 0.50 and 0.71 with correlation coefficients 0.88, 0.79 and 0.84 respectively.

$$\tau = \begin{cases} 0.943 Y_1^{1.64} & ; \quad H_R = 0.29 \\ 1.81 Y_1^{1.35} & ; \quad H_R = 0.50 \\ 2.63 Y_1^{1.23} & ; \quad H_R = 0.71 \end{cases} \qquad \ldots (11)$$

The results of previous studies [13] for $H_R = 0$ given by equation (7) were shown in the figure for comparison. The travelling time for the smoke front moving upward inside the shaft model would be significantly increased with higher height ratios H_R. It is observed that the non-dimensional time τ is about three times longer for H_R = 0.71 than for $H_R = 0$ at the early stage of smoke movement.

For smoke front moving downward inside the vertical shaft model, the compartment height H_c is used to evaluate the non-dimensional distance, i.e.,

$$Y_2 = \frac{(H_c - y)}{D} \qquad \ldots (12)$$

The values of τ were plotted against Y_2 as shown in Fig. 9. Correlation equations were derived from the measured results for H_R of 0.29, 0.50 and 0.71 with correlation coefficients 0.78, 0.76 and 0.73 respectively.

$$\tau = \begin{cases} 30.4 Y_2^{0.4} & ; \quad H_R = 0.29 \\ 27.4 Y_2^{0.5} & ; \quad H_R = 0.50 \\ 21.0 Y_2^{0.58} & ; \quad H_R = 0.71 \end{cases} \qquad \ldots (13)$$

The experimental results of previous studies [13] with $H_R = 0.93$ given by equation (8) were plotted in the figure for comparison. The travelling time for the smoke front moving downward inside the vertical shaft model would be significantly increased with lower height ratios H_R. It is observed that the non-dimensional travelling time τ for $H_R = 0.93$ is about half of that for $H_R = 0.29$ at the early stage of smoke movement.

6. Conclusion

Smoke filling process in vertical shafts in highrise buildings was studied experimentally with scale modeling technique. Smoke filling in a vertical shaft with a fire compartment next to the shaft at three different levels was considered. It is further confirmed that the location of fire would be an important factor in determining the smoke travelling time in vertical shafts. Following the concept of Fujita et al. [11] and Tanaka et al. [14], correlation relationships between the smoke and the travelling time are developed for the three cases. Equations (11) and (13) are useful for understanding the smoke filling process in vertical closed shafts in buildings.

Acknowledgement

This project is funded by The Hong Kong Polytechnic University with account number
G-V504.

References

1. Building Ordinance, Chapter 123, Laws of Hong Kong, Hong Kong (1997).
2. South China Morning Post, 21 November (1996).
3. Ming Pao, 22 November (1996).
4. Hong Kong Standard, 17 January (1997).
5. Chow, W.K., Preliminary studies of a large fire in Hong Kong, Journal of Applied Fire Science, Vol. 6, No. 3, pp. 243-268 (1997).
6. Chow, W.K., Numerical studies on recent large high-rise building fire, ASCE Journal of Architectural Engineering, Vol. 4, No. 2, pp. 65-74 (1998).
7. Woo, K.W., Final Report of the inquiry into the Garley Building fire on 20 November 1996. Printing Department, Hong Kong (1997).
8. Drysdale, D.D., Interpretation of evidence at the fire scene: The importance of fire dynamics, Proceedings of the Interflam '99 Conference, Edinburgh Conference Centre, Scotland, 29 June – 1 July 1999, Edited by Grayson, S., Interscience Communications Limited, London, UK, p. 233-244 (1999).
9. Cooper, L.Y. Simulating smoke movement through long vertical shafts in zone-type compartment fire models, Fire Safety Journal, Vol. 31, No. 2, pp. 85-99, (1998).
10. Zukoski, E.E., A review of flows driven by natural convection in adiabatic shafts, NIST-GCR-95-679 National Institute of Standards and Technology, U.S. Department of Commence, U.S.A. (1995).
11. Fujita, T., Yamaguchi, J. and Tanaka, T., Investigation into travel time of buoyant fire plume fronts, Proceedings of the First International Symposium on Engineering Performance-Based Fire Codes, Edited by Chow, W.K., Department of Building Services Engineering, The Hong Kong Polytechnic University, Hong Kong, China, 8 September 1998, pp. 220-228 (1998).
12. Friedman, T., An international survey of computer models for fire and smoke, Journal of Fire Protection Engineering, Vol. 4, No. 3, pp. 81-92 (1992).

13. Chow, W.K., Wong, L.T., Tang, P.M., and Kwan, Eric C.Y., Scale model studies on smoke filling in the lift shaft of an old highrise building, Journal of Applied Fire Science – Accepted to publish (2000).

14. Tanaka, T., Fujita, T. and Yamaguchi, J., Investigation into rise time of buoyant fire plume fronts, International Journal on Engineering Performance-Based Fire Codes, Edited by Chow, W.K., Department of Building Services Engineering, The Hong Kong Polytechnic University, Hong Kong, China, Vol. 2, No. 1, pp. 14-25 (2000).

NSFscale2a

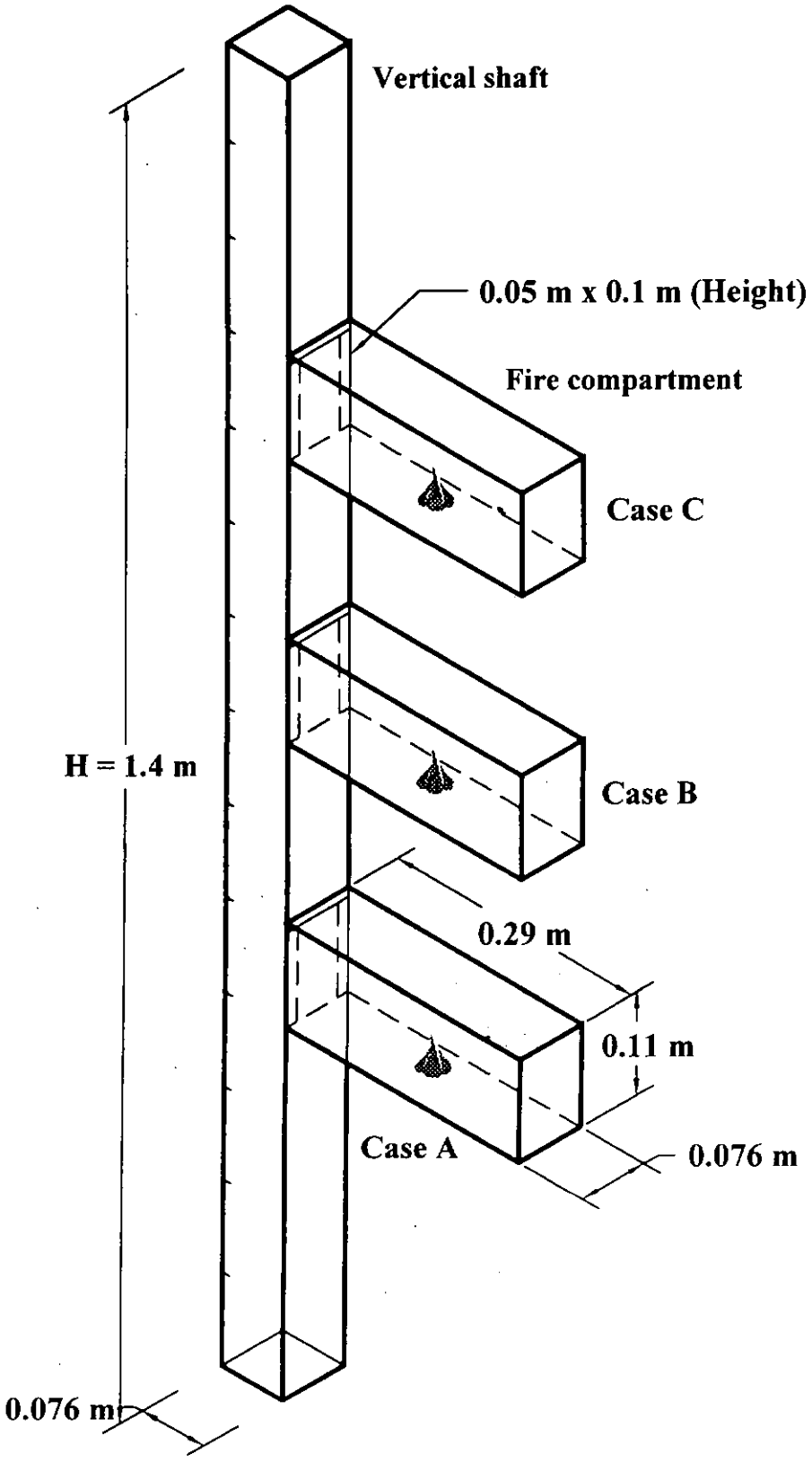

Figure 1: Scale model experiment

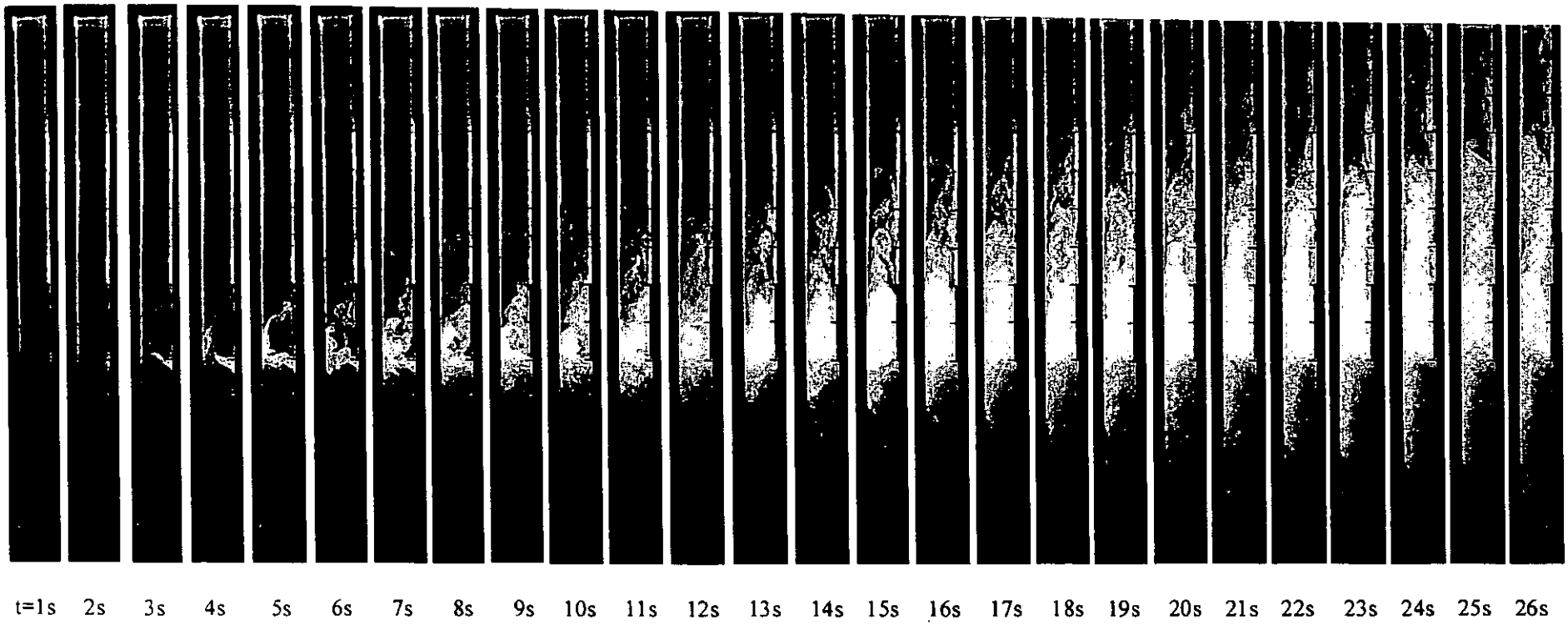

Figure 2: Smoke filling for Case A

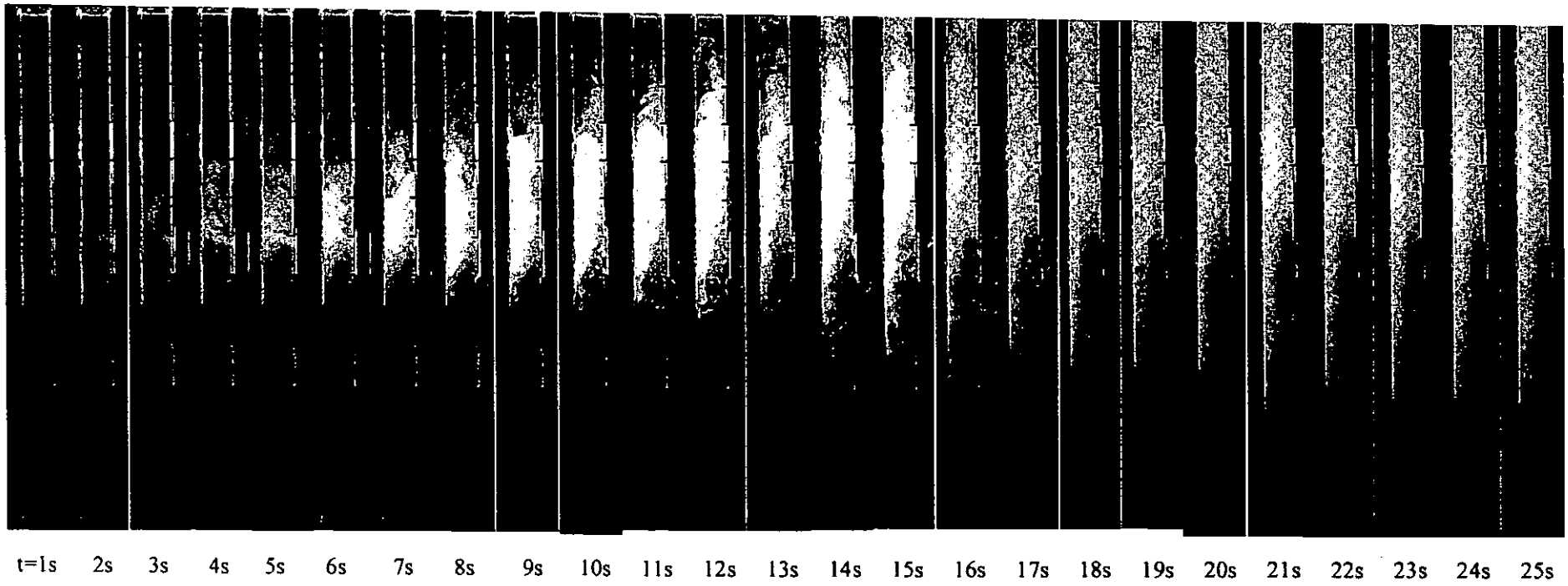

Figure 3: Smoke filling for Case B

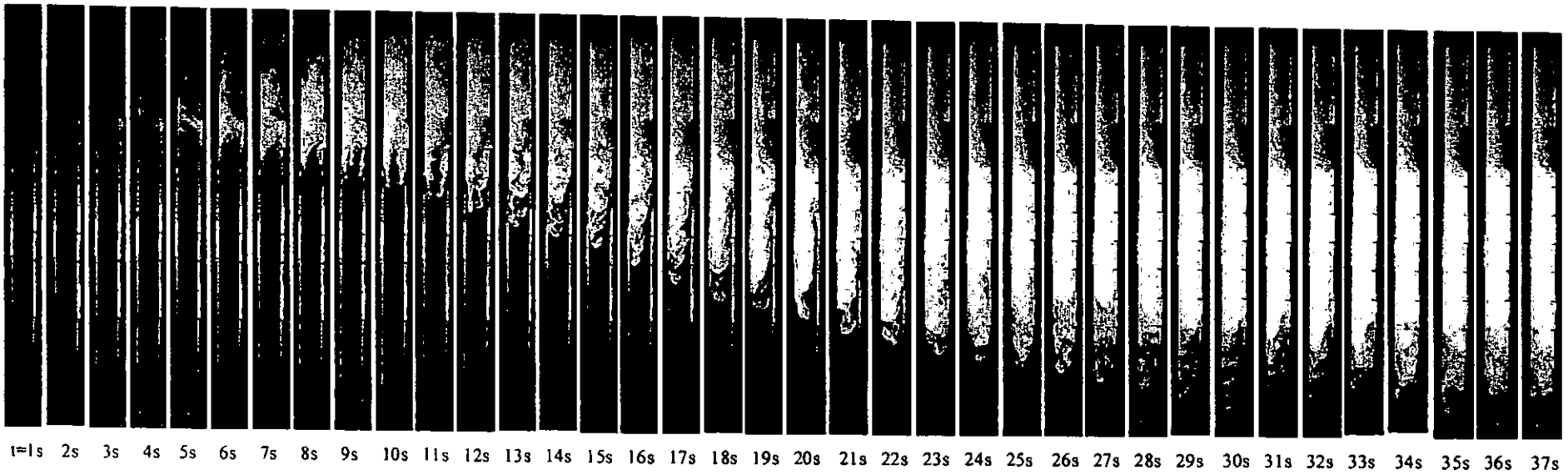

Figure 4: Smoke filling for Case C

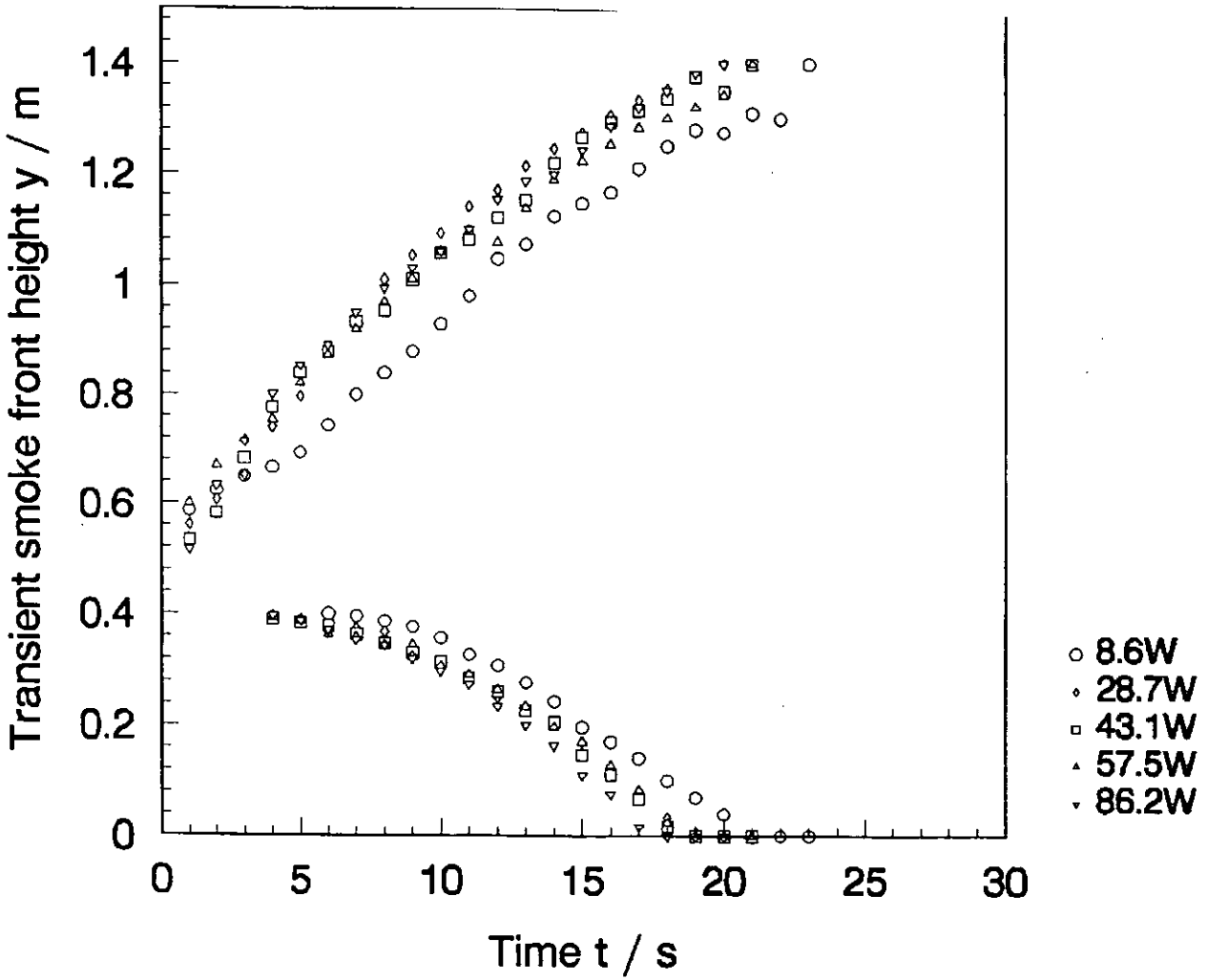

Figure 5: Height of transient smoke front for Case A

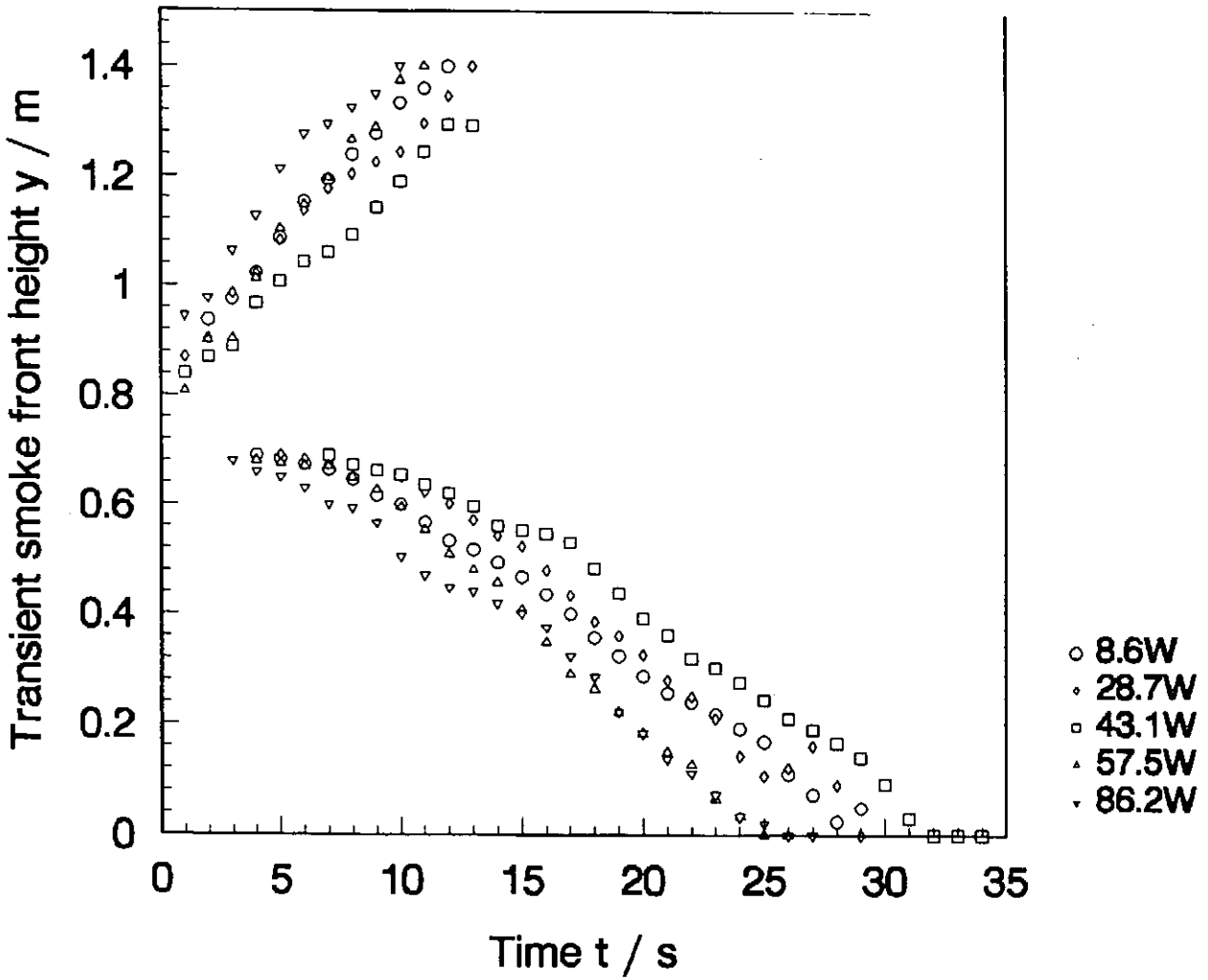

Figure 6: Height of transient smoke front for Case B

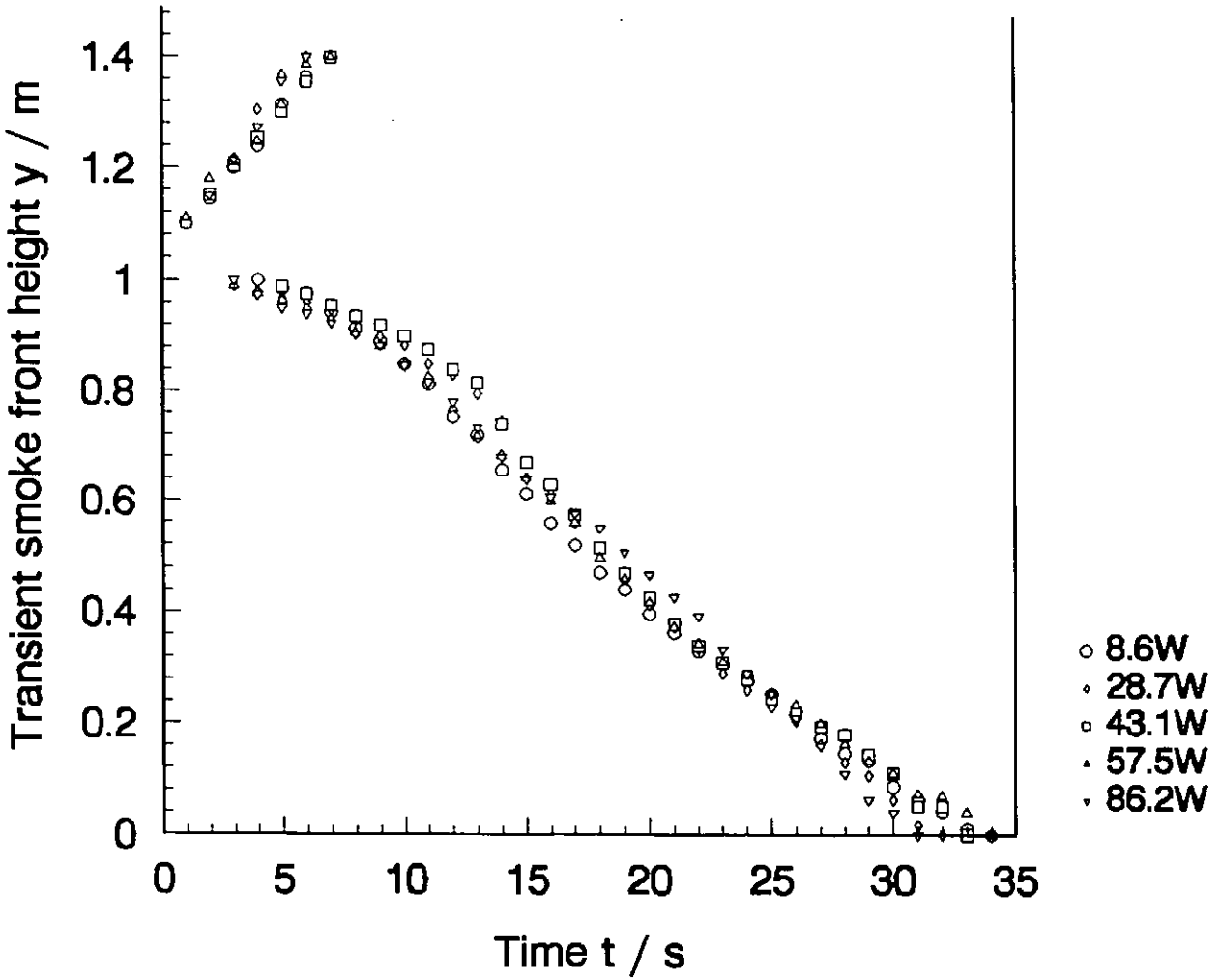

Figure 7: Height of transient smoke front for Case C

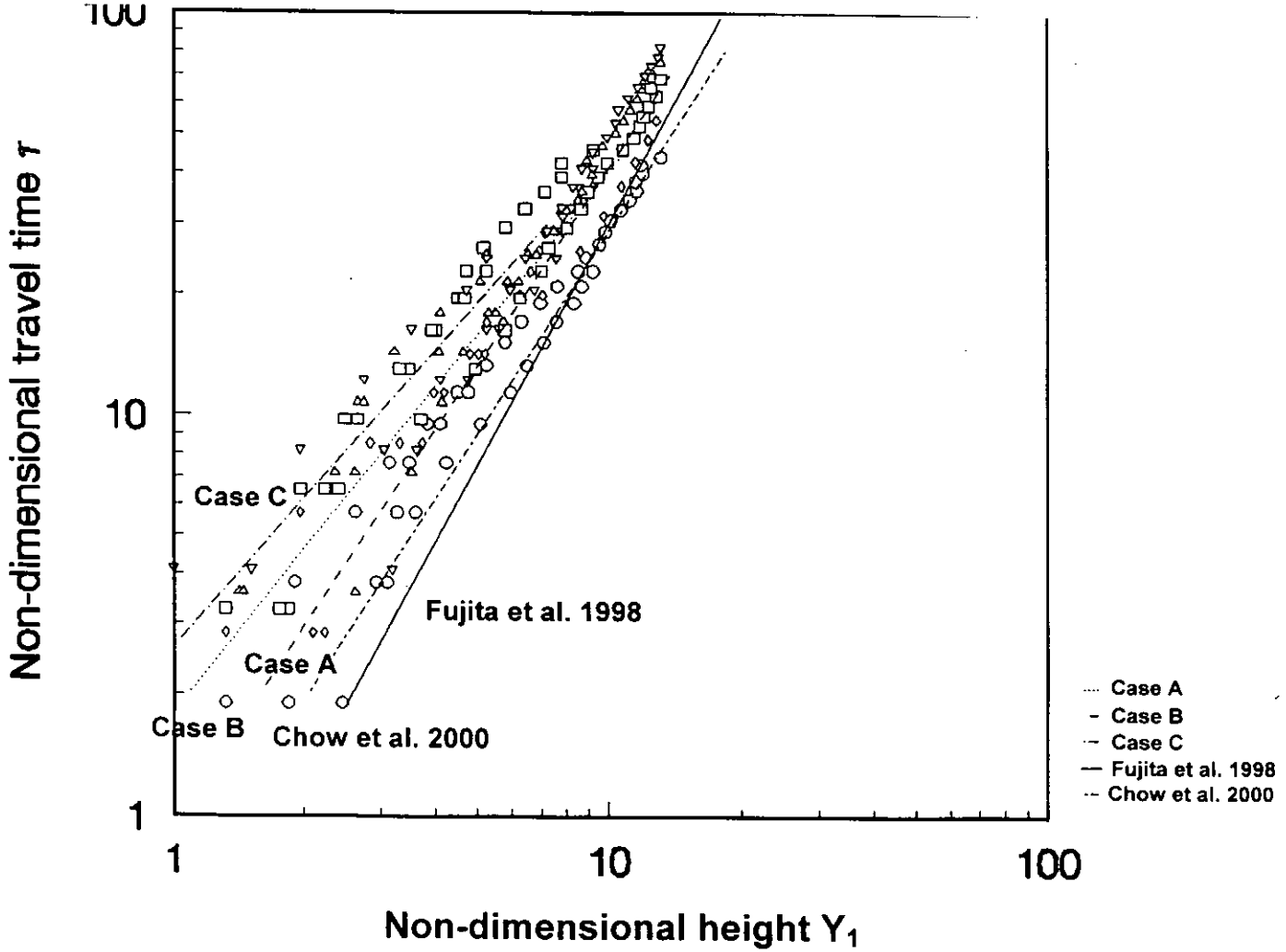

Figure 8: Correlation of non-dimensional travel time with non-dimensional height Y_1

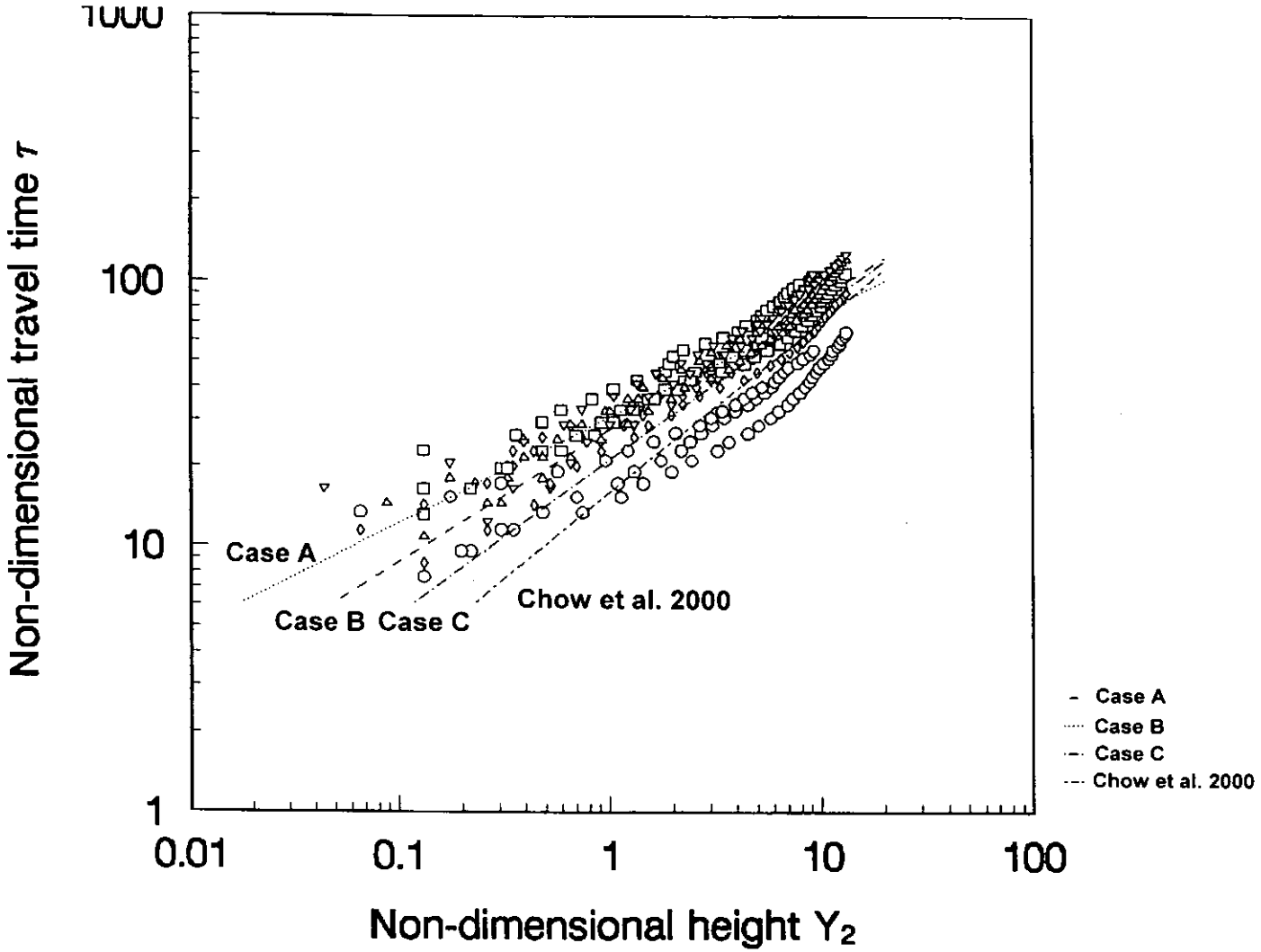

Figure 9: Correlation of non-dimensional travel time with non-dimensional height Y_2